Università degli Studi di Trento
Facoltà di Scienze Matematiche
Fisiche e Naturali
Dipartimento di Fisica

Tesi di Dottorato di Ricerca in Fisica
Ph.D. Thesis in Physics

Topological Dynamics in Low-Energy QCD

Candidato
Raffaele Millo

Relatore
Dr. Pietro Faccioli

Dottorato di Ricerca in Fisica, XXIII ciclo
Trento, 21 Febbraio 2010

Acknowledgments

I want to thank my advisor Dr. Pietro Faccioli for his continuous support; I also want to thank Dr. Luigi Scorzato, Dr. Francesco Di Renzo and Prof. Edward Shuryak for their help and interesting dicussions.
A particular thanks to Dr. Andre Sternbeck for giving us the Lattice configurations we used in chapter 5.

Contents

Chapter 1

Introduction

The understanding of the mechanisms driving the low-energy QCD dynamics in different conditions of temperatures and densities is still an open problem. The main difficulty arise from the fact that QCD becomes strongly coupled in the infrared regime, and hence perturbation theory cannot be applied.

A fundamental open question in non-perturbative QCD concerns the origin of color confinement. Another important non-perturbative process in strong interactions is the spontaneous breaking of chiral symmetry (SChSB). This mechanism is responsible for the emergence of light mesonic excitation in the hadronic spectrum, and hence is crucial for the description of strong interactions at low energies. Even if we still lack of a complete description of SChSB in terms of fundamental degrees of freedom, it is now understood that non-perturbative gauge configurations with non-trivial topological properties play an important role in this process.

In particular, in the N=4 supersymmetric gauge theory [1] and in the Schwinger Model [2] instantons have been shown to be responsible for both confinement and chiral symmetry breaking. On the other hand, the dynamical mechanism underlying these processes in QCD seems to be considerably more involved and role of the different topological configurations is still a matter of debate.

Topological gluonic configurations may in principle induce strong CP violation in hadronic processes. Indeed, it can be shown that the non-trivial non-perturbative structure of the vacuum leads to an additional pseudoscalar term in the QCD Lagrangian

$$\mathcal{L}_\theta = \theta \frac{g^2}{64\pi^2} \tilde{G}^{\mu\nu}_a G^a_{\mu\nu},$$

where θ is a free parameter. However, measurement of the neutron elec-

tric dipole moment sets an upper bound for the parameter in the QCD Lagrangian at $\theta \leq 10^{-10}$. The smallness of this number constitutes to the so-called Strong CP-problem; the reason why CP-symmetry is conserved at such a high precision in the hadronic interactions is still an open fundamental question and motivates further studies to provide better estimates of θ.

In the first part of this thesis we shall investigate the dynamics associated to topological gauge field configurations in connection to the breaking of the CP symmetry; in particular, we will discuss the possibility of observing violations of CP symmetry in hadronic processes in the presence of an extremely small but finite θ. In fact we will show that a system of quarks propagating in a background gauge field with non-trivial topology may be electrically polarized by an external magnetic field. At low energies this CP-odd polarization is proportional to θ and aligned along the external magnetic field,

$$\mathbf{P}_{odd} = k\,\theta B^n \hat{\mathbf{B}}.$$

Contributions of topological dynamics to very low-energy observables can be rigorously accounted for by means of Chiral Perturbation Theory (ChPT). In particular, in such a framework, it is possible to evaluate the factor k and the exponent n in a systematic expansion. In the ChPT approach, one considers light psuedoscalar mesons as relevant degrees of freedom, and the dynamics of fundamental degrees of freedom and topological configurations are taken into account by local interactions among pseudoscalar mesons.

Strong CP-violating $\theta-$dependent interactions can also have an influence on the dynamics of light propagating in a Fabry-Perot cavity permeated by an external electromagnetic field; in fact, topological dynamics induces CP-odd photon-photon interactions that can contribute to the non-linear properties of the QED vacuum, generating a CP-odd term for the vacuum birefringence. For particular orientation of the electric and magnetic field, CP-odd and CP-even channels are disentangled and signals of CP-odd birefringence may be in principle observed.

CP-symmetry can be globally broken only if $\theta \neq 0$. However, CP-odd observables may be non-zero in background field of specific topological configurations; this implies that fluctuation of topological fields may induce non-trivial dynamics which reflects the breaking of CP in subregions of space-time. For example, recently the STAR collaboration [3] have observed an asymmetry in pion distribution in relativistic heavy ion collisions at RHIC: such an asymmetry is a consequence of the Chiral Magnetic Effect (CME) [4] which consists in a polarization of quarks along the axis perpendicular to the collision plane, due to the local anomalous CP-violating interactions induced by specific topological gauge fields. Unfortunately this effect cannot

be investigated in ChPT because at energies $T \simeq T_c$ fundamental degrees of freedom become manifest and have to be explicitely included in the theoretical description.

The only approach which enables to solve QCD non-perturbatively from first principles is Lattice QCD (LQCD). Unfortunately, it is still unclear how to use LQCD to obtain qualitative information on the microscopic dynamics of topological degrees of freedom participating in processes such as CME.

In the second part of this project we will try to tackle this problem, and we will present a rigorous method for investigating the microscopic dynamics of non-perturbative processes. The main assumption is that it is possible to identify a specific family of non-perturbative configurations (e.g. constructed form a collection of instantons, or from a "cocktail" of monopoles and instantons or from other configurations) which drive the non-perturbative process of interest. In general, such a family of configurations will be parametrized by a set of collective coordinates, which e.g. specify the position, size and color orientation of each instanton. The QCD partition function can be rigorously rewritten in terms of such collective coordinates and of the path integral over all other field configurations which do not belong to the selected manifold of gauge fields. If such a path integral is evaluated non-perturbatively, one obtains an effective theory for QCD in which the role of low-energy degrees of freedom is played by the collective coordinates spanning the manifold of background field configurations.

In this work, we shall present an approach to achieve this goal by means of LQCD simulations. We will show the first application to gauge theories, which consist in the calculation of the instanton size distribution in pure gauge SU(2).
The advantage of this method is that it is not based on semiclssical arguments and does not depend on any arbitrary parameters. Hence it can be applied to other topological configurations and even at finite temperature, giving new insights on the microscopic dynamics of non-perturbative processes such as SChSB, or even confinement.

The work is then organized as follows. In chapter 2 we will discuss the properties of the QCD Lagrangian at the classical and quantum level, and we will analyze the non-trivial topological structure of the QCD vacuum; we will also present a phenomelogical explanation of axial anomaly and SChSB in terms of topological degrees of freedom. In chapter 3 we will outline ChPT formalism and we will briefly discuss LQCD formulation: these are the two main methods which enables to solve QCD non-perturbatively. In chapter 4 we will review our results for the CP-odd vacuum polarization in the presence of external magnetic fields, and we will discuss their im-

plications on low-energy photon-photon interactions. In chapter 5 we will introduce the projection technique which enables to gain information on the non-perturbative microscopic dynamics of the QCD vacuum in terms of effective degrees of freedom, and we will present the results for the instanton-density in pure gauge $SU(2)$ QCD at $T = 0$.
Results are summarized in the conclusions, chapter 6.

Results of this work have been published in Phys.Rev.**D79**(2010) 065020, Phys.Rev.**D82**(2010) 074019, and in two preprints which are being considered for publications.

Chapter 2

Quantum ChromoDynamics

Quantum ChromoDynamics is considered the fundamental theory of strong interactions. An important feature of this theory is that it is strongly coupled in the infrared and weakly coupled in the ultraviolet (asymptotic freedom). At the classical level, the theory displays a global $U_V(N_f) \times U_A(N_f)$ "chiral" invariance which is broken down to $U_V(N_f) \times SU_A(N_f)$ at the quantum level, due to the *axial anomaly*. In addition, an analysis of the hadronic spectrum reveals that *chiral symmetry is* also *spontaneously broken* down to $U_V(N_f)$ at low energies.

The anomalous breaking of $U_A(1)$ and SChSB are a consequence of the topological structure of the QCD vacuum, which implies the existence of gauge configurations with non-trivial topology, known as instantons, which can trigger P and CP breaking processes.

2.1 Classical QCD Lagrangian

We start our analysis by considering the $SU_C(3)$ gauge invariant classical QCD Lagrangian[1], which consists in the sum of two terms

$$\mathcal{L}_{QCD} = \sum_{f=1}^{N_f} \bar{q}_f (i\gamma^\mu D_\mu - m_f) q_f - \frac{1}{4g^2} G^a_{\mu\nu} G^{\mu\nu}_a. \tag{2.1}$$

The first term is the Lagrangian for N_f massive Dirac fields — quarks — to be intended as vectors in color space, each component labelled by a different

[1] In this work we use the so-called "non-perturbative notation", in which the strong coupling g is absorbed into A_μ. The standard notation can be obtained by replacing

$$A_\mu \longrightarrow g A_\mu,$$
$$G_{\mu\nu} \longrightarrow g G_{\mu\nu}.$$

color —*red, blue* and *green* —

$$\bar{q}_f = q_f^\dagger \gamma_0 = (\bar{q}_{f,r}, \bar{q}_{f,b}, \bar{q}_{f,g})\,; \qquad \text{for } N_c = 3.$$

Quarks are coupled to $N_C^2 - 1 = 8$ guage fields in the adjoint representation — gluons — via a covariant derivative

$$D^\mu = \partial^\mu - iA^\mu, \tag{2.2}$$

$$A^\mu(x) = \frac{\lambda_C^a}{2} A_a^\mu(x). \tag{2.3}$$

Gauge transformations are represented by unitary $N_C \times N_C$ matrices

$$U_C(x) = e^{i\xi_a^C(x)\frac{\lambda_C^a}{2}}, \tag{2.4}$$

with λ_C^a generators of $\mathfrak{su}(3)$ in color space — e.g. Gellmann matrices —; transformations law for q_f, $\bar{q}_f$, $D_\mu q_f$ and A_μ are given by

$$q_f \rightarrow q_f^{'} = U_C q_f, \tag{2.5}$$

$$\bar{q}_f \rightarrow \bar{q}_f^{'} = \bar{q}_f U_C^\dagger, \tag{2.6}$$

$$A^\mu \rightarrow A^{'\mu} = U_C A^\mu U_C^\dagger - i\left[\partial^\mu U_C\right] U_C^\dagger, \tag{2.7}$$

$$D_\mu q_f \rightarrow D_\mu^{'} q_f^{'} = U_C\left(D_\mu q_f\right). \tag{2.8}$$

The second term in the QCD Lagrangian is built up with chromoelectromagnetic fields, which define interactions among gluons

$$G_{\mu\nu} = \partial_\mu A_\nu - \partial_\nu A_\mu - i[A_\mu, A_\nu], \tag{2.9}$$

$$G^{\mu\nu} \rightarrow G_{\mu\nu}^{'} = U_C G^{\mu\nu} U_C^\dagger. \tag{2.10}$$

Using the ciclic property of the trace of matrices in color space, we can then write the gauge invariant pure gauge Lagrangian as

$$\mathcal{L}_{p.g.} = -\frac{1}{2g^2}\mathrm{Tr}\left[G^{\mu\nu}G_{\mu\nu}\right] = -\frac{1}{4g^2}G_a^{\mu\nu}G_{\mu\nu}^a.$$

In principle one might add to the Lagrangian another gauge invariant term

$$\mathcal{L}_\theta = \frac{\theta}{32\pi^2}G_a^{\mu\nu}\tilde{G}_{\mu\nu}^a; \quad \tilde{G}_{\mu\nu} = \frac{1}{2}\varepsilon_{\mu\nu\rho\sigma}G_{\rho\sigma}; \tag{2.11}$$

$$= \frac{\theta}{16\pi^2}\partial_\mu[\epsilon^{\mu\nu\alpha\beta}A_\nu^a\left(G_{a\alpha\beta} + \frac{1}{3}f_{abc}A_\alpha^b A_\beta^c\right)] \tag{2.12}$$

$$= \frac{\theta}{32\pi^2}E_{a,i}B_i^a, \tag{2.13}$$

where we have introduced the chromoelectric and chromomagnetic fields

$$E_{a,i} = G_{0,i}; \quad B_{a,i} = \frac{1}{2}\varepsilon_{ijk}G_{j,k}.$$

$\mathcal{L}_\theta$ is manifestly P, T and CP-odd, because E_a^i is a polar vector, whereas B_i^a is an axial vector: if $\theta \neq 0$ QCD may allow for the violation of P, T and CP symmetries. On the other hand this CP-violating term, to which we will refer as the "θ-term", is equivalent to a total derivative and hence one should naively expect that it cannot modify the QCD dynamics. In section 2.5 we will see that this statement is wrong, in particular we will see that gauge invariance not only allows but somehow *implies* CP-violation in pure gauge QCD: we will prove that this is a consequence of the non-trivial topological structure of the QCD vacuum.

2.2 Asymptotic Freedom

At low energies the hadronic spectrum is formed by meson and baryons which are bound states of quarks and gluons. More generally, the fundamental degrees of freedom of QCD are not directly manifest at low energies, because they are *confined* in bound states: this is a consequence of the strength of the strong coupling at low energies. After forty years from the foundation of QCD, it is still not clear which is the microscopic non-perturbative mechanism underlying confinement.
On the other hand since the '70s [5] it has been known that at energies much greater than $\Lambda_{QCD} \simeq 250MeV$, hadronic systems enter in a weakly coupled regime: quarks and gluons can be considered as "almost free" weekly interacting particles.

This so-called "asymptotic freedom" can be seen as a consequence of renormalization in quantum field theories, which implies that the couplings "constants" are actually a function of the energy scale of the process under considerations. The behaviour of the "running coupling" $\alpha_s = \frac{g_s^2}{2\pi^2}$ is determined by calculating the β function

$$\beta(g) = \frac{\mathrm{d}}{\mathrm{d}\,(\ln \mu)} g(\mu),$$

where μ is the energy scale of the process. In non-abelian $SU(N_C)$ gauge theory coupled to N_f fermions the β function at one loop is given by

$$\beta(\alpha_s) = -\frac{\alpha_s^2}{2\pi}\left[\frac{11}{3}N_c - \frac{2}{3}N_f\right] + O(\alpha_s^3) \tag{2.14}$$

$$\simeq -7\frac{\alpha_s^2}{2\pi} < 0, \tag{2.15}$$

which implies that the coupling decrease at high momenta if $N_c = 3$ and $N_f = 6$. The result for β implies the following "running" behaviour

$$\alpha_s(q^2) = \left[\frac{1}{2\pi}\left(\frac{11}{3}N_c - \frac{2}{3}N_f\right)\ln\frac{q^2}{\Lambda_{QCD}}\right]^{-1} \xrightarrow{q\to\infty} 0. \tag{2.16}$$

In this sense we can then distinguish between a "perturbative" and a "non-perturbative" energy regime, depending on the value assumed by the coupling constant $\alpha_s = \frac{g_S^2(q)}{4\pi}$.

2.3 Global Chiral $U_V(N_f) \times U_A(N_f)$ Symmetry

Local $SU_C(3)$ gauge invariance discussed in section 2.1 is not the only symmetry of $\mathcal{L}_{QCD}$: by considering unitary transformations of quarks in flavor space, we can define a global symmetry which is exact in the so-called *chiral limit*

$$m_f \to 0.$$

We start by defining two projection operators acting on quarks

$$P_{R/L} = \frac{1}{2}(1 \pm \gamma_5); \qquad \gamma_5 = i\gamma_0\gamma_1\gamma_2\gamma_3 = \gamma_5^\dagger; \tag{2.17}$$

$$\gamma_\mu P_{R/L} = P_{L/R}\gamma_\mu; \qquad \{\gamma_\mu, \gamma_5\} = 0;\ \gamma_5^2 = 1, \tag{2.18}$$

whose basic properties are

$$(P_R + P_L)q_f = q_f, \tag{2.19}$$

$$P_R P_L q_f = 0, \tag{2.20}$$

$$P_{R/L}^2 q_f = P_{R/L} q_f. \tag{2.21}$$

This complete set of operators enable us to separate the quark fields into a "left-handed" — q_L — and a "right-handed" — q_R — *chiral* component[2]

$$q_{f,R/L} = P_{R/L} q_f\ ; \quad \bar{q}_{f,R/L} = \bar{q}_f P_{L/R}.$$

By separating the chiral components in the Dirac Lagrangian we obtain

$$\begin{aligned}\mathcal{L}_q = \ & \textstyle\sum_f \big[\bar{q}_{f,L}(i\gamma^\mu D_\mu)q_{f,L} + \bar{q}_{f,R}(i\gamma^\mu D_\mu)q_{f,R} + \\ & -m_f(\bar{q}_{f,L}q_{f,R} + \bar{q}_{f,R}q_{f,L})\big].\end{aligned} \tag{2.22}$$

We immediately see that, in the chiral limit $m_f \to 0$, the quark Lagrangian can be rewritten as the sum of two independent terms: one for quarks with right-handed chirality, the other one for quarks with left-handed chirality. This implies that, at the classical level, chirality is conserved for massless fermions, since there are no-interactions that can change the chirality of quarks; this implies in particular that the difference between right-handed and left-handed (anti)quarks in a closed system is always a constant. By

[2] For massless spinors chirality coincides with *helicity*, which measures the orientation of spin and momentum of a particle; $(-)+1$ helicity implies that the spin and the momentum are (anti)aligned.

defining N_R (N_L) as the total number of right-handed (left-handed) particles in a system we have

$$\begin{aligned} Q_A(t) &= N_R(t) - N_L(t), & (2.23)\\ \frac{\mathrm{d}}{\mathrm{d}t}Q_A(t) &= 0. & (2.24) \end{aligned}$$

The constant Q_A is called axial charge.

The Lagrangian for N_f species of massless fermions has other $2N_f^2 - 1$ conserved charges associated to the "chiral" group of transformations $G_\chi = U_R(N_f) \times U_L(N_f)$ of the QCD Lagrangian, acting on flavor space as follows

$$\begin{aligned} U_R = e^{=i\Theta_a^R \frac{\lambda^a}{2}};\ U_L = e^{-i\Theta_a^L \frac{\lambda^a}{2}}, \qquad (2.25)\\ U_\chi q_f(x) = U_R q_{f,R} + U_L q_{f,L}, \end{aligned}$$

where λ^a are the generators of the $\mathfrak{u}(N_f)$ algebra, which in the adjoint representation are given by $\mathfrak{su}(N)$ generators plus the identity matrix.
The Noether currents are

$$R_\mu^a = \bar{q}_R \gamma_\mu \frac{\lambda^a}{2} q_R\ ; \qquad L_\mu^a = \bar{q}_L \gamma_\mu \frac{\lambda^a}{2} q_L. \qquad (2.26)$$

The properties of projection operators enables to define currents which are independent from the "R/L" labelling: these are the so-called vectorial and axial current

$$V_\mu^a = R_\mu^a + L_\mu^a = \bar{q}\gamma_\mu \tfrac{\lambda^a}{2} q\ ; \qquad A_\mu^a = R_\mu^a - L_\mu^a = \bar{q}\gamma_\mu\gamma_5 \tfrac{\lambda^a}{2} q. \qquad (2.27)$$

which are the conserved currents of a new set of transformations $U_V(N_f)$ and $U_A(N_f)$ consisting in a simultaneous chiral rotation of both q_L and q_R, s.t. $G_\chi = U_V(N_f) \times U_A(N_f)$.
The Noether charges for such transformations are defined as the integral over R^3 of the time-component of the Nother currents

$$\begin{aligned} Q_V^a(t) &= \int_{R^3} \mathrm{d}^3x V_0^a(t,\mathbf{x}), & (2.28)\\ Q_A^a(t) &= \int_{R^3} \mathrm{d}^3x A_0^a(t,\mathbf{x}), & (2.29) \end{aligned}$$

and we can then identify $Q_A(t)$ as the Noether charge of A_μ^0.

Divergence of vector and axial currents in the general case of massive fermions are given by

$$\begin{aligned} \partial_\mu V^{\mu,a} = i\bar{q}\left[M_q, \frac{\lambda^a}{2}\right] q\ ; \qquad \partial_\mu A^{\mu,a} = i\bar{q}\left\{M_q, \frac{\lambda^a}{2}\right\}\gamma_5 q\\ \partial_\mu V^{\mu,0} = 0\ ; \qquad \partial_\mu A^{\mu,0} = 2i\bar{q}M_q\gamma_5 q, \qquad (2.30) \end{aligned}$$

where M_q =diag(m_f) is the quark mass matrix.

Analyzing the system of Eq.s (2.30) we then conclude that:

- In the chiral limit G_χ is an exact symmetry of the QCD Lagrangian;
- The singlet vector current V_μ^0 is always conserved: the related conserved charge Q_V^0 is the *barion number*: $B = 0$ for mesons and $B = 1$ for baryons;
- If all the quark masses have the same value the non singlet vector currents V_μ^a are also conserved. Notice that since $m_u \simeq m_d \ll \Lambda_{QCD}$ we can conclude that the chiral vector $U_V(2)$ symmetry is an almost exact symmetry for the QCD Lagrangian. This is marginally true for $U_V(3)$, since $m_s \simeq 150MeV$ which is not so much smaller than Λ_{QCD};
- The axial $U_A(N_f)$ symmetry is only an approximate symmetry of the Lagrangian, if $M_q \neq 0$.

The invariance property of the QCD Lagrangian reflects on the hadronic spectrum, which is organized along almost degenerate multiple along irreducible representations of $U_V(3)$; on the other hand we will see in chapter 3 that $SU_A(3)$ and $SU_A(2)$ symmetries are not reflected in the hadronic spectrum, this is a consequence of the fact that chiral symmetry is spontaneously broken in the QCD vacuum at low energies: we will discuss this phenomenon in section 2.8.

In the next section we will see that, at the quantum level, $U_A(1)$ is not a symmetry of the QCD Lagrangian.

2.4 Quantum Anomalies: $U_A(1)$ Breaking

Let us now discuss global symmetries of QCD at the quantum level. In the path integral formalism the invariance of the QCD Lagrangian under a global group of transformation $\mathcal{G}$ is not a sufficient condition for $\mathcal{G}$ to be a symmetry of the theory: at the quantum level we have to request the invariance of the generating functional Z_{QCD} respect to the group $\mathcal{G}$. In practice, one just analyze how the measure $\mathcal{D}\bar{q}\mathcal{D}q$ transforms under a generic element of the group $\mathcal{G}$.

In the case of the chiral group $G_\chi = U_V(N_f) \times U_A(N_f)$ it can be shown that the measure is invariant unless one performs an abelian axial transformation of the spinors. In fact, by applying an $U_A(1)$ rotation to quark fields the path integral acquires a phase, which is equivalent to an additional $\mathcal{L}_{an}$

term in the Lagrangian

$$\mathcal{D}\bar{q}\mathcal{D}q \overset{U_A(1)}{\longrightarrow} \mathcal{D}\bar{q}\mathcal{D}q\, e^{iS_{an}}, \tag{2.31}$$

$$S_{an} = 2\Theta_A \int_{R^4} \mathrm{d}^4x \mathcal{L}_{an}(x), \tag{2.32}$$

where Θ_A is the parameter of the axial transformation

$$U_A = e^{-i\gamma_5\Theta_A} = e^{-i[P_R - P_L]\Theta_A}.$$

This is a general result for arbitrary gauge theories involving spin $\frac{1}{2}$ fermions: without entering in details, the structure of the anomalous term $\mathcal{L}_{an}$ can be related to the so-called triangle diagram in fig(2.1), which describes the anomalous interaction as a result of a loop of fermions interacting with a background gauge fields A_μ. In the case of quarks coupled to a chromoelectromagnetic field, the triangle diagram implies

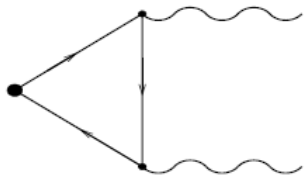

Figure 2.1: Triangle Diagram: Axial current (Big Black Dot) interacting with two external gluons (wavy lines), via a quark loop (straight lines).

$$\mathcal{L}_{an} = \frac{N_f}{16\pi^2}\tilde{G}^{\mu\nu}_a G^a_{\mu\nu} = 2N_f\mathcal{Q}[A_\mu].$$

By applying the Noether theorem to these new "transformation Laws" for the QCD Lagrangian we obtain the following expression for the divergence of the axial current in QCD with massive fermions

$$\partial_\mu A^{\mu,0} = 2i\bar{q}M_q\gamma_5 q + 2N_f\mathcal{Q}[A_\mu], \tag{2.33}$$

where $A^{\mu,0}$ is the iso-singlet axial current: the axial charge is not conserved if $\mathcal{Q}$ does not vanishes.

From a phenomenological point of view, the non vanishing of the axial charge in the chiral limit can be expressed in the following way: if massless quarks propagates in a background gauge field with A_μ whose operator $\mathcal{Q}$ is not vanishing, there is a change in the total chirality (or helicity) of the system Q_A. The amount of chirality change is given by

$$Q_A(T=\infty) - Q_A(T=-\infty) = 2N_f \int_{R^4} \mathrm{d}^4x \mathcal{Q}(x),$$

which implies that the integral of $\mathcal{Q}$ over all space must have an integer value

$$\frac{1}{32\pi^2}\int_{R^4} \mathrm{d}^4x G^{\rho\sigma}\tilde{G}_{\rho\sigma} \equiv \nu \ ; \quad \nu \in Z.$$

The operator $\mathcal{Q}$ is of the same form of the term $\mathcal{L}_\theta$ we have considered in section 2.1, i.e it is a total derivative: we would then expect $\nu = 0$ for every gauge field A_μ. On the other hand in the section 2.5 we will see that ν, to which we will refer as the *topological charge* of the background field A_μ, does not vanish in general due to the non-trivial topological structure of the vacuum.

2.4.1 Abelian Anomaly and CP-odd Polarization of the Vacuum

We conclude this section by discussing the role of gauge configurations A_μ with non-vanishing $\mathcal{Q}$ in CP-violating processes; this effect is related to another realization of the Abelian anomaly, the so-called "electromagnetic anomaly". For simplicity we will consider $N_f = 2$ massless QCD, with only u and d relevant degrees of freedom.

We start by considering QCD coupled to electromagnetic fields

$$\mathcal{L} = \mathcal{L}_{QCD} + \mathcal{L}_{e.m.}; \quad \mathcal{L}_{e.m.} = -\frac{1}{4}F^{\mu\nu}F_{\mu\nu},$$

and perform the following $U_A(1)$ chiral trnasformation to the u and d quarks in the path integral, s.t.

$$u \xrightarrow{U_A(1)} e^{i\gamma_5\Theta}u, \tag{2.34}$$

$$d \xrightarrow{U_A(1)} e^{\pm i\gamma_5\Theta}d. \tag{2.35}$$

If we take the "$-$ sign" in the d transformation, the system is anomaly free in QCD, but in the presence of photons the quark measure acquires an *electromagnetic dependent* phase which is equivalent to an anomalous term, similar to the QCD case

$$\partial_\mu A_0^\mu = -\frac{N_c e^2}{24\pi^2}F_{\mu\nu}\tilde{F}_{\mu\nu}. \tag{2.36}$$

On the other hand, if we take the "$+$ sign" the theory has both a gluonic and photonic anomalous contribution

$$\partial_\mu A_0^\mu = 4\mathcal{Q} - \frac{5}{3}\frac{N_c e^2}{24\pi^2}F_{\mu\nu}\tilde{F}_{\mu\nu}, \tag{2.37}$$

$$F_{\mu\nu}\tilde{F}_{\mu\nu} = \mathbf{E}\cdot\mathbf{B}, \tag{2.38}$$

where **E** and **B** are the electric and magnetic fields.
This relation is crucial in the calculationof CP-od polarization in the vacuum; in fact it can be shown that in the presence of a very intense magnetic field **B**, a system of quarks propagating in a background field with non-trivial topological charge ν is polarized: the external magnetic field induces an electromagnetic current whose amplitude is proportional to the topological charge

$$\mathbf{J} = -2Q\hat{\mathbf{B}},$$

for smaller magnetic fields, this relation is substituted by

$$\mathbf{J} = \frac{N_C}{2\pi^2}\frac{5}{9}\mu_5\mathbf{B},$$

where μ_5 represents the amount of $U_A(1)$ breaking in the system.
This is the so-called chiral magnetic effect [4], and relates the non-vanishing of the operator $\mathcal{Q}$ to the emergence of anomalous CP-odd electromagnetic currents in hadronic system.

We then conclude that the existence of gauge fields with a non-zero "topological charge" breaks the $U_A(1)$ chiral symmetry at the quantum level, and may imply the emergence of CP-violation in hadronic systems.

2.5 The QCD Vacuum

In the previous section we have shown that the operator

$$\mathcal{Q} = \frac{1}{32\pi^2}G_{\mu\nu}\tilde{G}^{\mu\nu},$$

is related to crucial properties of the QCD Lagrangian: we have seen that in the presence of a gauge configurations with non-vanishing $\mathcal{Q}$, the $U_A(1)$ axial symmetry is broken and hadronic systems may be CP-odd polarized by external magnetic field; in addition, we have seen in section 2.1 that Q is related to the possibility of breaking T, P and CP-symmetry in hadronic processes. In this section we will see that $\mathcal{Q}$ is related to the topological structure of the QCD vacuum.
Throughout the rest of the chapter, we will assume a Wick rotation and consider QCD in the Euclidean space[3].

[3]Note that since the operator $\mathcal{Q}$ is a total derivative, and $x_0 = ix_{0,E}$ and $\partial_0 = i\partial_{0,E}$ we obtain the following equivalence

$$\int \mathrm{d}^4x_E\mathcal{Q}_E = -\int \mathrm{d}^4x\mathcal{Q}. \tag{2.39}$$

The classical vacuum of pure gauge QCD can be identified by gauge configurations with vanishing chromoelectromagnetic field

$$G^a_{\mu\nu} = 0. \tag{2.40}$$

In Abelian theories the ground state solution is trivial

$$U(1) \text{ Vacuum:} \quad \longrightarrow \quad A_\mu = 0.$$

On the other hand, in $SU(N)$-gauge theories one can satisfy the non-linear relation in Eq.(2.40) also if $A_\mu \neq 0$; in fact, the chromoelectromagnetic field vanishes also if the gauge field is in the so-called "pure gauge" form[4]

$$A^{'}_{\mu}(x) = -i\big[\partial_\mu U^{'}(x)\big]U^{'\dagger}(x), \tag{2.41}$$

$$G^{'}_{\mu\nu} = 0. \tag{2.42}$$

We immediately notice that in temporal gauge $A^{'}_0(x) = 0$, the vanishing of the chromoelectromagnetic field implies

$$\partial_0 A^{'}_i(x) = 0; \quad i = 1, 2, 3,$$

by setting boundary conditions for the $A^{'}_\mu$ vacuum gauge fields

$$A^{'}(x) \overset{|x|\to\infty}{\longrightarrow} 0, \tag{2.43}$$

$$\Downarrow \tag{2.44}$$

$$U^{'}(x) \overset{|x|\to\infty}{\longrightarrow} I_{3\times 3}, \tag{2.45}$$

we can "compactify" R^3 into S^3: this implies that there is a one-to-one correspondence between the ground states of the theory and S^3 mappings into $SU(N)$.

The mappings of S^3 into $SU(N)$ can be distinguished into so-called *homotopy classes*, which are elements of the third homotopy group[5] $\pi_3\,[SU(N)]$: homotopy classes describe how the $SU(N)$ manifold can be wrapped with tri-spheres $\in S^3$. In the $SU(N)$ case different "wrappings", i.e. different homotopy classes, are labelled by an integer number $\nu \in Z$, due to the fact that

$$\pi_3[SU(3)] = Z,$$

[4]Note that the pure gauge field is intrinsecally non-perturbative, in fact in perturbative notation we have

$$A^{'}_{\mu}(x) = -\frac{i}{g}\big[\partial_\mu U^{'}(x)\big]U^{'\dagger}(x).$$

hence

[5]For a discussion on Lie groups and topology, see A.1.

which implies that we have an infinite number of degenerate vacua classified by an integer number $\nu \in Z$

$$SU(N) \text{ Vacuum:} \quad \longrightarrow \quad |\nu\rangle;\ \nu \in Z.$$

The homotopy class ν of a given vacuum $|\nu\rangle$ can be calculated by means of a topological invariant functional, the Cartan-Maurer integral $\mathcal{J}^3[A^{'}]$

$$\mathcal{J}^3_{SU(N)}[A^{'}] = f^{abc}\varepsilon^{ijk}\int_{S^3} \mathrm{d}^3x[A^{'}_{a,i}A^{'}_{b,j}A^{'}_{c,k}] = 24\pi^2\nu; \qquad \nu \in Z.$$

The Cartan-Maurer integral can be re-casted in a gauge invariant form in terms of the operator $\mathcal{Q}$: in fact, by simple manipulations we obtain

$$\int_{R^4} \mathrm{d}^4x\mathcal{Q}[A] = \frac{1}{24\pi^2}\mathcal{J}^3_{SU(N)}[A] = \nu,$$

which implies that the operator $\mathcal{Q}$ does not vanish in general.

2.5.1 Gauge Invariance of the QCD Vacuum and the θ-term

In the previous section we have seen that the vacuum gauge fields are expressed, by definition, in a "pure gauge" form, that is to say that there always exists a gauge transformation Q_μ that can connect a vacuum $|\nu\rangle$ into a vacuum $|\mu + \nu\rangle$. On the other hand we have also seen that the homotopy class of a gauge field can be obtained by integrating a *gauge invariant* operator — $\mathcal{Q}$ — over all space.

This apparent contraddiction can be solved by defining two different classes of gauge transformation: the first can be called the class of "small" gauge transformation, that comprehend all continuous transformations which leave the homotopy class of the field invariant. The second class is that of "large" gauge transformations: these are all the gauge transformations Q_μ that change the homotopy class of the gauge field. In this section we will discuss the gauge invariant properties of the vacuum under such Q_μ transformations, in section 2.6 we will interpret such transformations with gluonic configurations with finite topological charge.

As we said, large gauge transformations act as operators on the homotopy class ν; in particular, they do not leave the $|\nu\rangle$ vacua invariant

$$Q_\mu|\nu\rangle = |\mu + \nu\rangle.$$

On the other hand, in order for gauge invariance to be a symmetry of hadronic systems, the true vacuum $|VAC\rangle$ must be invariant both under "small" and "large" gauge transformations: this can be achieved if $|VAC\rangle$ is an eigenstate of Q_μ with eigenvalue of unitary modulus $|e^{i\phi(\mu)}| = 1$. If

this is the case, the partition function is left invariant under the action of a generic operator Q_μ, and physical observables are left gauge invariant

$$Q_\mu|VAC\rangle = |VAC'\rangle = e^{i\phi(\mu)}|VAC\rangle, \tag{2.46}$$

$$\Downarrow \tag{2.47}$$

$$Z'_{QCD} = \langle VAC'|VAC'\rangle = \langle VAC|VAC\rangle = Z_{QCD}. \tag{2.48}$$

To obtain such a vacuum it is sufficient to combine the $|\nu\rangle$ vacua in the following way

$$|VAC\rangle| := |\theta\rangle = \sum_\nu e^{i\nu\theta}|\nu\rangle,$$

so that

$$Q_\mu|VAC\rangle = e^{-i\mu\theta}|VAC\rangle.$$

The QCD gauge invariant vacuum is usually called "θ-vacuum" $|\theta\rangle$, since it depends on a free parameter θ, and the partition function can be written in terms of the gauge dependent vacua $|\nu\rangle$ as a sum over homotopy classes

$$Z_{QCD}(\theta) = \sum_\mu \sum_\nu e^{i\theta\nu}\langle\mu|\mu+\nu\rangle. \tag{2.49}$$

A simple interpretation for the action of the operator Q_μ on the degenerate vacua can be given in terms of tunneling configurations, the so-called *instantons*[6]: as we will see in the next section, tunneling events are linked to gauge A^I_μ configurations with non-trivial topology, whose boundary conditions at $T = \pm\infty$ coincide with two degenerate vacua. This implies that A^I_μ must carry a topological charge, $\mathcal{Q}_\mu = \mu$ that is to say

$$\mathcal{Q}_\mu = \exp\left\{ i \int_{R^4} \mathcal{Q}[A^I] = i\mu \right\}; \quad \mu \in Z. \tag{2.50}$$

which implies that $\mathcal{Q}$ represents the topological charge density operator.

We can then rewrite the partition function of QCD as a sum over topological charges ν

$$Z_{QCD} = \sum_\nu \int \mathcal{D}q\mathcal{D}\bar{q}\mathcal{D}A_\mu e^{iS_{QCD}+i\theta\mathcal{Q}_\nu}.$$

This relation motivates the choice of the parameter θ as label for the QCD vacuum; in fact, we can take account of the topological structure of the vacuum by simply adding the CP-violating θ-term of Eq.(2.9) to the QCD Lagrangian

$$\mathcal{L}_\theta = \frac{\theta}{32\pi^2}\tilde{G}^a_{\mu\nu}G^{\mu\nu}_a, \tag{2.51}$$

[6] At higher temperatures we can also have "hoppings" from a vacuum to another, the so-called sphalerons.

in order to reproduce the correct vacuum amplitudes and preserve gauge invariance at the quantum level. Hence the non-trivial topological structure of the vacuum and the requirement of invariance under "large" gauge transformations *imply* that the most general renormalizable Lagrangian is P, T and therefore CP-violating, if $\theta \neq n\pi$, with $n \in Z$.

2.5.2 The Strong-CP Problem

Since θ is a free parameter, we would then expect it to assume any possible value

$$\theta \in [0, \pi].$$

On the other hand, experimental bounds for this parameter obtained from the measurement of the neutron electric dipole moment d_n and Baryon Perturbation Theory calculations [6] tells us that QCD conserves CP symmetry at an extremely precise level

$$d_n < 0.63 \times 10^{-25} e\,\text{cm}, \quad [7] \tag{2.52}$$

$$\simeq 5 \times 10^{-16}\theta \ldots \implies \theta < 10^{-10}. \tag{2.53}$$

This value is unnaturally small and leads to the so-called strong CP Problem. Many solutions have been proposed, but no one has proved conclusive.

The "Zero-Mass" Solution

The Strong-CP Problem could be solved at the quantum level if at least one of the quark masses vanishes, that is to say $\det M_q = 0$. In fact, in section 2.4 we have seen that by performing a $U_A(1)$ chiral transformation in the path integral, the Lagrangian acquires a term proportional to the $\mathcal{Q}$: this implies that a $U_A(1)$ rotation on the quark fields shifts the parameter θ to a different value

$$\theta \xrightarrow{U_A(1)} \theta(\Theta_f^A) = \theta - 2\sum_f \Theta_f^A,$$

where Θ_f^A are the parameters which charachterize the $U_A(1)$ transformations acting on q_f. Such a chiral transformation would obviously also change the mass terms in the fermionic part of the Lagrangian[7]; the change consists in multiplying by a complex phase the quark masses

$$m_f \bar{q}_f q_f \xrightarrow{U_A(1)} e^{-2i\Theta_f^A} m_f \bar{q}_f q_f.$$

[7] We know that the other terms are left unchanged since, in che chiral limit, the Lagrangian is G_χ invariant.

Hence, if there is at least one massless quark $q_{f'}$, we can always choose an axial transformation which leaves invariant the QCD Lagrangian but absorbs the θ-term, that is to say

$$\theta(\Theta^A_{f'}) = 0, \tag{2.54}$$

$$\Downarrow \tag{2.55}$$

$$\Theta^A_{f'} = \tfrac{\theta}{2}. \tag{2.56}$$

This implies that if just one of the quarks is massless, one could completely cancel the effects of θ from the theory: on the other hand, in QCD all the known quark masses range between $m_u \sim 5MeV$ to $m_t \sim 10^2 GeV$.

The axion solution

In the 1977 Peccei and Quinn [8] proved that the introduction of an additional $U_{PQ}(1)$ axial symmetry which is spontaneously broken at some energy scales $\Lambda_{PQ} \sim \frac{1}{f_a}$ would account for a solution of the strong CP problem. In fact a new dynamical variable —the axion— would appear as the Goldstone boson of the broken $U_{PQ}(1)$ symmetry, resulting in an additional term in the QCD Lagrangian, due to axial anomaly,

$$\mathcal{L}_{ax} = \frac{\xi g^2}{64\pi^2 f_a} a(x) \tilde{G}^{\mu\nu}_b G^b_{\mu\nu}.$$

By minimization of the associated effective potential one then finds that the axion is connected to the θ parameter by the following relation

$$\langle a \rangle = -\frac{f_a}{\xi}\,\theta.$$

Hence, θ is controlled by the vacuum expectation value of the axion, which dynamically relaxes to zero for the vacuum energy to be minimized. This would explain why today we observe $\theta \sim 0$. On the other hand at energy scales higher than Λ_{PQ}, θ could have assumed a generic value. So, according to the axion picture, even if today θ has a definitely small value, we can suppose that it was bigger and in general of order 1 at some early time.

Nowadays there is no experimental evidence for the existence of the axion. To account for the present experimental constraints, variations from the original Peccei-Quinn model have been proposed: in the Invisible Axion Model, this particle is supposed to be very light and very weakly interacting [9, 10, 11, 12].

2.6 Tunneling Between Degenerate Vacua

We turn back to the QCD vacuum and analyze the operator Q_μ which represent a transition between two different classical $\nu^{'} - \nu = \mu$ vacua.

As we said, these can be easily identified with non-perturbative vacuum gauge configurations with non-trivial topological charge μ. At very low energies, the only possible transitions are represented by tunneling configurations, which are localized solutions of the imaginary time Equation of Motion (EoM)

$$D_\mu G_{\mu\nu} = \partial_\mu G_{\mu\nu} + [A_\mu, G_{\mu\nu}] = 0.$$

The boundary conditions specify the topological charge of the configuration

$$A_\mu(\mathbf{x}, T = -\infty) \longrightarrow |\nu\rangle,$$

and

$$A_\mu(\mathbf{x}, T = \infty) \longrightarrow |\nu^{'}\rangle,$$

these solutions are the so-called $SU(N)$ *instantons*.
In temporal gauge we can identify the imaginary time Lagrangian with the real time Hamiltonian; hence, tunneling configurations are stationary configurations with minimal energy: this condition, as we will see, makes them good candidates for describing low-energy non-perturbative dynamics in terms of effective degrees of freedom.

We now briefly discuss instantons properties in $SU(N)$ gauge theories. First of all they are (anti)selfdual fields, that is to say

$$G^I_{\mu\nu} = \pm \tilde{G}^I_{\mu\nu}.$$

(Anti)Selfduality of tunneling configurations is a consequence of the instanton being solutions of the imaginary time EoM. This in fact implies that they have to minimize — at least "locally", that is to say within an homotopy class — the Euclidean action

$$S_E = \frac{1}{4g^2} \int_{R^4} \mathrm{d}^4 x_E G^a_{\mu\nu} G_{a,\mu\nu} \tag{2.57}$$

$$= \pm \frac{1}{4g^2} \int_{R^4} \mathrm{d}^4 x_E \left[G^a_{\mu\nu} \tilde{G}_{a,\mu\nu} + (G^a_{\mu\nu} \mp \tilde{G}_{a,\mu\nu})^2 \right], \tag{2.58}$$

since the first term is nothing more than the topological charge of the instanton, we can conclude that within a homotopy class the action is minimized if the second term, which is always positive, vanishes.
It is easy to show that selfdual solutions (instantons) have a positive topological charge, while antiselfdual (antiinstantons) have negative topological charge. This implies that within an homotopy class, the gauge fields with

minimal energy have a finite action proportional to the topological charge ν. This condition implies that their action is finite — localized due to their tunneling nature — and equal to

$$S_E = 8\frac{\pi^2}{g^2}|\nu|.$$

In the next section we will see that, since they are localized configurations with finite action, instanstons can be interpreted as pseudoparticles with proper size, euclidean coordinates, and color orientation. We could in principle rewrite the partition function as an integral over these effective degrees of freedom and integrate-out all the other gluonic degrees of freedom, which can be intepreted as quantum fluctuations around these classical solutions. On the other hand it is simple to show that not all instantons give the same contribution to the path interal; this can be seen by calculating the tunneling rate, which gives an estimate of the probability of finding an instanton in a volume V_4: at tree level in pure gauge QCD this is given by

$$P[\nu] = V_4 e^{-|\nu|8\frac{\pi^2}{g^2}},$$

which implies that instantons with big topological charge are exponentially suppressed. Calculations at one-loop in pure gauge QCD, the introduction of quarks and thermal fluctuations can change the tunneling rate: we will not discuss this results in details, but results show that configuration with high topological charge are still exponentially suppressed.
We can then rewrite the partition function in Eq. (2.5.1) as

$$Z_{QCD}(\theta) = \sum_{\mu}[e^{i\theta}\langle\mu|\mu+1\rangle + e^{-i\theta}\langle\mu|\mu-1\rangle], \tag{2.59}$$

that is to say a tunneling from two vacua separated by a topological charge $\mu \neq 1$ can be effectively described in terms of a series of a number μ of single tunnelings: we can effectively describe the QCD vacuum in terms of a $\nu = \pm 1$-instantons ensemble.

In the next section we present the analytical expression for these two (anti)selfdual fields.

2.7 BPST Instantons

In this section we present the tunnelings solutions with total topological charge $\nu = \pm 1$. From now on we will refer to these as (anti)instantons.

As we said, (anti)instantons are solutions of the Euclidean EoM

$$\frac{\delta S_E[A^I]}{\delta A_\mu} = D_\mu[A^I]G^I_{\mu\nu} = 0,$$

this implies that they are a family of gauge configurations parametrized by $4N_c$ collective coordinates. These collective coordinates reflects the symmetries of the classical Lagrangian:

- Traslational invariance: 4 collective coordinates, x^I_μ.
  They represent the instanton coordinate in spacetime;

- Scale invariance: 1 collective coordinate, ρ^I.
  It represents the size of the instanton.

- Gauge invariance: $4N_c - 5$ in $SU(N_c)$, $U(\mathbf{\Delta}^I) = exp(i\frac{\lambda^a a}{2}\Delta^I_a)$.
  They represents the instanton orientation in color space.

The instanton solutions with topological charge $\nu = 1$ are usually expressed in two forms: the so-called *regular gauge instanton* [13]

$$A_\mu(x; x^I, \rho^I, \Delta^I) = U(\Delta^I)\tau^a U^\dagger(\Delta^I)\eta^a{}_{\mu\nu}\frac{(x-x^I)_\nu}{(x-x^I)^2+\rho_I^2},$$

or *singular gauge instanton*

$$A_\mu(x; x^I, \rho^I, \Delta^I) = U(\Delta^I)\tau^a U^\dagger(\Delta^I)\bar{\eta}^a{}_{\mu\nu}\frac{\rho_I^2}{(x-x^I)^2}\frac{(x-x^I)_\nu}{(x-x^I)^2+\rho_I^2}.$$

The (anti)selfdual properties of the instanton are reflected by the 't Hooft coefficient, which mix color and lorentz indices

$$\eta_{a\mu\nu} = \varepsilon_{a\mu\nu} + \delta_{a\mu}\delta_{\nu 4} - \delta_{a\nu}\delta_{\mu 4}, \tag{2.60}$$

$$\bar{\eta}_{a\mu\nu} = \varepsilon_{a\mu\nu} - \delta_{a\mu}\delta_{\nu 4} + \delta_{a\nu}\delta_{\mu 4} \quad a = 1, 2, 3. \tag{2.61}$$

The antiinstanton solutions with topological charge $\nu = -1$ are obtained by changing

$$\eta \leftrightarrow \bar{\eta},$$

in the instanton solution.
Regular and singular gauge instantons are both in the Landau gauge $\partial_\mu A_\mu = 0$, but in the former case the topological charge is localized at infinity while, in the latter is localized at the center of the instanton.

Note that the $SU(N)$ instanton solutions are just "embedding" of the $SU(2)$ solutions, in fact τ^a in Eq.s (2.7) and (2.7) are the Pauli matrices: that is to say that by applying a generic $SU(N)$ color rotation to the $SU(2)$ instanton solution constructed in the 2×2 minor of an $N_c \times N_c$ color matrix, we get the more general instanton solution in $SU(N)$.
Note also that by construction, the instanton action — i.e. topological

charge density — is localized, and depends only on the instanton size parameter ρ; this can be easily seen by evaluating the chromomagnetic field: in the singular gauge one finds

$$G^{s,a}_{\mu\nu}(x;x^I,\rho,\Delta) = -4U(\Delta^I)\tau^a U^\dagger(\Delta^I)\eta^a_{\mu\nu}\frac{\rho^2}{[(x-x^I)^2+\rho^2]^2}, \tag{2.62}$$

which implies that the action density is equal to

$$\mathcal{S}^s = \frac{1}{4g^2}\mathcal{Q}^s = \frac{1}{4g^2}G^{s,a}_{\mu\nu}G^s_{a,\mu\nu} = \frac{48}{g^2}\frac{\rho^4}{[(x-x^I)^2+\rho^2]^4}. \tag{2.63}$$

Fluctuation Operator and Bosonic Zero Modes

Another property of instanton solutions is that to every collective coordinate one can assign a bosonic zero-mode, that is to say a solution of the so-called "fluctuation operator" with zero eigenvalue. In chapter 5 we will see the importance of the existence of these zero-modes and we will give a geometric interpretation of their properties.

The fluctuation operator $\mathcal{F}_{\mu\nu}[A]$ is built by functionally differentiating twice the action with respect to the gluon fields

$$\mathcal{F}_{\mu\nu}[A] = \frac{\delta^2 S_E[A]}{\delta A_\mu \delta A_\nu},$$

and gets his name from its role in one loop calculations of instanton tunneling rate: if we taylor expand the action around a given gauge field $\bar{A}_\mu$ we obtain

$$S[A_\mu] = S[\bar{A}_\mu] + \frac{\delta S[\bar{A}_\mu]}{\delta A_\mu}A_\mu + A_\mu\mathcal{F}_{\mu\nu}[\bar{A}]A_\nu + O(A^2), \tag{2.64}$$

which implies that $\mathcal{F}$ rules the gaussian "gauge field fluctuations" around $\bar{A}_\mu$. If $\bar{A}_\mu$ is a solution of the EoM — i.e. an $|\nu| = 1$ instanton — one can easily show that the fluctuation operator has one eigenstate with eigenvalue "0" for each instanton collective coordinate, in fact

$$0 = \partial_\gamma\left\{\frac{\delta S_E[A^I]}{\delta A_\mu}\right\} = \frac{\delta^2 S_E[A^I]}{\delta A_\mu \delta A_\nu}\partial_\gamma A^I_\nu = \mathcal{F}_{\mu\nu}[A^I]\{\partial_\gamma A^I_\nu\}.$$

These zero-mode eigenstates are called "bosonic zero-mode" of instantons.

The expansion in Eq.(2.64) can be used to evaluate the instanton tunneling rate at one loop, by integrating the partition function over $\mathcal{F}$ dependent gaussian fluctuations in a perturbative way. The leading order result due to 't Hooft [14] is given by

$$P_I \propto \frac{\mathrm{d}\rho}{\rho^5}\rho^{\frac{11}{3}N_C}.$$

This expression shows that small sized instantons are suppressed. On the other hand, the same equation implies that infinitely large instantons are dominant: this infrared divergence implies that semi-classical treatment cannot be applied in instanton calculations, we will turn back to this problem in section 2.9.

2.8 Topology and Light Fermions

In this section we discuss how topological configurations, in particular instantons, provide a link between the anomalous breaking of axial symmetry and the spontaneous breaking of chiral symmetry.

2.8.1 Index Theorem: Microscopic Dynamics of Axial $U_A(1)$ Breaking

One of the most important properties of (anti)instantons is that the Dirac operator calculated in such a background field has a zero-mode with definite (right)left-handed chirality, where by zero-modes we intend eigenstates of the Dirac equation[8] with vanishing eigenvalue. In singular gauge we have

$$i\gamma_\mu D_\mu \psi^0 = 0, \tag{2.65}$$

$$\psi^0[A^I] = \frac{\rho}{\pi}\frac{1}{[(x-x^I)^2+\rho^2]^{\frac{3}{2}}}\frac{\gamma_\mu x_\mu}{|x-x^I|}P_{R(L)}u, \tag{2.66}$$

where u is a constant spinor in which color and spinor indices are coupled. The importance of such modes is related to the Index Theorem, which states that: *the difference of the number n_L left-handed and n_R right-handed zero-modes of fermions in a background field, is equivalent to the topological carge ν of the field*

$$\nu = n_L - n_R$$

This will be proved in the end of the section.

We start our discussion by showing that only eigenstate with vanishing eigenvalue have definite chirality. In fact, due to the properties of Euclidean γ_μ matrices we have

$$\{i\gamma_\mu D_\mu, \gamma_5\} = 0,$$

that is to say that there always exists an eigenstate of eigenvalue $-\lambda \neq 0$ for every eigenstate with eigenvalue $\lambda \neq 0$

$$i\gamma_\mu D_\mu \psi^l = \lambda_l \psi^l \quad \Longrightarrow \quad i\gamma_\mu D_\mu(\gamma_5\psi^l) = -\lambda_l(\gamma_5\psi^l). \tag{2.67}$$

[8] We recall that the discussion considers QCD in the Euclidean and not Minkowskian space: the Dirac operator is Hermitian in the Euclidean.

This implies that the eigenstates of the Dirac operator with non-vanishing eigenvalue do not have a definite chirality

$$i\gamma_\mu D_\mu[(1 \pm \gamma_5)\psi^l] = (1 \mp \gamma_5)\lambda_l \psi^l, \tag{2.68}$$

$$\Downarrow \tag{2.69}$$

$$i\gamma_\mu D_\mu \psi^l_{R/L} = \lambda_l \psi^l_{L/R}, \tag{2.70}$$

$$\Downarrow \tag{2.71}$$

$$i\gamma_\mu D_\mu \psi^n_{R/L} = \lambda^n \psi^n_{R/L} \quad \Leftrightarrow \quad \lambda^n = 0, \tag{2.72}$$

that is to say, that eigenstates with definite parity must have vanishing eigenvalue.

We now show that if the Dirac operator is calculated in an selfdual gauge field background, the chirality of the zero-mode is left-handed. In fact, consider the following equation

$$(iD_\mu\gamma_\mu)^2[\psi^0_L + \psi^0_R] = (-D^2 + \frac{1}{2}\sigma_{\mu\nu}G^{\mu\nu})[\psi^0_L + \psi^0_R] = 0, \tag{2.73}$$

where we have used the matrix

$$\sigma_{\mu\nu} = \frac{i}{2}[\gamma_\mu, \gamma_\nu].$$

Since $G_\mu\nu$ is selfdual one obtains the following equality

$$\sigma^{\mu\nu}G^{\mu\nu} = -\gamma_5\sigma_{\mu\nu}G_{\mu\nu},$$

which implies

$$\sigma^{\mu\nu}G^{\mu\nu} = \sigma_{\mu\nu}G_{\mu\nu}P_L,$$

so that we can separate Eq.(2.73) into

$$(-D^2 + \tfrac{1}{2}\sigma_{\mu\nu}G^{\mu\nu})\psi^0_L = 0, \tag{2.74}$$

$$-D^2\psi^0_R = 0, \tag{2.75}$$

but since $-D^2$ is a positive definite operator, it means that the second condition is fulfilled only if $\psi^0_R = 0$: if we considered an antiselfdual field we would have obtained ψ^0_L.
Notice that this result is independent on the flavor of the fermion, this means that to every (anti)instanton we can associate N_f (right)left-handed zero-modes.

As we have seen, the zero-mode in the background of an (anti)selffual field must be (right)left-handed. We now prove that this condition has

crucial consequences on the breaking of $U_A(1)$ axial symmetry.
Consider the axial singlet current of massless quarks

$$A^0_\mu = \sum_f \bar{q}_f i\gamma_\mu\gamma_5 q_f,$$

the change in axial charge in a system of quarks propagating in a generic background field $\bar{A}_\mu$ is given by

$$\Delta Q_A = Q_A(T=\infty) - Q_A(T=-\infty) = \int_{R^4} \mathrm{d}^4x \partial_\mu A^0_\mu,$$

which due to the relation

$$\partial_\mu A^0_\mu = \sum_f [\bar{q}_f i\gamma_\mu\gamma_5 q_f] = \sum_f \sum_n \lambda_n [\bar{\psi}_{f,n} i\gamma_5 \psi_{f,n}], \tag{2.76}$$

can be expressed in terms of the fermion propagator

$$S[x,y] = -\langle x|\frac{1}{i\gamma_\mu D_\mu}|y\rangle = \sum_n \frac{\psi_n\psi_n^\dagger}{\lambda_n}, \tag{2.77}$$

$$\Delta Q_A = -2N_f \sum_n \int_{R^4} \mathrm{d}^4x \mathrm{Tr}[\lambda_n \frac{\psi_n^\dagger\gamma_5\psi_n}{\lambda_n}], \tag{2.78}$$

where λ_n and ψ_n are the eigenvalues and eigenfuntions of the Dirac operator in the background field.
Since Eq.(2.73) implies that $\gamma_5\psi_n$ and ψ_n are different eigenstates, hence they must be orthonormal, the only surviving terms in the sum are those with vanishing eigenvalue, which implies that

$$\Delta Q_A = -2N_f \sum_k \int_{R^4} \mathrm{d}^4x \mathrm{Tr}[\psi_0^\dagger(P_r - P_l)\psi_0] \tag{2.79}$$

$$= 2N_f(n_L - n_R), \tag{2.80}$$

where the last equivalence is given by the fact that we have chosen an orthonormal basis.

Since we know from section 2.4 that the change in axial charge is proportional to the total topological charge of the vackground field

$$\Delta Q_A = 2N_f\nu \tag{2.81}$$

We can then conclude that the difference between left-handed and right-handed fermionic zero-modes is equivalent to the topological charge of the background field in which the fermions propagate.

$$n_L - n_R = \nu.$$

This result is the so-called Atiyah-Singer Index Theorem [15].

We now return to the Minkowski space and recall that due to the Eq.(2.39) the result of Eq.(2.81) should be rewritten as

$$Q_A(T=\infty) - Q_A(T=-\infty) = -2N_f\nu.$$

We can then give a phenomenological description of the anomalous breaking of $U_A(1)$ symmetry in terms of fundamental degrees of freedom.
A quark propagating in a background gauge field with non-trivial topology, e.g. instantons and antiinstantons, can change its chirality by a modification of its zero-mode spectrum, that is to say that when a system of quarks propagates through a background with $\nu = (-)1$ topological charge N_f zero-mode state with (right)left-handed chirality are created and N_f zero-mode with (left)right-handed chirality are destroyed. This result in an effective flipping of the chirality of quarks.

2.8.2 Bank-Casher Relation

As we have seen, in the previous section, the presence of topological structures such as (anti)instantons is related to the existence of fermionic zero-modes and hence the breaking of $U_A(1)$ axial symmetry. We now show that the SChSB in the QCD vacuum has a similar explanation in terms of quarks propagating in an instanton backgrouns.

First of all we start our discussion by showing that the parameter related to the spontaneous breaking of axial symmetry in the vacuum is the quark condensate

$$\sum_f \frac{\partial}{\partial m_f} Z_{QCD} = \langle \bar{q}_f q_f \rangle = -230(MeV)^3.$$

In fact, by simple manipulations we can show that if $\langle \bar{q}q \rangle$ does not vanish, there is a set of operators Q_A^a, generators of $U_A(N_f)$, which do not annihilate the vacuum

$$\begin{aligned} 0 \neq \langle \bar{q}_f q_f \rangle &= -\frac{3}{2}\langle [Q_A^a, \bar{q}\gamma_5\lambda_a q] \rangle, && (2.82)\\ &\Downarrow && (2.83)\\ Q_A^a|\theta\rangle &\neq 0, && (2.84) \end{aligned}$$

where Q_A^a are the axial charges, which are also a representation of the generators of $U_A(N_f)$. Hence chiral symmetry is spontaneously broken to $U_V(N_f)$, if the quark condensate does not vanish.

If chiral symmetry is spontaneously broken in the vacuum, we know from the goldstone theorem that there must be a set of goldstone bosons with the

same quantum number of the generators of the broken symmetries. We will discuss the property of such pseudoscalar bosons in chapter 3, what we are interested in right now is that these are the result of the non-conservation of axial currents

$$A^a_\mu = \bar{q}_R \gamma_\mu \gamma_5 \frac{\lambda^a}{2} q_R - \bar{q}_L \gamma_\mu \gamma_5 \frac{\lambda^a}{2} q_L, \tag{2.85}$$

in the vacuum. As we have seen in the last section, a quark can change its chirality when propagating through a backgorund gauge field with non-trivial topology, we would then expect that if quarks propagates through a vacuum permeated by an ensemble of such background fields, e.g. instantons and antiinstantons, they would keep on changing their chirality, and $SU_A(N_f)$ would be effectively broken.

These considerations can be expressed in mathematical form: if we calculate the quark condensate in terms of eigenstates and eigenvalues of the Dirac operator as in the previous section, but now for massive quarks

$$\langle \bar{q}q \rangle = -i \sum_n \frac{1}{\lambda_n + im} = \ldots = -\int_0^\infty \mathrm{d}\lambda \mathfrak{d}(\lambda) \frac{2m}{m^2 + \lambda^2},$$

we obtain a result which relates it to the density of eigenvalues $\mathfrak{d}(\lambda)$. Without entering in details, by considering the system as infinite and by taking the chiral limit the former equation results in

$$\langle \bar{q}q \rangle = -\pi \mathfrak{d}(\lambda = 0).$$

This is the so-called Bank-Casher relation [16], and can be conidered as a "generalization of the index theorem".

The calculation of $\mathfrak{d}(\lambda = 0)$ requires an ab-initio non-perturbative calculation of the quark condensate.

2.9 Instanton Models

In the previous section we have shown that both the anomalous breaking of the $U_A(1)$ symmetry and the spontaneous breaking of chiral symmetry are related to the topological properties of the vacuum.
Based on such an observation, a large effort has been put towards investigating the role of instantons in various processes, see e.g. [17] [18] [19]. In the impossibility of performing rigorous semi-classical calculations, these studies have relied on phenomenological description of the properties of the instanton ensemble, i.e. on instanton models. see [20] and references therein.

In such approaches instantons are treated as pseudo-particles with charachteristic position, size, and color orientations: the so-called collective coordinates. By defining a generic family of topological configurations as, for example[9]

$$\tilde{A}^N_\mu(x;\gamma) = \sum_{i=0}^{N} A^I_\mu(a;\hat{\gamma}_i) + \sum_{i=0}^{N} A^{\bar{I}}_\mu(a;\hat{\gamma}_i),$$

where I stands for instantons and $\bar{I}$ stands for antiinstantons and

$$\hat{\gamma}_i = (x^I_{\nu,i}, \rho_i, \mathbf{\Delta}_i),$$

is the set of collective coordinates of the i-th (anti)-instantons, one can rigorously parametrize the QCD partition function in terms of γ, which represent a set of effective low-energy degrees of freedom: all other infinite degrees of freedom are explicitly integrated out from the path integral[10]

$$\begin{aligned} Z_{QCD} \;=\; & \sum_{N_+=0}^{\infty}\sum_{N_-=0}^{\infty}\int \prod_{i^+=0}^{N_+}(\mathrm{d}\hat{\gamma}_{i^+}) \prod_{i^-=0}^{N_-}(\mathrm{d}\hat{\gamma}_{i^-}) \times \\ & \times e^{i\theta[i^+-i^-]} e^{-\frac{8}{\pi^2}g^2[i^++i^-]} \times G\left\{\hat{\gamma}_{i^+},\hat{\gamma}_{i^-},\det[i\gamma_\mu \hat{D}^{i^+,i^-}_\mu + m_f]\right\}. \end{aligned} \tag{2.86}$$

The parameters in the path integral are defined as

- $N^{+/-}$ is the number of instantons/antiinstantons;
- the function $G(\hat{\gamma})$ is formally obtained by integrating over all gluonic degrees of freedom B^μ which are not topological: we will discuss this fucntion in much more details in the chapter 5. Note that $-\log[G(\hat{\gamma})]$ can be interpreted as an effective instanton interaction;
- $\det[i\gamma_\mu \hat{D}_\mu + m_f]$ is the determinant one obtains after the grassman integration of quarks in the path integral;
- the covariant derivative is to be intended as

$$\hat{i}D^{i^+,i^-}_\mu = i\partial_\mu + \sum_{j=0}^{i^+} A^I_\mu[\hat{\gamma}_j] + \sum_{j=0}^{i^+} A^{\bar{I}}_\mu[\hat{\gamma}_j] + \tilde{B}_\mu.$$

Once the form of the $G(\hat{\gamma})$ has ben specified, Eq.(2.86) allows to evaluate approximatively matrix elements by computing statistical averages over the instanton ensemble. This statistical average is expressed by a set of ordinary integrals over collective coordinates γ, and not by an infinite dimensional

[9] This is the so-called *sum ansatz*, for other realizations see [20].

[10] As we seen in section 2.6 omitting the contribution of gauge configuration with topological charge bigger than $|\nu| = 1$ is a very good approximation.

integral.

The partition function in Eq. (2.86), on the other hand, cannot be even approximately calculated using perturbative methods such as semi-classical expansion because of the infrared divergence that we discssed in section 2.7. If the instanton vacuum is sufficiently dilute, on the other hand, we can rewrite $G(\gamma)$ as a sum of $n-$body correlation functions

$$G(\gamma_1, \ldots, \gamma_n) = \sum_i G_1(\gamma_i) + \sum_{i<j} G_2(\gamma_i, \gamma_j) + \ldots,$$

that can be set by phenomenological considerations.
Shuryak and Diakonov [20] proposed the following choice of phenomenological parameters: for G_1 an average (anti)instanton size

$$\bar{\rho} = 0.3fm,$$

and a low average density

$$\bar{n}_{I/\bar{I}} = 1fm^{-4},$$

Short range interaction, i.e. G_2, can be chosen to be constant (random instanton liquid model), or repulsive (interacting instanton liquid model).

This is a crude approximation, nonetheless it is possible to obtain phenomenologically interesting results for the quark condensate in Instanton Models: the density of eigenvalues of the Dirac operator is non-vanishing at zero-temperatures, which implies that chiral symmetry is spontaneously broken down to $U_V(3)$ at low-energy; at high temperature T, chiral symmetry is restored [21].

In chapter 5 we tackle the problem of performing a rigorous and model independent calculation of the term $G(\bar{\gamma})$ using Lattice QCD simulations.

Chapter 3

Non-Perturbative Methods in QCD

In this chapter we present two approaches which enable to perform ab-initio calculations in non-perturbative QCD: Chiral Perturbation Theory and lattice gauge theories, such as lattice QCD.

ChPT is a rigorous Effective Field Theory (EFT) which enables to obtain exact results for low-energy amplitudes up to corrections $O(\frac{\mu}{\Lambda_{SChSB}})$, where μ represents the energy scale of the process under considerations, and $\Lambda_{SChSB} \simeq 1GeV$ is a characteristic scale which separates low-energy and high-energy dynamics in QCD.

LQCD is a gauge invariant regularization of QCD based on the discretization of the Euclidian space-time. The analytic continuation to imaginary time makes such a formulation of the theory amenable to Monte Carlo simulations. This way it is possible to obtain in principle exact numerical calculation of the properties of the hadronic spectrum, and to obtain ab-initio results of matrix elements for any operator in terms of the fundamental quark and gluonic degrees of freedom.

3.1 Chiral Perturbation Theory

The aim of ChPT is constructing a theory which enables to calculate non-perturbative Green's functions in the low-energy limit of a fundamental theory, with a perturbative expansion in momenta rather than coupling constants: this makes it possible to use Feynman diagram formalism to obtain ab-initio information on non-perturbative processes. The relevant degrees of freedom of such a theory are the lightest particles of the spectrum and their interaction mimic — and are dictated by — the interactions of the fundamental degrees of freedom.

3.1.1 Weinberg's Theorem

Effective Field Theories provide a general and rigorous formalism to describe the low-energy dynamics of arbitrary fundamental theories with a gap in energy momentum scale. In QED, for example, the electron mass provides a natural scale and low-energy dynamics can be described by effective photon-photon interactions, see chapter 4.

In QCD the gap is $\Lambda_{SChSB} \simeq 1GeV$, and the low-energy QCD dynamics can be described by the Goldstone bosons of the spontaneous breaking of chiral symmetry, $U(\varphi_a(x))$. The scale of the symmetry breaking Λ_{SChSB} is then the natural threshold for the low-energy QCD dynamics, since a process at energies higher than Λ_{SChSB} would involves other degrees of freedom. We now introduce the EFT fomalism.

EFT foundation is a theorem by Weinberg [22]:
We can reproduce the low-energy dynamics of a fundamental theory, by constructing the most general effective Lagrangian $\mathcal{L}_{EFT}$ containing all possible terms compatible with the global simmetries $\mathcal{G}_i$ of a given fundamental theory. To every global symmetry $\mathcal{G}_i$ of the fundamental theory, will correspond a local symmetry $\mathcal{G}_i(\xi)$ of $\mathcal{L}_{EFT}$. If this construction is consistent with QFT principles (unitarity, causality...), the S-matrix (and hence the correlation functions) of such a theory will exactly reproduce that of the fundamental theory.

In the case of QCD we can then expect to describe low-energy dynamics with a Lagrangian $\mathcal{L}_{ChPT}$ which is a function of the pseudoscalar mesons $U(\varphi_a(x))$ and contains all terms compatibles with chiral symmetry. All non-perturbative high-energy processes (small distances interaction, massive particle exchange, resonances, etc..) will be taken into account in the coupling constant of local-interaction terms —not renormalizable in general—. Each of those information which was manifest in the fundamental theory is now contained in the coupling constant of the interaction terms in $\mathcal{L}_{EFT}$: this will be true also for the topological properties of the vacuum.

Power Counting: Perturbative Expansion in Momenta.

Such a Lagrangian $\mathcal{L}_{ChPT}$ contains an infinite number of terms. In fact, if a term $U^\dagger \Box U$ is allowed by symmetry, we also have to include all other terms $U^\dagger \Box^n U$ with $n = 1, 2, 3...$ In order to retain predictive power, Weinberg outlined a procedure which enables to consider only a finite numeber of terms in the effective Lagrangian. This procedure [22] consists in the so-called "power counting scheme": by assigning to every parameter in the Lagrangian (the fields and their derivatives, the external sources, the masses, etc..) a weight

α in terms of powers of momenta, we can organize the EFT Lagrangian as a sum of $\mathcal{L}^{(\alpha)}$ terms with the same order $O(p^\alpha)$. The meaning of this procedure resides in the fact that terms with a high number of, for example, derivatives should give a small contribution to *any* amplitude: they describe the exchange of a large number of momenta —and hence energy— and these processes are suppressed in the low-energy approximation because they are statistically unlikely to happen. The Lagrangian should then be ordered as a sum of terms $\mathcal{L}^{(n)}_{EFT}$ whose contribution is suppressed by a factor $\left(\frac{p}{\Lambda_{EFT}}\right)^n$.

"Power Counting" also implies that the generating functional has a natural perturbative expansion in terms of powers of momenta: it is possible to assign an order $O(p^\alpha)$ also to the Feynman diagrams which contribute to a given process. Without entering in details, the general formula for the effective dimension D of a diagram is

$$D = 2L + 2 + \sum_d (d-2)N_d,$$

where N_d are the number of vertices at order $O(p^d)$, and L is the number of loops of the diagrams.

The expectation value of the operator at a given order is then obtained by summing all possible diagram which contribute at that order: at the lowest $O(p^D)$ order D=2 one should consider only tree level diagram built with vertices of $\mathcal{L}^{(2)}$; at D=4 all tree level diagrams built with one vertex from $\mathcal{L}^{(4)}$ and one-loop diagram with vertices of $\mathcal{L}^{(2)}$; at D=6, one needs to include all tree diagram with one vertex of $\mathcal{L}^{(6)}$, one-loop diagram with one vertex from $\mathcal{L}^{(4)}$, a tree diagram with two vertices from $\mathcal{L}^{(4)}$, or a two-loop diagram with vertices from $\mathcal{L}^{(2)}$; and so on. According to this procedure, even if the terms in the Lagrangian are not renormalizable, every amplitude will be finite. In fact the terms at order $O(p^n)$ behave like counterterms for the terms at order $O(p^{n-2})$.

Our main goal in the following sections will then consist in determining the ChPT Lagrangian at the lowest chiral order which allows us to evaluate perturbatively amplitudes in the hadronic sector for CP violating processes. Such a Lagrangian will have to reproduce the anomalous properties of the QCD partition function and will have to take into account the topological properties of the QCD vacuum.

We now analyze the low-energy hadronic spectrum, in order to motivate the choice of pseudoscalar mesons, as relevant low-energy degrees of freedom in QCD.

3.1.2 Chiral Symmetry and the Hadronic Spectrum

In order to analyze the low-energy hadronic spectrum, we have to recall the its properties are directly inherited by the symmetries of the QCD Lagrangian:

1) at the classical level, the QCD Lagrangian is invariant under a global $U_V(N_f) \times U_A(N_F)$ in the limit $m_f \to 0$;

2) in the physical case of massive quarks, we have an exact $U_V(1)$ symmetry and $\mathcal{L}_{QCD}$ is almost — perfectly — invariant under chiral $U_V(3)$ — $U_V(2)$ — transformations;

3) at the quantum level $U_A(1)$ is broken by the existence of configurations with non-trivial topology;

4) $U_V(N_f) \times SU_A(N_F)$ is dynamically broken down to $U_V(N_f)$ due to the non-vanishing of chiral condensate.

The hadronic spectrum has then the following properties.

Baryon Number Conservation

$U_V(1)$ is related to the baryon number conservation; quarks and antiquarks are assigned the baryon numbers $B = \frac{1}{3}$ and $B = -\frac{1}{3}$ respectively: depending on the quark content of the excitations, the hadronic spectrum devides into mesons $B = 0$ and baryons $B = 1$.

Degenerate Multiplets

$SU_V(N_f)$ invariance implies that baryons and mesons are organized along irreducible representation of $U_V(N_f)$. For $N_f = 2$, the degeneracy is almost perfect: e.g. the neutron and the proton are in the **2** representation of $SU_V(N_f = 2)$ and have almost degenerate mass

$$m_n - m_p \simeq 1.3 MeV;$$

Missing Parity Partners

$U_A(N_f)$ axial transformations would mix states with different P-parity, and if they were symmetries of the QCD vacuum we would also expect a mass degeneracy between parity partners, but such a degeneracy is not present: for example both vector ρ and axial a_1 meson, and the neutron and N^* have a mass gap of $\simeq 0.5 GeV$

$$m_{a_1} - m_\rho \simeq (1260 - 770) MeV = 510 MeV, \tag{3.1}$$
$$m_{N^*} - m_n \simeq (1535 - 940) MeV = 595 MeV. \tag{3.2}$$

SChSB and Goldstone Theorem

At energy scales below $\Lambda_{SChSB} \simeq 1GeV$ chiral symmetry is spontaneously broken: the parameter ruling this phase transition is the quark condensate $\langle \bar{q}_f q_f \rangle$. The non-vanishing of $\langle \bar{q}_f q_f \rangle$ implies the existence of a set of operators Q^a, generators of the broken symmetry, which do not annihilate the vacuum.
The Goldstone theroem states that these generators are promoted to dynamical fields. At the quantum level, the QCD Lagrangian is approximately invariant under $SU_A(3)$ chiral transformations, we would expect to find an octet of almost degenerate pseudoscalar mesons. These mesons would have the same quantum number of the generators of the broken symmetry, and masses proportional to the symmetry breaking paramters, i.e. the quark masses and the chiral condensate. Their masses would then be much lower than the masses of other hadrons.
Such an octet is observed in the hadronic spectrum: particles are displayed

Quantum Numbers	$Q=-1$	$Q=0$	$Q=1$
$S=-1$	K^- (493.7)	$\bar{K}^0$ (497.7)	—
$S=0$	π^- (139.6)	π^0 (135); η (547.8)	π^+ (139.6)
$S=1$	—	K^0 (497.7)	K^+ (493.7)

Table 3.1: Quantum numbers and Masses (in MeV) of the mesons' octet: S=Strangeness; Q=Electric Charge.

in table (3.1). The mass gap of these particle respect to the other hadrons — $m_\rho \simeq 770MeV$, $m_n \simeq 1GeV$ — is of the order of $\sim 0.5GeV$.
In addition, since the QCD Lagrangian is *almost perfectly invariant* to $SU_A(2)$ chiral transformations we would expect to find a triplet, within this octet, of almost perfectly degenerate pseudoscalar mesons. Such a triplet is present, and is given by the pions

$$\pi^-(139.6MeV)\ ; \qquad \pi^0(135MeV)\ ; \qquad \pi^+(139.6MeV).$$

At very low-energy, the strange degrees of freedom are somehow "freezed" so we might exclude all the kaons.

The $U_A(1)$ Symmetry in the Large N_c Limit

We have seen in section 2.4 that the iso-singlet axial current is not cunserved in the chiral limit, because axial symmetry is broken in the background of a configuration of non-trivial topological charge.
A quantitative analysis for $U_A(1)$ as an approximate symmetry, on the other hand, can be performed in the so-called *large N_C limit*.

In 1974, 't Hooft [23] introduced the notion of large N_c analysis of gauge theories. The idea consists in expanding correlation functions in power of the inverse of the number of colors $\frac{1}{N_c}$. He showed that in the large N_c limit quark loops are suppressed. Witten demonstrated [24] that in the large N_C limit the quantum chiral anomaly vanishes, and hence the axial symmetry is conserved in both the chiral and large N_C limit. That is to say that the limit

$$m_q \to 0 \quad \wedge \quad N_C \to \infty,$$

the axial symmetry can be considered an approximate symmetry of the QCD Lagrangian. Since this symmetry is not reproduced in the hadronic spectrum (SChSB), we can define a new Goldstone boson:

$$\eta^{'}(957.6MeV); \quad \mathrm{S} = \mathrm{Q} = 0,$$

whose mass is $\simeq 0.5GeV$ greater than the masses of the other goldstone bosons.

All these considerations about the $\eta^{'}$ meson are important for the low-energy theory we want to build, because they tell us that its presence in the low-energy effective Lagrangian is crucial in order to reproduce the properties of the QCD vacuum: it is strictly related to the axial anomaly and hence to the dynamics of topological configurations. In addition, even if this field is more massive than the other mesons and quite equal to Λ_{ChSB}, Pich et al.[25, 26] also showed that with the introduction of $\eta^{'}$ the convergence of amplitudes in ChPT is improved.

From now on we will then consider $\eta^{'}$ as a member of the *low-energy hadornic spectrum.*

Non-Linear Representation of SChSB Goldstone Bosons

The Goldstone theorem implies that the golstone boson fields are elements of the adjoint representation of $U_A(N_f)$ and can be casted in a compact non-linear form

$$U\left(\varphi_a(x)\right) \;=\; e^{\frac{i}{F}\lambda_a\varphi^a(x)},$$

with F a parameter which will be set in the ChPT formalism. In our discussion we will restrict to $N_f = 2$, so we just present the unitary representation of the low-energy degrees of freedom in terms of pions and $\eta^{'}$, which we will

call η from now on for simplicity[1]

$$\pi_0 = \phi_3 \ ; \ \ \pi^{\mp} = \frac{1}{\sqrt{2}}\left(\varphi^1 \pm i\varphi^2\right) \ ; \ \ \eta = \phi_0, \tag{3.3}$$

$$U(\phi_a) = \exp\left\{\frac{1}{\sqrt{2}}\tau^a\varphi_a = \begin{pmatrix} \frac{1}{\sqrt{2}}\pi^0 + \frac{1}{\sqrt{2}}\eta & \pi^+ \\ \pi^- & -\frac{1}{\sqrt{2}}\pi^0 + \frac{1}{\sqrt{2}}\eta \end{pmatrix}\right\}, \tag{3.4}$$

with $U(\varphi_a)$ in the adjoint representation of the coset $G_{ch}/U_V(2)$, and τ^a the Pauli matrices: for simplicity here we have also excluded the possibility of π_0 and η mixing.

3.1.3 ChPT Lagrangian at Leading $O(p^2)$ Order

We now use the Effective Field Theory framework to construct *ab-initio* an effective Lagrangian in terms of pseudoscalar mesons. The EFT formalism will then allow for the perturbative description of non-perturbative dynamics at energies below Λ_{SChSB}.

Following the prescriptions of the previous sections, the ChPT Lagrangian will be the most general Lagrangian containing all possible terms compatible with the global symmetries of QCD, organized as a sum of terms suppressed by increasing powers of momenta, quark masses and $\frac{1}{N_C}$ terms. Our counting rules will then be the following

$$U = O(p^0) \ ; \quad \partial_\mu = O(p) \ ; \quad m_q \simeq m_\varphi^2 = O(p^2) \ ; \quad \frac{1}{N_C} = O(m_q) = O(p^2).$$

Since the $U(x)$ fields are Goldstone bosons of the broken $SU_A(N_f)$ plus $U_A(1)$ they can be represented as the coordinates of the broken symmetry transformation: hence they are element in the coset $G_{ch}/U_V(N_f)$. Under a generic $g_{ch} \in G_{ch}$ they will transform as

$$U(x) \to U^{'}(x) = g_R(x)U(x)g_L^{\dagger}(x),$$

or if the transformations are only $g_V \in U_V(N_f)$ or $g_A \in U_A(N_f)$ respectively

$$U(x) \to U^{'}(x) = g_V(x)U(x)g_V^{\dagger}(x) \qquad U(x) \to U^{'}(x) = g_A(x)U(x)g_A(x).$$

These transformation properties will enable us to construct the leading order $O(p^2)$ ChPT Lagrangian; before proceding with the calculation of $\mathcal{L}^{(2)}_{ChPT}$, we recall that the Lagrangian is a Lorentz scalar, and:

a) the only possible way of building a scalar out of a unitary matrix is by using the trace Tr[...] or the determinant det[...];

[1] From the point of view of quarks content, η and $\eta^{'}$ are indistinguishable in $N_f = 2$.

b) the only possible way of building a scalar out of derivatives of a unitary matrix, is using an even number of derivatives;

c) the lowest order ChPT Lagrangian is $O(p^2)$: in fact it has to have a mass term and hence should be at least $O(m_q)$;

We now construct piece by piece the ChPT Lagrangian, by mimiking the invariance properties under chiral transformation of the QCD Lagrangian. We will start with global G_χ invariance: we will consider local G_χ invariance in section 3.1.5.

Chiral Invariant Term

The lowest non trivial $O(p^2)$ order term which is full G_{ch} invariant, is the following

$$\frac{F^2}{4} Tr\left[\partial_\mu U(x) \partial^\mu U^\dagger(x)\right],$$

where the factor $\frac{F^2}{4}$ has been chosen to reproduce the correct normalization for the cinematic terms of the meson fields, as one can see in section (**??**). Another possible term involving trace and derivatives and fully G_{ch} invariant could be

$$Tr\left[(\partial_\mu \partial^\mu U(x)) U^\dagger(x)\right] = \partial_\mu \left[Tr\left((\partial^\mu U(x)) U^\dagger(x)\right)\right] - Tr\left(\partial_\mu U(x) \partial^\mu U^\dagger(x)\right),$$

which aside from a total derivative is equivalent to the previous term;

Mass Term

Let us now construct the mass terms in the ChPT Lagrangian. To this end we analyze the divergence of the vector and axial currents in Eq.(2.30) and recall that in the chiral limit, the chiral symmetry G_{ch} is unbroken. In $\mathcal{L}_{QCD}$, the mass terms breaks the chiral group to $G_{ch} \to U_V(3)$ in the limit of equal quark masses, that is to say that the mass term has to lay in the regular representation of the coset $G/U(3)_V$, that is to say it has to be $U(x)$ itself. So we can define a 3×3 constant —complex, in general— matrix M_c, which has to be proportional to the quark mass matrix M_q; we set $M_c = \rho e^{i\theta} M_q$ to obtain

$$\frac{F^2}{4} \rho Tr\left[e^{i\theta} M_q U^\dagger(x) + e^{-i\theta} U(x) M_q\right].$$

CP-violating/AxialSymmetryBreaking Term

The term we are looking for should transform as the an element in the coset $G_{ch}/[U_V(N_f) \times SU_A(N_f)]$. This is the way the logarithm of the determinant of the field $U(x)$ transform

$$\ln \det U(x) = Tr(\ln U(x)) = \frac{i}{F} \varphi_a(x) Tr\left[\frac{\lambda_a}{2}\right] = \frac{i}{2F} \varphi_0(x) Tr[\lambda_0].$$

Then we can construct the part of $\mathcal{L}_{ChPT}$ which parametrizes low-energy CP violating dynamics in $\mathcal{L}_{QCD}$ in terms of the determinant of the field

$$-\frac{F^2 a}{4N_C}\left[i\ln\det U(x)\right]^2. \tag{3.5}$$

The reason why the square of the determinant $(\det U)^2 \simeq (\varphi^0)^2$ appears, is that we only need a term quadratic in φ^0: we want this term to behave as a mass term, since ϕ^0 must have a mass gap respect to the pions. Notice that this term is of order $O(N_c^{-1})$, i.e. the same order of the axial anomaly.

Apparently the term in Eq. (3.5) does not display any θ dependance. However if we recall that in QCD the CP violating θ dependent term is equivalent to a complex mass term then we extract the phase from the mass matrix $M_c = e^{i\theta}\rho M_q$, by performing a $U_A(1)$ rotation

$$U(x) \xrightarrow{U_A(1)} e^{i\frac{\theta}{2}} U(x) e^{i\frac{\theta}{2}},$$

one obtains the complete $O(p^2)$ chiral Lagrangian

$$\begin{aligned}\mathcal{L}_\theta^{(2)} &= \frac{F^2}{4}\left\{Tr\left[(\partial_\mu U)^\dagger \partial^\mu U + \rho M_q\left(U^\dagger + U\right)\right] - \frac{a}{N_c}\left[i\ln\det U - \theta\right]^2\right\} \\ &= \frac{F^2}{4}Tr\left[(\partial_\mu U)^\dagger \partial^\mu U\right] - V(U).\end{aligned} \tag{3.6}$$

3.1.4 The θ-Vacuum in ChPT

In order to apply perturbation theory to (3.6) it is convenient to change variables and introduce the fields which describe fluctuations around the physical vacuum.
This can be achieved by finding the U_0 field s.t. the energy density

$$H[U] = \frac{F^2}{4}Tr\left[(\partial_\mu U)^\dagger \partial^\mu U\right] + V(U),$$

is minimized; this obviously implies that U_0 is a constant field which can be identified with the vacuum expectation value $U_0 = \langle U(x)\rangle$ of the chiral fields. Note that since $V(x)$ in Eq.(3.6) is of order $O(p^2)$, the vacuum U_0 itself will be correct at otder $O(p^2)$. Nonetheless, this calculation will also allow to determine the θ dependance of the ChPT vacuum — which is non-perturbative by construction —. This will be a direct proof that ChPT enables us to obtain information on non-perturnative amplitudes in terms of a perturbative expansion in momenta: we will also check this by calculating the θ dependance of some amplitudes.

For completeness, we will consider the $N_f = 3$ case.
In order to calculate the true ground state of the theory we have to extract $U_0 = \langle U(x) \rangle$ from $U(x)$. To this end, we note that in ChPT the vacuum is invariant under any $g_V \in U_V(3)$ transformation

$$U_0 = U[g_V(x)] U_0 U^\dagger[g_V(x)],$$

but since the right handside is equivalent to the expression of the diagonalization of a non singular matrix and $U[g_V(x)]$ is unitary by definition, we realise that the vacuum has the following expression

$$U_0 = \begin{pmatrix} e^{-i\varphi_1} & 0 & 0 \\ 0 & e^{-i\varphi_2} & 0 \\ 0 & 0 & e^{-i\varphi_3} \end{pmatrix},$$

where φ_1, φ_2 and φ_3 are three constant phases. The minima are thus obtained by solving the following set of equations

$$\partial_{\varphi_i} V(U_0) = 0 = \rho m_i \left[i e^{i\varphi_i} - i e^{-i\varphi_i} \right] - \frac{2a}{N_C} \left[\sum_j \varphi_j - \theta \right],$$

which give

$$\rho m_u \sin\varphi_u = \rho m_d \sin\varphi_d = \rho m_s \sin\varphi_s = \frac{a}{N_c} \left[\theta - \sum_i \varphi_i \right] = \frac{a}{N_c} \bar{\theta}. \quad (3.7)$$

In the $m_u, m_d << m_s << \frac{a}{N_c}$ limit[2] we obtain the following approximate solutions [27] for the phases $\varphi_i(\theta)$

$$\begin{aligned} \varphi_s &\simeq 0, \\ \sin\varphi_u &\simeq \frac{m_d \sin\theta}{\sqrt{m_u^2 + m_d^2 + 2 m_u m_d \cos\theta}} \simeq \frac{m_d}{m_u + m_d}\theta, \\ \sin\varphi_d &\simeq \frac{m_u \sin\theta}{\sqrt{m_u^2 + m_d^2 + 2 m_u m_d \cos\theta}} \simeq \frac{m_u}{m_u + m_d}\theta, \end{aligned}$$

which in the approximation $m = m_u = m_d$ relate the unknown parameter $\bar{\theta}$ with θ in the following way [29]

$$\frac{a}{N_c}\,\bar{\theta} \simeq \frac{\rho m}{2} \cos\varphi\,\theta \left(= \frac{1}{2}\, m_\pi^2\, \theta \right).$$

This relation will be useful in chapter 4.
In any case we are not interested in the φ_i angles themselfes, but on the two matrices

$$M(\varphi_i) = \frac{1}{2} \left(M_q U_0 + (M_q U_0)^\dagger \right) \; ; \qquad B = \frac{\rho}{2} \left((M_q U_0)^\dagger - M_q U_0 \right) = \frac{a}{N_C} \bar{\theta} I_{3\times 3}.$$

[2] We recall that $\frac{a}{N_C}$ represents the mass gap of η.

B is an antihermitian θ-dependent matrix; $M(\varphi_i)$ is a real diagonal matrix proportional to the quark mass matrix

$$M(\varphi_i) = \begin{pmatrix} m_1 = m_u \cos\varphi_1 & 0 & 0 \\ 0 & m_2 = m_d \cos\varphi_2 & 0 \\ 0 & 0 & m_3 = m_s \cos\varphi_3 \end{pmatrix},$$

this means that the pion masses depend on the values of the φ_i angles. So, by defining a new field $U(x)$ whose vacuum expectation value is equal to $\langle U(x)\rangle = 1$, we obtain

$$\begin{aligned} V(U) &= \frac{F^2}{4}\rho Tr\left[M(\varphi_i)\left(U(x)+U^\dagger(x)\right)\right] + \\ &- \frac{F^2 a}{4N_C}\left[\bar{\theta}^2 - (\ln\det U)^2\right] - i\frac{F^2 a}{4N_C}\bar{\theta}\left[Tr\left(U(x)-U^\dagger(x)\right) - 2\ln\det U(x)\right], \end{aligned}$$

which we will consider from now on.

We can now determine what exactly are the constant ρ and a.
Since in QCD the chiral condensate $\langle q\bar{q}\rangle$ can be defined as

$$\begin{aligned} \langle q\bar{q}\rangle &= \sum_f \frac{\partial}{\partial m_f}\log[Z_{QCD}] \qquad (3.8) \\ &= \sum_f \frac{\partial}{\partial m_f}\log[Z_{ChPT}] = -\frac{F^2}{4}\rho\sum_f \cos\phi_f \langle K_f\cdot[U(x)+U^\dagger(x)]\rangle_{ChPT} \\ &\simeq -\frac{F^2}{2}\rho N_f\cos\phi; \qquad (K_f)_{ij} = \delta_{if}\delta_{jf}, \qquad (3.9) \end{aligned}$$

we obtain the equality

$$\rho = -\frac{\langle q\bar{q}\rangle}{F^2\cos\varphi}; \quad N_f = 2.$$

We also have the relation

$$\chi_{TOP} = \partial_\theta^2 \log[Z_{QCD}] = \frac{F^2}{2}\frac{a}{N_C}.$$

Note that this implies

$$n_{TOP} = \chi_{TOP}\bar{\theta} = F^2 m_\pi^2 \theta. \qquad (3.10)$$

That is to say that the topological charge density and the topological susceptibility vanish in the chiral limit: the first limit is the ChPT realization of the "vanishing-quark-mass solution" of the Strong-CP Problem; the second limit is the ChPT realization of the so-called *screening of topological charge*,

a consequence of quark-induced instantons interactions whose correlation-length set the strength of value of $U_A(1)$ breaking in a finite volume and the value of the η mass gap. In the presence of vanishing quark mass the topological charge is completely screened. This is a clear signal that ChPT can perfectly reproduce the non-perturbative dynamics of topological degrees of freedom.

3.1.5 ChPT and Chiral currents

In the previous section we have calculated the full ChPT Lagrangian to $O(p^2)$. Now we have to ensure that the correlation fucntions which are obtained functional differentiating the generating functional

$$Z_{ChPT} = \int \mathcal{D}U(\varphi_a) e^{i\int \mathrm{d}^4 y \mathcal{L}^{(2)}_{ChPT}},$$

are consistent with those obtained in QCD. This is achieved by examining how are considered symmetries in path integral formalism.

In classical physics symmetries can be treated by the Noether formalism, which states that for any infinitesimal transformation of the fields which leaves the Lagrangian invariant there is a conserved current. At the quantum level, symmetries are encoded by Ward identities, which are relations between correletion functions: a fundamental requirement for ChPT to represent low-energy QCD dynamics, is that the Ward Identities of QCD are respected. This is achieved by ensuring that to each transformation of the fields in the fundamental theory for which the generating functional is globally invariant, there correspond in the effective theory a *local* transformation of the fields for which the generating functional is invariant. In our case, since the QCD Lagrangian is invariant under a global chiral group, we have to introduce in $\mathcal{L}^{(2)}_{ChPT}$ a set of external sources which will promote global G_{ch} into a local G_{ch} symmetry.

We will outline this procedure in QCD, for the ChPT construction will be straightforward. In Eq.(2.27) we showed the chiral noether currents V^b_μ and A^b_μ. The easiest way to introduce the external sources v^b_μ and a^b_μ is adding a term

$$\mathcal{L}_{ext} = V^b_\mu v^\mu_b + A^b_\mu a^\mu_b = \bar{q}\gamma_\mu \frac{\lambda^b}{2} q v^\mu_b + \bar{q}\gamma_\mu\gamma_5 \frac{\lambda^b}{2} q a^\mu_b,$$

to the QCD Lagrangian, which is equivalent to a new covariant derivative

$$D^{'}_\mu = D_\mu + v_\mu + \gamma_5 a_\mu,$$

with the usual notation

$$v_\mu = v^b_\mu \frac{\lambda_b}{2} \quad ; \quad a_\mu = a^b_\mu \frac{\lambda_b}{2}.$$

It is now trivial to determine the transformation rules for $l_\mu = v_\mu - a_\mu$ and $r_\mu = v_\mu + a_\mu$ under a local $g_{ch}(x) \in G_{ch}$

$$\begin{aligned} l_\mu(x) &\rightarrow l'_\mu(x) = g_L(x) l_\mu(x) g_L^\dagger(x) + i g_L(x) \partial_\mu g_L^\dagger(x), \\ r_\mu(x) &\rightarrow r'_\mu(x) = g_R(x) r_\mu(x) g_R^\dagger(x) + i g_R(x) \partial_\mu g_R^\dagger(x). \end{aligned} \tag{3.11}$$

Due to these transformation rules the Lagrangian

$$\mathcal{L}_{tot} = \mathcal{L}_{QCD} + \mathcal{L}_{ext},$$

is invariant, in the chiral limit, under a generic local chiral transformation $g_{ch}(x)$.

To make the ChPT Lagrangian invariant under a local chiral transformation it is sufficient to define a set of external sources in ChPT which transform exactly as in QCD, Eq. (3.11). Then we have to define a covariant derivative

$$D_\mu U(x) = \partial_\mu U(x) - i r_\mu(x) U(x) + i U(x) l_\mu(x).$$

Note that this is equivalent to define a power counting rule for the external fields as well

$$r_\mu, l_\mu = O(p) = \partial_\mu.$$

So that the full ChPT Lagrangian at $O(p^2)$ becomes

$$\begin{aligned} \mathcal{L}_\theta^{(2)} &= \frac{F^2}{4} Tr\left[(D_\mu U)^\dagger D^\mu U + \rho M_q \left(U(x) + U^\dagger(x) \right) \right] + \\ &- \frac{F^2 a}{4 N_C} \left[\bar{\theta}^2 - (\ln \det U)^2 \right] - i \frac{F^2 a}{4 N_C} \bar{\theta} \left[Tr\left(U(x) - U^\dagger(x) \right) - 2 \ln \det U(x) \right]. \end{aligned}$$

We recall that this Lagrangian has been obtained ab-initio, using the EFT formalism.

3.1.6 Vector and Axial Currents in ChPT

Having introduced the external sources in the generating functional we can determine the chiral Noether currents in ChPT in a straightforward way by

$$J_\mu(x) = \frac{\delta}{\delta A_J^\mu(x)} S = \frac{\delta}{\delta A_J^\mu(x)} \int \mathrm{d}^4 y \mathcal{L}(y).$$

In our case we then obtain

We can now read off the physical meaning of the effective parameter F: since in the absence of external fields and to the lowest order in the fields expansion the axial current is

$$J_\mu^a = -F \partial_\mu \varphi^a,$$

$$L^a_\mu(x) = i\tfrac{F^2}{4} Tr\left[\lambda^a \left(D_\mu U(x)\right)^\dagger U(x)\right]; \qquad R^a_\mu(x) = -i\tfrac{F^2}{4} Tr\left[\lambda^a U(x) \left(D_\mu U(x)\right)^\dagger\right];$$

$$V^a_\mu(x) = -i\tfrac{F^2}{4} Tr\left\{\lambda^a \left[U(x), \left(D_\mu U(x)\right)^\dagger\right]\right\}; \quad A^a_\mu(x) = -i\tfrac{F^2}{4} Tr\left\{\lambda^a \left\{U(x), \left(D_\mu U(x)\right)^\dagger\right\}\right\}.$$

Table 3.2: Chiral currents to $O(p^2)$ in chiral perturbation theory.

and since by definition the decay constant D^b of the mesons are given by

$$\langle \Omega | J^b_\mu | \varphi^b(p) \rangle = i p_\mu D^b,$$

we obtain that $D^b = F$ is the pion decay constant.

These ChPT currents are equivalent to the chiral QCD currents in Eq.(2.27) at low-energies. Without entering in details, using the Noether formalism we can calculate the divergences of currents

$$\begin{aligned}
\partial_\mu V^\mu_a &= -i\frac{F^2}{4} Tr\left(\left[M_q, \frac{\lambda_a}{2}\right](U + U^\dagger) + i\left(\left[\frac{\lambda_a}{2}, v_\mu\right] + \left\{\frac{\lambda_a}{2}, a_\mu\right\}\right)\left[U, (D^\mu U)^\dagger\right]\right); \\
\partial_\mu A^\mu_a &= -i\frac{F^2}{4} Tr\left(\left\{M_q, \frac{\lambda_a}{2}\right\}(U + U^\dagger) + i\left(\left[\frac{\lambda_a}{2}, v_\mu\right] + \left\{\frac{\lambda_a}{2}, a_\mu\right\}\right)\left\{U, (D^\mu U)^\dagger\right\}\right) + \\
&- \frac{F^2 a}{2N_c}\bar{\theta}\, Tr\Big(\lambda_a(U + U^\dagger)\Big) + \frac{F^2 a}{N_c}\Big(\bar{\theta} - i \ln \det U\Big) Tr(\lambda_0).
\end{aligned}$$

As expected, chiral currents have the following properties (in the absence of external currents)

- in the limit of equal masses for all quarks the vectorial currents are conserved, in fact $M_q = m_q I_{N_f \times N_f}$;
- in the chiral limit $M_q \to 0$ the vectorial currents are conserved and the axial currents, except for the axial singlet, are conserved as well;
- in both the chiral and the large N_c limits the axial singlet is conserved.

Electromagnetic Current in ChPT

In QCD the electromagnetic current is defined as

$$J^\mu_{e.m.} = \frac{2}{3} e J^u_\mu - \frac{1}{3} e J^d_\mu - \frac{1}{3} e J^s_\mu.$$

This is equivalent to consider $r_\mu = l_\mu = eQA_\mu$, with $Q = \mathrm{diag}(\frac{2}{3}, -\frac{1}{3}, -\frac{1}{3})$ the charge matrix and A_μ the vector potential of the external electromagnetic field.

We can then construct an electromagnetic current in ChPT as well: in $N_f = 2$ we have

$$J^u_\mu = \frac{1}{2}\left(V^0_\mu + V^3_\mu\right),$$
$$J^d_\mu = \frac{1}{2}\left(V^0_\mu - V^3_\mu\right).$$

But since the trace of a commutator is alway zero we have $V^\mu_0 = 0$ and the following relation

$$J^\mu_{e.m.} = \frac{e}{2}V^{\mu,3} = eJ^{\mu,u} = -eJ^{\mu,d}. \tag{3.12}$$

Explicit ChPT Lagrangian

As a conclusion of this section we are going to expand $U(x)$ in terms of meson fields. In fact the Lagrangian in Eq.(3.12) and the currents in table (3.2) are useless from the point of view of perturbation theory, because the physical fields are not explicit.

Since in chapter 4 we will use EFT method to calculate CP-odd interactions in external electromagnetic fields, for our purpose it is sufficient to consider only electromagnetic and CP violating interactions. This is $O(\varphi_a^3)$ and gives for $N_f = 2$ and $m = m_u = m_d$, the following ChPT Lagrangian[3] (for simplicity we will restrict to the $r_\mu = l_\mu = eQA_\mu$ case)

$$\begin{aligned}\mathcal{L}^{(2)}_\theta &= \frac{1}{2}\partial_\mu\pi^0\partial^\mu\pi^0 + \frac{1}{2}\partial_\mu\eta\partial^\mu\eta + \partial_\mu\pi^+\partial^\mu\pi^- - \rho\frac{m\cos\varphi}{2}\left(\pi^0\pi^0 + \eta\eta + 2\pi^+\pi^-\right) + \\ &- \frac{a}{N_c}\eta\eta - \frac{a}{N_c}\bar\theta\frac{1}{F}\left[\frac{1}{6}\eta\eta\eta + \frac{1}{2}\eta\pi^0\pi^0 + \eta\pi^+\pi^-\right] + \\ &- ieA_\mu\left(\pi^+\partial^\mu\pi^- - \partial^\mu\pi^+\pi^-\right) + e^2A_\mu A^\mu\pi^+\pi^-. \end{aligned} \tag{3.13}$$

From this equation we can read-off the pseudoscalar masses

$$m^2_\pi = -\frac{m\langle q\bar q\rangle}{F^2}\ ; \qquad m^2_\eta = -\frac{m\langle q\bar q\rangle}{F^2} + 2\frac{a}{N_c}, \tag{3.14}$$

as we expected η has a mass gap proportional to the topological susceptibility, as expected

$$m^2_\eta - m^2_\pi = 4\frac{\chi_{TOP}}{F^2} \simeq (350MeV^2).$$

In term of pion fields, the electromagnetic current reads

$$J^\mu_{e.m.} = -ie\left(\pi^+\partial^\mu\pi^- - \partial^\mu\pi^+\pi^-\right) + 2e^2A^\mu\pi^+\pi^-.$$

[3] In these limits and in the $N_f = 2$ case $\varphi^3 = \pi^0$ and $\varphi^0 = \eta$.

Notice that it depends on the charged scalar only and it is equivalent to the electromagnetic current we would have found in a theory of a complex scalar field $\varphi = \pi^-$, $\varphi^\dagger = \pi^+$.

Notice that all terms except the CP violating θ interactions, have an even number of pion fields: i.e. their Feynman vertices have an even number of pion legs. Notice also that as we expected the CP violating term it is always η dependent, for this meson it is strongly connected with the anomalous dynamics: CP violating dynamics at very low-energy is mediated by the η field.

3.1.7 Realization of Electromagnetic Anomaly

As we said in section 3.1.1, every non-perturbative process in low-energy QCD must be reproduced in the ChPT Lagrangian. Electromagnetic anomaly, on the other hand, is not reproduced in $\mathcal{L}^2_{ChPT}$: this is not a surprise, because due to power counting electromagnetic anomaly should count as an $O(p^4)$ term, in fact

$$\mathcal{L}^{e.m.}_{an} \propto \mathbf{E}\cdot\mathbf{B}; \qquad O(\mathbf{E}) = O(\mathbf{B}) = O(p^2).$$

Wess, Zumino [30] and Witten [28] have shown that the electromagnetic anomaly can be accounted for by an interaction term

$$\begin{aligned}\mathcal{L}^{(4)}_{WZ} &= -\frac{N_c\epsilon_{\mu\nu\alpha\beta}}{48\pi^2}\Big[eA_\mu Tr\left(-QR_\nu R_\alpha R_\beta + QL_\nu L_\alpha L_\beta\right) + \\ &+ ie^2F_{\mu\nu}A_\alpha Tr\left(Q^2L_\beta - Q^2R_\beta + \frac{1}{2}(QUQU^\dagger L_\beta - QU^\dagger QUR_\beta)\right)\Big],\end{aligned}$$

which is the so-called WZW term, with $L_\mu = (\partial_\mu U)U^\dagger$ and $R_\mu = U(\partial_\mu U)^\dagger$. As we can show by expanding at lowest order in the meson fields, this term has the same form of the anomalous term in section 2.4

$$\mathcal{L}_{WZW} = \frac{e^2N_c}{48\pi^2F}\varepsilon^{\mu\nu\alpha\beta}F_{\mu\nu}A_\alpha\partial_\beta\left(\pi^0 + \frac{5}{3}\eta\right),$$

which contributes to the elecromagnetic current with an $O(p^4)$ term equivalent to

$$J^\mu_{WZW,e.m.} = \frac{e^2N_c}{48\pi^2}\varepsilon^{\mu\nu\alpha\beta}F_{\nu\alpha}\partial_\beta\left(\pi^0 + \frac{5}{3}\eta\right).$$

From the point of view of perturbation theory, this is equivalent to an electromagnetic vertex with two external "photonic legs" and a single "mesonic leg". Due to this term, ChPT allows anomalous electromagnetic interactions: neutral mesons can interact with photons. The most famous example is the decay of a neutral pion into two photons: $\pi^0 \to \gamma\gamma$.

In chapter 4 we will discuss the role of WZW anomalous current in the realization of CP-odd vacuum polarization and we will see that the results will be qualitatively equivalent to the phenomenological discussion in terms of fundamental degrees of freedom in section 2.4: the interplay between topologically induced and electromagnetically induced anomaly enables to polarize quantum vacuum fluctuations.

3.2 Lattice Gauge Theories

Chiral Perturbation Theory cannot be applied in processes where the exchanged momenta is of the order of $\simeq 150MeV$, beacuse fundamental degrees of freedom have to be explicitely included in the theoretical description. Lattice gauge theories, on the other hand, provides a framework in which correlation functions can be obtained by means of numerical simulations.

Lattice QCD, in particular, is the ab-initio realization of QCD in a discretized Euclidean space-time: LQCD configurations ate generated according to their path integral weight — e.g. using Markov chains, ... —

$$P[\text{Conf}] \propto e^{-S_{LQCD}[\text{Conf}]},$$

and calculations of matrix elements are performed numerically using a discretized version of the path integral formalism

$$\langle \mathcal{O} \rangle_{LQCD} = \frac{1}{Z_{LQCD}} \sum_{\text{Conf}} \mathcal{O}\{\text{Conf}\} e^{-S_{LQCD}[\text{Conf}]}.$$

Lattice discretization removes UV and IR divergences, i.e. the theory is regularized to all order by a cutoff on momenta

$$\frac{\pi}{aN} \leq |p| \leq \frac{\pi}{a},$$

where N is the number of lattice points per size and a the spacing between lattice points[4]. Calculations can then be linked to observable quantities in the well behaved continuum limit $a \to 0$.

Since LQCD is a fundamental theory, it is formulated in terms of the same parameter which appear in the continuum formulation, that is to say that it enables to test ab-initio the behaviour of non-abelian theories, and validate QCD by reproducing physical quantities in the physical limit

$$m_q^{LQCD} \to m_q^{QCD}; \quad g_s^{LQCD} \to g_s^{QCD}; \ldots.$$

In this section we will not enter in details of computational techniques: we only want to give a very basic introduction to LQCD. We will present the properties of the fundamental QCD degrees on freedom on the lattice and we will discuss LQCD actions and their behaviour in the continuum limit. For a more comprehensive and extensive discussion, see [31].

[4] We assume for simplicity that the lattice has the same numebr of points and the same lattice spacing per all sizes.

3.2.1 Quarks and Gluons on the Lattice

We start our review, by showing how quarks and gluons can be discretized on the lattice. Since QCD is the quantum field theory of quarks whose interactions are mediated by gluon fields in the adjoint representation, the most intuitive way of discretize such fields is to put fermions on the *lattice sites* and define gauge fields on *lattice links*, that is to say the lines which connect two neighbour lattice sites.

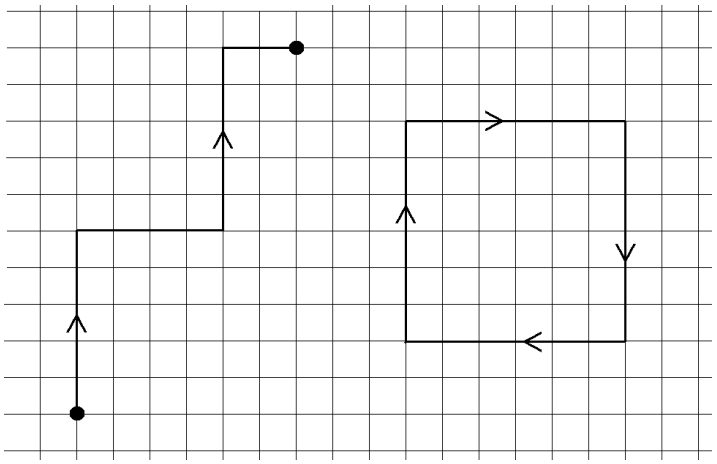

Figure 3.1: Quarks are on the lattice sites and gauge fields are on the lattice links. Example of Wilson line (on the left) and Wilson loop (on the right).

The reason of putting gluons on gauge links resides on the geometrical interpretation of the covariant derivative

$$D_\mu q = (\partial_\mu - iA_\mu)q.$$

If we consider two vectors defined on different points x and y of a $SU(N_C)$ manifold, the correct way of comparing them consist in perform a "parallel transport" of the one in y to the point x, that is to say

$$U(x,y)q(y) = q^{'}(y),$$

where $U(y,x)$ is some unitary $SU(N_C)$ matrix.
If we consider an infinitesimal transformation we have

$$q^{'}(x+\mathrm{d}x) - q(x) = U^{-1}(x+\mathrm{d}x,x)q(x+\mathrm{d}x) - q(x) := [D_\mu q(x)]\mathrm{d}x_\mu,$$

where $D_\mu q(x)$ is, by definition, the covariant derivative on the $SU(N_C)$ manifold. We then conclude that the infinitesimal transformation is equivalent to

$$U^{-1}(x+\mathrm{d}x,x) = I - iA_\mu \mathrm{d}x_\mu,$$

which implies that

$$U(x,y) = \mathcal{P} e^{i \int_x^y \mathrm{d} z_\mu A_\mu(z)}.$$

Hence, we can effectively describe interactions among quarks at a distance x and y by means of a path-ordered gluon operator $U(y,x)$.

On the lattice we would then have

$$\begin{aligned} U_\mu(x) &:= U(x + a\hat{\mu}, x) = U^\dagger(x, x + a\hat{\mu}) && (3.15) \\ &= e^{iaA_\mu(x)} \simeq I + iaA_\mu(x) + O(a^2). && (3.16) \end{aligned}$$

3.2.2 Gauge Invariance on the Lattice

Discretized theory is not translationally and rotationally invariant: invariance in an hypercubic lattice would be that of the *hypercubic group*, that is to say invariance under 90° rotation and unit $a\hat{\mu}$ translations.
On the other hand, we insist in requiring that gauge invariance should be satisfied even on the lattice.

On the lattice, local $SU(N_C)$ gauge transformation can be defined by means of $G(x)$ unitary matrices as in the QCD case

$$\begin{aligned} q(x) &\rightarrow q^{'}(x) = G(x)q(x), && (3.17) \\ \bar{q}(x) &\rightarrow \bar{q}^{'}(x) = \bar{q}(x)G^\dagger(x), && (3.18) \\ U_\mu(x) &\rightarrow U_\mu^{'}(x) = G(x)U_\mu(x)G^\dagger(x + a\hat{\mu}). && (3.19) \end{aligned}$$

Such a definition enables to define two classes of invariant operators: "Wilson lines" and "Wilson loops", see Fig(3.2.1):

- Wilson lines are given by a path-ordered product of gauge-links closed by a quark and an anti-quark at their endings

  $$\mathrm{Tr}[W^L(x,y)] \Longrightarrow \mathrm{Tr}[\bar{q}(x)U_\mu(x)U_\nu(x + a\hat{\mu}) \dots U\alpha(y - a\hat{\alpha})q(y)],$$

  where the trace is over color space. Obviously one could also interpolate different lines obtaining a composite operator

  $$\mathrm{Tr}[W^L(x,y)W^{L^{'}}(y,z)W^{L^{''}}(z,q)].$$

  These operators are also gauge invariant;

- Wilson loops are closed lines without quarks at their endings

  $$Tr[W^{\mathcal{L}}] = Tr[U_\mu(x)U_\nu(x + a\hat{\mu}) \dots U_\alpha^\dagger(x)].$$

The shortest loop is given by

$$Tr[W_{\mu\nu}^{1\times 1}] = Tr[U_\mu(x)U_\nu(x + a\hat{\mu})U_\mu^\dagger(x + a\hat{\nu})U_\nu^\dagger(x)],$$

such a Wilson loop is called plaquette.

3.2.3 LQCD Gauge Action

As we have seen gauge invariant term are given by Wilson lines and Wilson loops: out of these two classes of terms one can build a gauge invariant LQCD Lagrangian, recalling that in the limit $a \to 0$ limit, we have to obtain the QCD Lagrangian.

We restrict for a moment to the pure gauge case: it can be shown that by expanding in a the real part of the plaquette $W^{1\times1}_{\mu\nu}(x)$ one obtain

$$Re\{W^{1\times1}_{\mu\nu}(x)\} \simeq 2N_c + a^4 Tr[G_{\mu\nu}(x)G_{\mu\nu}(x)] + O(a^5).$$

Which implies that by choosing the following as LQCD gauge action

$$S_{LQCD} = \beta \sum_p \{1 - \frac{1}{N_C} Re\{W^{1\times1}_p\}\}$$

where p runs over all possible plaquette and β is a LQCD coupling parameter, we obtain

$$\begin{aligned} S_{LQCD} &= -\frac{\beta}{4N} \sum_x a^4 Tr[G_{\mu\nu}(x)G_{\mu\nu}(x)] + O(a^5) && (3.20) \\ &\overset{a\to0}{\to} -\frac{1}{4g^2} \int_V \mathrm{d}^4x G^a_{\mu\nu}(x) G_{a,\mu\nu}(x), && (3.21) \end{aligned}$$

which sets the LQCD coupling to

$$\beta = \frac{2N_C}{g^2}.$$

Note that instead of S_{LQCD}, which is called Wilson action, we could have also used other definitions: $W^{1\times1}$ and $W^{1\times2}$ combined, etc. . ..

3.2.4 LQCD Fermion Action

We now discuss the construction of quark LQCD Lagrangian. One can easily show that the Lagrangian

$$\mathcal{L}_q = m_q \bar{q}(x)q(x) + \frac{1}{2a}\bar{q}(x) \sum_\mu \gamma_\mu [U_\mu(x)q(x + a\hat{\mu}) - U^\dagger_\mu(x - a\hat{\mu})q(x - a\hat{\mu})\psi],$$

is equivalent to the Dirac Lagrangian in the $a \to 0$ limit.

Such a Lagrangian give raise to an action

$$\begin{aligned} S_q &= \sum_x \bar{q}(x) M^q_{xy}[U] q(y), && (3.22) \\ M^q_{ab}[U] &= m_q \delta_{ab} + \frac{1}{2a} \sum \mu\gamma_\mu [U_{i\mu}\delta_{i,j-\mu} - U^\dagger_{i-\mu,\mu}\delta_{i,j+\mu}]. && (3.23) \end{aligned}$$

The nature of the operator M^q_{ab} is very peculiar: in the continuum limit it gives rise to $16 = 2^d$ different quarks flavors per each quark flavor in the LQCD fermionic action.
In fact, it can be shown that the free quark propagator in momentum space

$$S^{-1}(p) = m_q + \frac{1}{a}\sum_\mu \gamma_\mu \sin[ap_\mu],$$

has 16 poles in the continuum limit: in addition, these poles have definite chirality: 8 left-handed and 8 right-handed. This implies that such an action cannot reproduce the chiral invariance properties of the QCD Lagrangian, shown in section 2.4.
The emergence of fermionic copies is the so-called "doubling": in order to reproduce $\mathcal{L}_{QCD}$ phenomenology, doubling must be removed.

Doubling and Nielsen-Ninomiya's Theorem

The emergence of doubling in discretized actions is a consequence of the Nielsen-Ninomiya theorem:
If a fermion action $S_F = \bar{q}D[U]q$ satisfies the following conditions:

- *is translationally invariant;*
- *is chirally symmetric, that is to say*: $D\gamma_5 + \gamma_5 D = 0$;
- *is hermitian*;
- *is bilinear in the fields*;
- *is local.*

Then, there must be doublers in the continuum limit.
To remove doublings, we then have to define different actions: Wilson [32] proposed to add a term to Eq.(3.22)

$$\mathcal{L}_W = 4\frac{r}{a}\bar{q}(x)q(x) + \frac{r}{2a}\bar{q}(x)\sum_\mu \gamma_\mu[U_\mu(x)q(x+a\hat{\mu}) + U^\dagger_\mu(x-a\hat{\mu})q(x-a\hat{\mu})\psi],$$

such a term leads to a rescaling of fermion fields

$$\psi^W = \sqrt{am_q + 4r}q,$$

which enables to reabsorb the lattice parameter a; these are the so-called *Wilson Fermions* (WF): they remove doubling in the continuum limit, but break chiral symmetry at finite lattice spacing.
Another way of reducing doubling is by definition of the so-called *Staggered Fermions* (SF) [33]: doubling is only reduced to $16 \to 4$ and they have a

complicatedd flavor structure, but chiral symmetry is reproduced at finite a.
The use of staggered or wilson fermions is then motivated by the type of calculations one wants to perform: SF are applied to studies in which the chiral symmetry plays essential role, otherwise WF are prefered due to their corresponence to QCD quarks.

3.2.5 Strong Coupling and Lattice Spacing

We conclude our basic review by discussing the relation between the lattice spacing parameter a and the lattice coupling constant β.

By looking at the gauge and fermion actions of previous sections one immediately notice that there is no explicit way to set the lattice spacing parameter in the calculations: it is only possible to set the value for β, and obviously the number of lattice sites. On the other hand, this is not suprising: by setting a cut-off in the momenta, the lattice spacing also sets a specific energy scale $\mu = \frac{1}{a}$ in the calculations, this implies that due to renormalization in LQCD, the LQCD coupling has a specific Λ_{LQCD} scale and the coupling β has a running behaviour similar to that of the QCD coupling $\alpha_s(\mu)$

$$\Lambda_{QCD} \propto \Lambda_{LQCD}, \tag{3.24}$$

$$\beta := \beta(a) \Longrightarrow a := a(\beta). \tag{3.25}$$

The best way to determine the lattice spacing for a given lattice configuration at a fixed value of β and lattice points, is that of comparing the lattice result for a given observable at β to that of the QCD observable at the corresponding α_s value. The lattice observables in fact, are a dependent

$$\mathcal{O}_{LQCD} := \mathcal{O}_{LQCD}(a).$$

Among the most used quantities there is the string tension σ which can be extracted by Wilson lines correlation functions.

3.2.6 LQCD and Topology

We conclude this section, by presenting some of the available methods for extracting information on the topological structure of QCD, from LQCD configurations.

As we have seen in the previous sections LQCD enables to have access to gluon field configurations. This would in principle allow to analyze the microscopic structure of gauge field configurations just by direct calculation of the action density. This operation, on the other hand, reveals that lattice

gauge configurations are dominated by UV fluctuations whose correlation length is of the order of the lattice spacing: these $O(a)$ fluctuations forbid to have a direct access to long-range structures, such as non-perturbative topological configurations.
To overcome this problem several method have been proposed, based on the filtering (or even removal) of UV fluctuations.

UV Filtering

UV filtering methods can be distinguished into *cooling, smearing* and *eigenvalue filtering.*

Cooling essentially consists in removing UV fluctuations by driving the configuration into a smooth classical solution. This can be achieve by taking a LQCD configuration and performing Monte Carlo updates which accepts only changes that lower the action.

Smearing techniques consist in a local average of gauge field configurations, which result in a removal of UV fluctuations. Every gauge link is replaced by a combination of neighbours link, with the link itself

$$U_\mu(x) \longrightarrow U^{sm}_\mu(x) = \alpha U_\mu(x) + \gamma \sum_{\nu \neq \mu} U^\nu(x) U_\mu(x + a\hat{\nu}) U^\dagger_\nu(x + a\hat{\mu}),$$

in general, the resulting *smeared link* needs to be projected back to the gauge group: in the $SU(2)$ case the operation consists in a rescaling of $U^{sm}_\mu(x)$ by a scalar.
If one takes $\alpha = 0$ smearing coincides with cooling.

Eigenvalue filtering is a technique based on the assumption that slow modes of the Dirac operators are correlated with the location of relevant non-perturbative gluonic (topologic) excitations, e.g. instantons and fermionic zero-modes. Gluonic observables (or the link variables themselfs) are then represented through an expansion in eigenmode of lattice Dirac operators, with a truncation of the spectral sum at low eigenvalues. For a complete discussion, see [34].

These methods are all based on the filtering (or even removal) of UV fluctuations, and hence on the modification either of the lattice configuration or the structure of gluonic observables. In chapter 5 we will propose a technique which enable to obtain direct information on long-range gluonic structures without requiring a manipulation of LQCD configurations.

Chapter 4

Electromagnetic Implications of Strong CP-Violation in Vacuum

In the previous chapters we have seen that topological degrees of freedom are responsible for the violation of CP-symmetry in hadronic systems, we have also seen that these effects can be quantitative taken into account at low energies using ChPT formalism. In this chapter we will present the results for the calculation of CP-odd polarization in $N_f = 2$ QCD $\theta-$vacuum induced by strong CP violating interactions, in the presence of an external electromagnetic field

$$\nabla \cdot \mathbf{P}^{odd} = \langle J^{0,e.m.}_{CP-odd} \rangle_{\theta, A^\mu}. \tag{4.1}$$

The calculation will be performed both at zero and finite temperature, in the large N_c limit: the results are correct at leading chiral order.

These results will enable us to discuss the conditions under which effects of topology can be directly observed in low-energy systems: we will see that a necessary condition is that the system under consideration is permeated by an intense magnetic field, coherent over large scales. In particular we will discuss effects of Strong-CP violation in astrophysical objects such as Magnetars (i.e. neutron stars with a magnetic field of the order of $B \simeq 10^{15}$Gauss).

In the second part of the chapter we will use these results to discuss effects of topology in very low-energy photon-photon interactions: we will calculate the QCD-dependent part of the first order coefficient regulating CP-odd interactions in Effective QED, and we will calculate the CP-odd contribution to the vacuum birefringence. A discussion on the possibility of observing CP-violating effects on monochromatic polarized light propagating in a Fabry-Perot cavity permeated by an external electromagnetic field

will be presented.

4.1 CP-odd Vacuum Polarization in QCD

Results in this section have been published in [35].
Here we will calculate the CP-odd contribution to the electromagnetic-charge density at low energies, using the ChPT formalism

$$\langle\theta|J^{0,e.m.}_{CP-odd}|\theta\rangle_{A_\mu,ChPT} \simeq \langle\theta|J^{0,e.m.}_{CP-odd}|\theta\rangle_{A_\mu,QCD}, \tag{4.2}$$

at leading chiral order; by looking at Eq.(4.1) we realize that this is the only ingredient we need to calculate CP-odd contribution to vacuum polarization.

In general a CP-violating QFT would admit not only for a $\mathbf{P}^{odd}$ contribution, but for both CP-even and CP-odd polarization

$$\mathbf{P} = \mathbf{P}^{CPeven} + \mathbf{P}^{CPodd},$$

the contributions, on the other hand, can be separated only if the contrbutions of the induced electromagnetic charge density are independent

$$\langle\theta|J^0_{e.m.}(x)|\theta\rangle_{A_\mu,QCD} = \langle\theta|J^0_{e.m.}(x)|\theta\rangle^{CPeven}_{A_\mu} + \langle\theta|J^0_{e.m.}(x)|\theta\rangle^{CPodd}_{A_\mu}.$$

Since the calculations are performed in an external electromagnetic field, this can be achieved by imposing the vanishing of the electric field $\mathbf{E}$ in a given reference frame: due to the invariance properties of the Lorentz scalar

$$F_{\mu\nu}\tilde{F}^{\mu\nu} = \mathbf{E}\cdot\mathbf{B},$$

the CP-even and the CP-odd components of the vector polarization will be perpendicular in every reference frame and aligned along the electric and the magnetic field respectively

$$\begin{gathered}\mathbf{E}\cdot\mathbf{B} = 0,\\ \Downarrow\\ \mathbf{P}^{CPeven} \parallel \mathbf{E} \;\;;\;\; \mathbf{P}^{CPodd} \parallel \mathbf{B}.\end{gathered}$$

Hence, throughout this section we will consider $F\tilde{F} = 0$.

4.1.1 Diagramatic Analysis

In chapter (3) we have seen that matrix elements in the EFT approach can be evaluated perturbatively in momentum expansion: the perturbative expansion is ruled by "chiral power counting" and stress that any vacuum amplitude at a given chiral order $O(p^\alpha)$ is obtained by summing all diagrams whose effective dimension is equal to α.

This implies that in order to perform a calculation of the matrix element in Eq.(4.1) at leading chiral order we have to consider diagrams with the lowest possible number of loops, and the lowest possible number of vertices. The former requests motivates our choice in section 3.13 of expanding ChPT interactions at lowest order in the pseudoscalar fields: the higher is the number of "legs" in the vertices, the higher is the number of loops in the diagrams; the latter request implies that we have consider the lowest possible number of such vertices.
But, which vertices should we use, and in what combination?

In chapter (2) we have seen that the combination of axial and electromagnetic anomaly may lead to the emergence of a non-vanishing anomalous CP-odd electromagnetic current, in the presence of an external electroagnetic field; at low-energy such effects of axial and electromagnetic anomaly are reproduced respectively by CP-odd $\eta-$dependent θ-vertices

$$\mathcal{L}^{(2)}_{\theta,O(\varphi^3)} = -\frac{1}{2F} m_\pi^2 \theta \left[\frac{1}{6}\eta\eta\eta + \frac{1}{2}\eta\pi^0\pi^0 + \eta\pi^+\pi^- \right],$$

and WZW anomalous interaction vertices

$$\mathcal{L}^{(4)}_{WZW} = \frac{\alpha}{12\pi F}\varepsilon^{\mu\nu\alpha\beta} F_{\mu\nu} A_\alpha \partial_\beta \left(\pi^0 + \frac{5}{3}\eta \right) \tag{4.3}$$

$$= \frac{\alpha}{12\pi F} \mathbf{E}\cdot\mathbf{B} \left(\pi^0 + \frac{5}{3}\eta \right). \tag{4.4}$$

We would then expect that CP-odd electromagnetic charge density may be calculated by assembling diagrams with a certain number of $N_{d,\theta}$ and $N_{d,WZW}$ vertices.

Diagrams Contributing at Leading Chiral Order

It is easy to show that requiring the presence of both WZW and $\theta-$dependent interactions is not only a sufficient, but also necessary conditions to construct a diagram describing CP-odd vacuum polarization.

Both WZW and $\theta-$dependent interactions are of odd order in the meson fields $O(\phi^{2n+1})$; for geometrical reasons, it is impossible to construct a diagram describing a vacuum amplitude using an odd number of such terms: the total number of vertices must be even

$$N_{d,\theta} + N_{d,WZW} = 2n \; ; \quad n \in N.$$

In addition, we cannot build a CP-violating diagram using an even number of $\theta-$dependent terms because the overall amplitude would be CP-even —

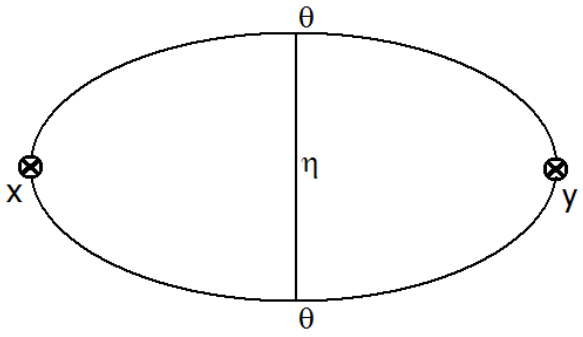

Figure 4.1: Diagram belonging to the process $\langle\theta|J_1^\mu(x)J_1^\nu(y)|\theta\rangle_{A_\nu}$, the diagram is of order α^2, chiral order $O\left(p^6\right)$, and $O(\theta^2)$: it is a correction to CP-even vacuum polarization.

e.g. diagram in Fig.(4.1) —: we have to consider diagrams with an odd number of θ vertices. This implies that at lowest chiral order we have

$$N_{d,\theta} = 1\ ; \quad N_{d,WZW} = 1.$$

Eventually, since we have requested the vanishing of $\mathbf{E}\cdot\mathbf{B}$, the only way the WZW term could enter in a diagram is through an anomalous current

$$J^\mu_{WZW} = \frac{\alpha}{12\pi F}\varepsilon^{\mu\nu\alpha\beta}F_{\mu\nu}\partial_\beta\left(\pi^0 + \frac{5}{3}\eta\right).$$

Thus, the diagrams which contribute to the matrix element in Eq. (4.1) at leading chiral order, are the ones in fig. (4.2) relative to the amplitude

$$\langle J^0_{WZW}(x)\rangle_{A_\mu} = \sum_{m_1}\sum_{m_2} D[m_1, m_2],$$

where m_1 and m_2 are the number of external J_1^μ and J_2^μ vertices

$$J^1_\mu = -ie(\pi^+\partial^\mu\pi^- - \partial^\mu\pi^+\pi^-), \tag{4.5}$$
$$J^2_\mu = e^2A^\mu\pi^+\pi^-. \tag{4.6}$$

The effective dimension of this diagram is equal to $D = 6$: one loop L, plus one vertex of $\mathcal{L}^{(4)}$. So, the leading chiral order for the CP violating vacuum polarization is $O(p^6)$.

The amplitude for the CP-odd electromagnetic current is then given by

$$\langle J^{0,e.m.}_{CP-odd}(x)\rangle_{A_\mu} = \sum_{m_1=0}^{\infty}\sum_{m_2=0}^{\infty} D[m_1, m_2](x) + O(p^6). \tag{4.7}$$

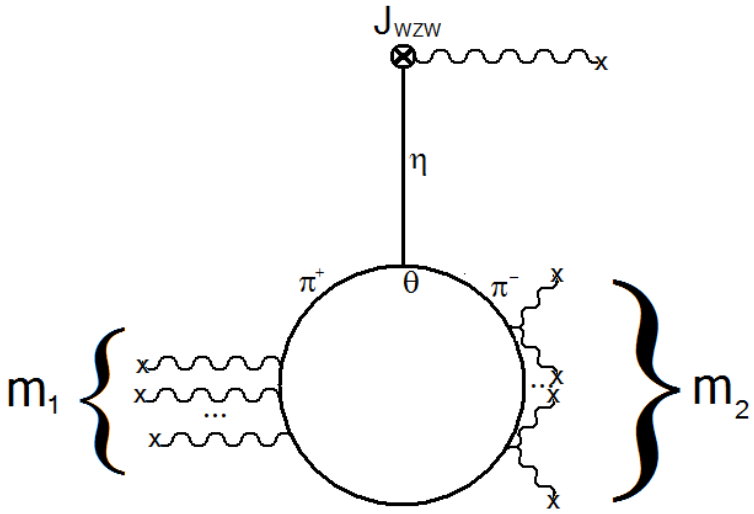

Figure 4.2: Diagrams $D[m_1, m_2]$ related to the amplitude $\langle\theta|J^0_{WZ}|\theta\rangle_{A_\nu}$; m_1 and m_2 are the number of J^μ_1 and J^μ_2 vertices in the pion loop.

Diagrams Contributing at Leading Order in $\alpha_{e.m.}$

$D[m_1, m_2]$ have different numbers of external electromagnetic interaction vertices, each of these diagrams contribute with a factor $\alpha^{\frac{m_1}{2}+m_2}$ to the process, where $\alpha \simeq \frac{1}{137}$. We are then also interested in considering diagrams with the lowest number of such vertices, since the other would account for a small correction $\leq 0.7\%$ to the leading order.

It is easy to show that at leading order in α we have the diagrams $D[2, 0]$ and $D[0, 1]$. Notice that these diagrams are very similar to the diagrams one should calculate to obtain the CP-even contribution to the electromagnetic charge density: the only difference is the insertion of a CP violating θ vertex and an anomalous electromagnetic interaction in the CP-odd ones.

4.1.2 Results: Uniform Oscillating Magnetic Field

In this work we will just present the results for $P^{odd}(t, \theta)$, in the presence of an uniform oscillating magnetic field; for the full calculation, we remand the reader to my Master Thesis [36].

If we restrict to the case of an external uniform oscillating magnetic field

$$\mathbf{B}(x) = B_0 \cos(\bar{\omega} t)\hat{\mathbf{z}},$$

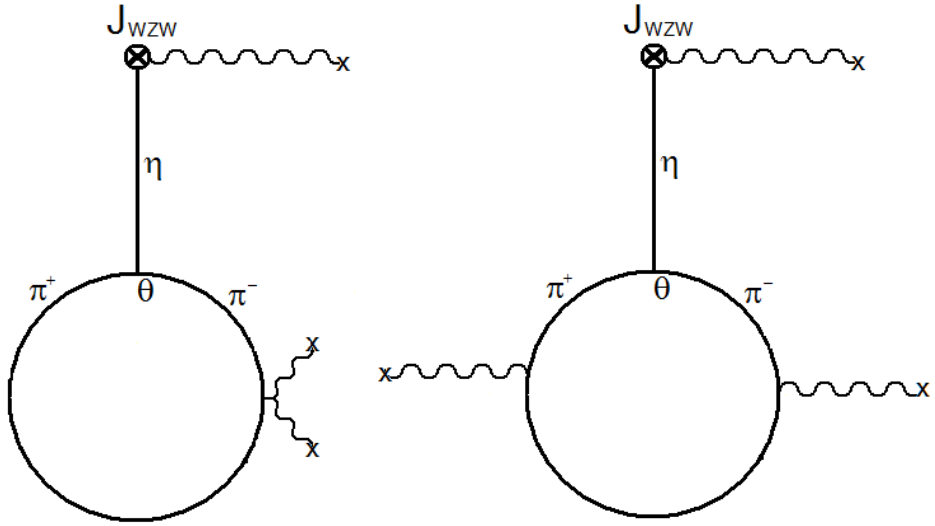

Figure 4.3: (Left Panel:) $D[0,1]$ Diagram. (Right Panel:) $D[2,0]$ Diagram.

we obtain the following result [35] for the CP-odd vacuum polarization

$$\boxed{\mathbf{P}(t) = \frac{5}{6}\frac{\alpha^2\theta B_0^3}{m_\eta^2(4\pi F)^2}\left\{\left[\frac{1}{6}+\frac{\bar{\omega}^2}{m_\eta^2}+\frac{1}{10}\frac{\bar{\omega}^2}{m_\pi^2}\right]\cos(3\bar{\omega}t)+\left[\frac{1}{2}-\frac{1}{3}\frac{\bar{\omega}^2}{m_\eta^2}+\frac{11}{45}\frac{\bar{\omega}^2}{m_\pi^2}\right]\cos(\bar{\omega}t)\right\}\hat{\mathbf{z}}} \tag{4.8}$$

where the amplitude B_0 and the frequency $\bar{\omega}$ are bounded by the ChPT counting rules — in natural units —

$$\sqrt{B_0}; \bar{\omega} \ll \Lambda_{ChPT} = 1GeV \ ; \quad \bar{\omega} = O(p) = \sqrt{B_0},$$

which implies

$$\bar{\omega} \ll 1.52 \times 10^{24} Hz, \tag{4.9}$$

$$B_0 \ll 5.11 \times 10^{15} Tesla. \tag{4.10}$$

In the presence of an external magnetic field the QCD vacuum behaves as a medium with a non linear response: the effect is cubic in $|B_0|$. This is a pure quantum effect, since we have a non zero polarization if and only if we consider η-mediated, θ-dependent and anomalous interactions. We also notice the response of the QCD vacuum to a uniform magnetic field oscillating with frequency $\bar{\omega}$ is given by a sum of two contribution, with $\bar{\omega}$ and $3\bar{\omega}$ frequencies.

It is interesting to address the question why oscillation modes with frequency $3\bar{\omega}$ and $\bar{\omega}$ emerge in response of a driving field characterized by a single frequency $\bar{\omega}$. If we take a look at the diagrams which describe the

induced CP violating polarization — Fig(4.3) — we immediately realise that the vacuum interacts with the external fields via three external field interaction vertices. This means that we can distinguish two types of interaction. In the first one the QCD θ-vacuum "absorb" or "emit" only a single quantum of energy from the external field. In the second one the QCD θ-vacuum "absorb" or "emit" three quanta of energy from the external field.

So, the responce of the vacuum responce is equivalent to a sum of two contributions: the first one is an oscillation with frequency $\bar{\omega}$; the second one an oscillatio with frequency $3\bar{\omega}$. These are the two "modes" which are present in the expression (4.8). We can also infer what would happen if we considered diagrams at higher order in α: we would have had more external field interaction vertices so that the vacuum could have exchanged an higher number of quanta $\bar{\omega}$ (which for gauge invariance are always equal to an odd number $2m_1 * 1 + m_2 * 2 + 1$).

This means that in the presence of an external scillating magnetic field and strong CP violating interactions, we should be able to observe a sum of oscillating modes, such that the spectrum of the response is $(2n+1)\bar{\omega}$, with $n = 0, 1, 2...$ However, note that each term $(2n+1)\bar{\omega}$ is suppressed by α^{n+1}.

4.1.3 Results: Uniform Static Magnetic Field

By setting $\bar{\omega} = 0$ in Eq.(4.8) we obtain the vacuum response to an uniform and static magnetic field oriented along the z axis

$$\boxed{\mathbf{P}(\theta) = \frac{5}{9}\frac{\alpha^2\ \theta\ B_0^3}{m_\eta^2\,(4\pi F)^2}\,\hat{\mathbf{z}}} \tag{4.11}$$

which is equivalent to an induced electric dipole moment

$$\mathbf{D}^{odd}(\theta) = \int_V \mathrm{d}^3x\,\mathbf{P}^{odd}(\theta). \tag{4.12}$$

We now present an ex example which allows us to estimate the strength of this CP-odd effect. Consider a "table-top experiment" consisting in a box of volume $V = 1m^3$ permeated by a magnetic field of $B_0 = 1Tesla$: the strength of the induced vacuum-edm would then be

$$D_{t-top}(\theta) = 1.52 \times 10^{-18}\theta e\,cm.$$

Notice that this value is extremely small, in fact vacuum-edm results to be two order of magnitudes smaller in strength than the electric dipole moment of a *single neutron*

$$D_{t-top}(\theta) \simeq 10^{-2} D_{n-edm,\theta}.$$

If $\theta \simeq 10^{-10}$, the only possibility of observing Strong CP-odd effects is by looking at systems permeated by much stronger magnetic fields coherent over much larger volumes.

Before considering such systems, we also perform a finite temperature calculation: we will see that at finite temperature the polarization effect is enhanced.

4.1.4 CP-odd Vacuum Polarization at Finite Temperature

In this section we will present the results for CP-odd vacuum polarization at finite temperature. We, will see that thermal fluctuations give raise to a much stronger effect; in fact, anomalous interactions can interact directly with pion fluctuations in the heat bath, thus reducing the number of loops and hence the chiral dimension of the diagram.

Without entering in the details, at low temperatures it is possible to expand the matrix elements so that any vacuum expectaion value gets the following expression

$$\langle \mathcal{O} \rangle_T = \langle \mathcal{O} \rangle_{T=0} + \int \frac{\mathrm{d}^3 k}{(2\pi)^3 2k} \frac{1}{e^{\beta k} - 1} \sum_a \langle \varphi_a(k) \mathcal{O} \varphi_a(k) \rangle,$$

where the sum is over all excitations $\phi_a(k)$ with energy $\ll T$, that is to say our pseudoscalar mesons with momentum k. In our case this gives

$$\begin{aligned} \langle J^0_{e.m.} \rangle_T &= \langle J^0_{e.m.} \rangle_{T=0} + \\ + &\int \frac{\mathrm{d}^3 k}{(2\pi)^3 2k} \frac{1}{e^{\beta k} - 1} \left(\langle \pi^0(k) | J^0_{e.m.} | \pi^0(k) \rangle + \langle \pi^+ | J^0_{e.m.} | \pi^-(k) \rangle \right), \end{aligned}$$

where the first term is equivalent, at lowest order, to the chiral $O(p^6)$ zero temperature vacuum polarization we evaluated in the previous part of the chapter. The second part needs the evaluation of a pion-pion amplitude: we have then to consider which is the lowest chiral order contribution to this matrix element.

For the same considerations of section (4.1.1) we require this matrix element to have $N_{d,\theta} = 1$ $\theta-$vertices and $N_{d,WZW} = 1$ WZW anomalous interactions, and we require the latter to be under the form of an anomalous current: this implies that the diagrams are of the kind in Fig (4.4). For a detailed calculations, see again [36]; at finite temperature, at the lowest chiral order $O(p^4)$ in the presence of an external magnetic field the vacuum has a linear response

$$\mathbf{P}(x) = \frac{25 \alpha m_\pi^2}{96 \pi F m_\eta^2} \theta \mathbf{B}(x) \int \frac{\mathrm{d}^3 k}{(2\pi)^3 2k} \frac{1}{e^{\beta k} - 1}. \tag{4.13}$$

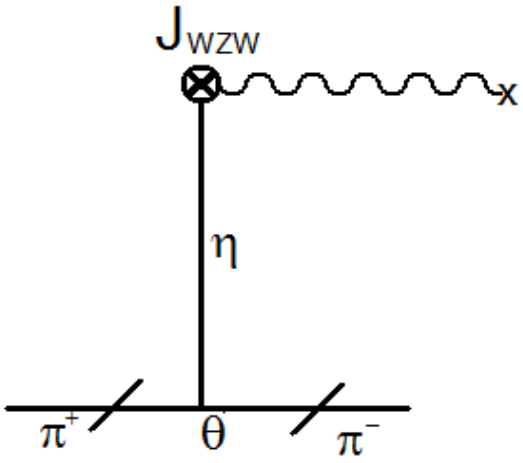

Figure 4.4: Lowest order $O(p^4)$ amplitude: equivalent to $\langle\pi|J^0_{WZ,e.m.}|\pi\rangle$.

Since in ChPT we deal with energies much lower than $\Lambda_{SChSB} \simeq 1GeV$, we can approximate the integral over momenta by imposing a cutoff at m_π:

$$\mathbf{P}(x) = \frac{5}{9}\frac{\alpha\,\theta}{m_\eta^2(4\pi F)^2}\frac{5\pi m_\pi^2}{16}\mathbf{B}(x)T^2. \tag{4.14}$$

In conclusion, both at zero and finite temperature, the QCD θ vacuum is electrically polarized by an external magnetic field. The polarization vector due to CP violating interactions is aligned along the axis of the field. The vacuum behaves as a material medium with a non linear response, as it can be seen by the frequency spectrum of the polarization in the presence of an oscillating external field. The link between strong and electromagnetic interaction is the η field. Hence the process represents a purely quantum-mechanical effect, because of the connection of the η field with axial anomaly.

4.1.5 CP-odd Effects in Magnetars

As we have seen in section 4.1.2 CP-odd effects at zero temperature are extremely small. We now consider an astrophysical object which possess an extremely intense magnetic field $B \simeq 10^{15}Gauss$ and which in its early lifetime has a surface temperature of $T \simeq 1MeV$: this is the Magnetar, a neutron star and the observed astrophysical object with the most intense magnetic field ever observed.

Up to now there are only few known magnetars, and it is still not clear what is the mechanism which enables them to possess such an intense mag-

netic field; on the other hand, as any other typical neutron star, it is supposed that they must have a mass of the order of the solar mass, a dimater of $d \simeq 10^4 m$, and that their rotation frequency should be $\omega \simeq 1Hz$.
Their magnetic field is supposed to have a dipolar form and due to their rotation they are also embedded with a quadrupolar electric field generated by an induced electric charge density

$$\rho_\omega = -\frac{1}{2\pi}\omega \cdot \mathbf{B}.$$

Rotation effects on the distribution of electric charge could be considered as a "classic" CP-even polarization effect: we are now going to show that in the pesence of a non-vanishing θ a neutron star is also embedded with an effective CP-odd dipolar electric field, induced by an effective CP-odd polarization of the neutron star magnetosphere.

Magnetars: CP-odd Dipolar Electric Field

In the following calculations we will not consider effects of Strong-CP violation within the neutron star: such an object is too dense for ChPT to be applied. We will just consider the contribution of $\theta \neq 0$ to the polarization of the magnetosphere of the neutron star, which can be considered in good approximation as a $T \simeq 0$ vacuum permeated by the magnetic field of the star.

It can be shown that at large distances the effects of a dipolar magnetic field if $\mathbf{B}_M(x)$, if integrated over all the magnetosphere, results in an effective dipolar field — see Fig (4.5)—

$$\mathbf{B}_M(\mathbf{x}) = \frac{1}{r^3}[3(\mathbf{M}\cdot\hat{\mathbf{r}})\hat{\mathbf{r}} - \mathbf{M}], \tag{4.15}$$

$$\Downarrow \tag{4.16}$$

$$\mathbf{E}_M(\mathbf{x}) = \frac{1}{r^3}[3(\mathbf{D}_M\cdot\hat{\mathbf{r}})\hat{\mathbf{r}} - \mathbf{D}_M], \tag{4.17}$$

where the CP-odd EDM is given by

$$|\mathbf{D}_M(\theta)| = 3\times 10^{26}\theta \; e\,cm.$$

That is to say that *the non-vanishing of CP-odd $\theta-$interactions would imply the existence of a finite electric dipole aligned along the magnetic dipole of the neutron star.*

We recall that this is a pure quantum mechanical effect and that measurements of effects related to the presence of such a dipolar electric field may be the first direct evidence for a finite θ background.

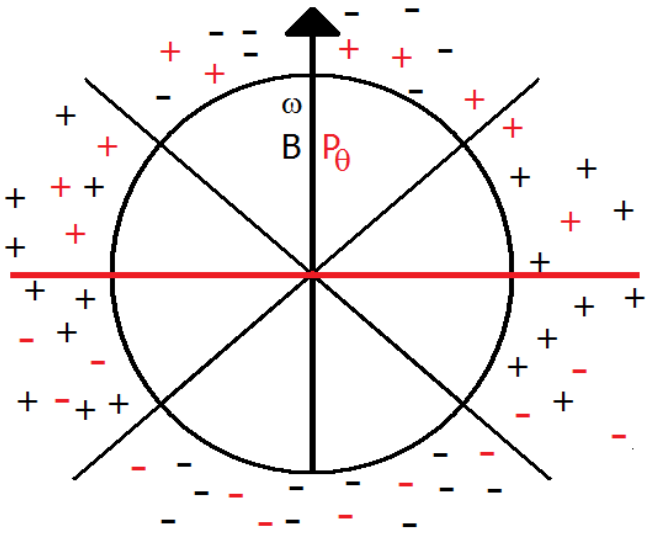

Figure 4.5: Qualitative CP-odd effect on a Neutron Star, with $\mathbf{B}||\omega$: the CP-even quadrupolar electric field (black + and - signs) is accompanied with a CP-odd $\theta-$dependent dipolar electric field (red + and - signs)

Magnetars: Acceleration of Charges

In the previous section we have seen that the presence of CP-odd interactions may lead to peculiar qualitative effects, such as the presence of an electric dipole moment in neutron stars; we now consider possible quantitative effects, by studying the dynamics of charged particles closed to the surface of the magnetar.

The existence of an electric dipole moment in magnetars has, as a first direct implication, that of modifying the distribution of charges in the magnetar surface. In fact, a positively (negatively) charged particle closed to the south (north) magnetic pole, may be accelerated along the magnetic field lines by CP-violating interactions. This can be expressed in terms of an effective CP-odd induced difference of potential V_θ:

$$V_\theta(T) = \theta \left\{ 3 \left(\frac{B}{10^{15} G} \right)^2 + 2 \times 10^6 \left(\frac{T}{1 MeV}^2 \right) \right\} \times 10^6 \left(\frac{L}{1m} \right) \left(\frac{B}{10^{15} G} \right) Volt.$$

Which implies that

T=0: if $\theta \simeq 10^{-10}$ an electron at rest may be accelerated at energies of the order of $3eV \div 3MeV$, assuming $B = 10^{15} \div 10^{17} G$: note that the typical electron energy on the neutron star surface is $\simeq 1KeV$;

T=1MeV: if $\theta \simeq 10^{-10}$ an electron at rest may be accelerated at energies of the

order of $2 \div 200 MeV$, assuming $B = 10^{15} \div 10^{17} G$: where that typical electron energy on the neutron star surface is obviously $\simeq 1 MeV$;

These results are obtained with a value of θ *extremely small*: if θ was of order 1, the transferred energies would be of the order of $1 GeV/1m$ even at zero temperature.

Results at values of the upper bound for θ are nonetheless interesting: the energy transferred to electrons is comparable with the typical energy of electrons on the surface of the neutron star. This energy may be dissipated by electrons on the north magnetic pole of the star: this might increase the temperature of the neutron star in certain "spots". Astrophysical observation actually signals the presence of "hot spots" on neutron stars, with temperatures of the order of few KeV, but we cannot conclude with certainty that these are CP-odd induced.

4.2 CP-odd Vacuum-Birefringence

Results in this section have been published in [37].
In this second part of the chapter, we discuss the implications of Strong CP-violation in the dynamics of photons at very low energies. We will show in particular that induced CP-odd photon-photon interactions may have observables effects on the dynamics of photon in a Fabry-Perot cavity permeated by an external electromagnetic field. These effects are a consequence of a $\theta-$dependent CP-odd vacuum birefringence.

Vacuum birefringence is one of the many consequences of the non-linear response of the quantum vacuum, in the presence of external electromagnetic fields: a linearly polarized wave propagating in a region permeated by a magnetic field would acquire a finite ellipticity Ψ [38][39][40][41]. In particular, if CP symmetry is conserved the acquired ellipticity has the following general structure,

$$\Psi_{\text{CP-even}}(\mathbf{B}, L) = \frac{\pi}{\lambda}(n_2(\mathbf{B}) - n_1(\mathbf{B}))\ L \times \sin 2\alpha_0, \tag{4.18}$$

where λ is the wavelength of the electromagnetic wave, L is the distance travelled in the cavity, n_1 and n_2 are the refraction indexes along the axes perpendicular and parallel to the external field and, α_0 is the angle between the polarization axis of the incoming wave and the direction selected by the external field (see Fig. 4.6).

A small amount of CP violation inside the quantum loops mediating photon-photon interactions would imply an additional contribution to the acquired ellipticity, in the form

$$\Psi = \Psi_{\text{CP-even}} + \Psi_{\text{CP-odd}}. \tag{4.19}$$

The correction from CP-odd term reads

$$\Psi_{\text{CP-odd}} = \epsilon\ \frac{\pi}{\lambda}(n_2(\mathbf{B}) - n_1(\mathbf{B}))\ L \times \cos 2\alpha_0, \tag{4.20}$$

where ϵ is a small parameter, which measures the amount of CP violation. The QCD contribution to $\Psi_{\text{CP-odd}}$ obviously comes from the θ-term, and can be calculated using the EFT approach, i.e. by matching the results of the very low-energy theory — QED's EFT — with the "fundamental theory" — ChPT —. In the following sections we will then first of all use the result of the ChPT calculation to determine the effective coefficient of the leading CP-odd term in the effective field theory for low-energy photon dynamics; we will then express $\Psi_{\text{CP-odd}}$ in terms of such a coefficient.

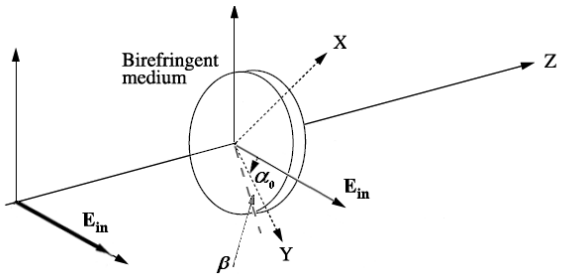

Figure 4.6: Polarization planes and refraction indexes in an electromagnetic wave propagating in a resonant cavity (see the details in the text).

4.2.1 Effective QED Lagrangian

At energy scales much below the electron mass, the quantum dynamics of the electromagnetic field can be rigorously formulated in terms of an effective theory, in which the only dynamical degrees of freedom are soft photons. As for QCD, in order to describe the low-energy non-perturbative QED dynamics, we consider the most general effective Lagrangian compatible with $U_{e.m.}(1)$ gauge and Lorentz symmetries: $\mathcal{L}_{eff}$ contains an infinite tower of CP-even and CP-odd operators of increasing effective dimension. The effective coefficients, as in ChPT, encode information on the physics above the cut-off scale Λ, and can in principle be determined explicitely, by means of microscopic calculations in the underlying, more fundamental theory.

The most general effective Lagrangian is constructed by combining powers of Lorentz invariant operators: the scalar

$$X = \mathbf{B}^2 - \mathbf{E}^2 = \frac{1}{2} F_{\mu\nu} F^{\mu\nu}, \tag{4.21}$$

and the pseudoscalar,

$$Y = \mathbf{B} \cdot \mathbf{E} = \frac{1}{2} F_{\mu\nu} \tilde{F}^{\mu\nu}. \tag{4.22}$$

Clearly, the CP-odd dynamics is encoded in the terms containing an odd number of Y operators. The lowest-order terms in the effective Lagrangian read

$$\mathcal{L}_{eff} = -\frac{1}{2} X + a\, Y + b\, X^2 + c\, Y^2 + d\, XY + \dots \tag{4.23}$$

The effective coefficient a can be set to zero, since the pseudo-scalar operator Y is a total derivative, while the effective coefficients b, c and d appear only at the quantum level. In principle, these coefficients receive contributions from the electro-weak and strong sectors of the Standard Model and, possibly,

also from dynamics beyond the Standard Model. In particular, the leading contribution to b and c comes from QED and has long been calculated[42]

$$b = \frac{2\alpha^2}{45m_e^4}, \qquad c = 7b. \tag{4.24}$$

The coefficient d in Eq. (4.23) parametrizes the short-distance CP-violating dynamics. Within the Standard Model, if the QCD θ-angle is greater than 10^{-13}, the leading contribution to d comes from the strong sector. On the other hand, for smaller values of θ, d is dominated by the weak interactions. In this work, we shall assume the first scenario and in the remaining part of this section we compute the QCD contribution to d.

4.2.2 Calculation of the CP-odd Effective Coefficient

Let us consider the response of the vacuum to an external electro-magnetic field $F^{\text{ext.}}_{\mu\nu} = (\mathbf{E}, \mathbf{B})$. It is convenient to introduce the electric displacement field $\mathbf{D}$ and the auxiliary magnetic field $\mathbf{H}$, defined as

$$\mathbf{D} = \frac{\partial \mathcal{L}}{\partial \mathbf{E}} = \mathbf{E} + \mathbf{P}, \tag{4.25}$$

$$\mathbf{H} = -\frac{\partial \mathcal{L}}{\partial \mathbf{B}} = \mathbf{B} - \mathbf{M}. \tag{4.26}$$

where $\mathbf{P}$ and $\mathbf{M}$ are the polarization and magnetization vectors, respectively. From Eq. (4.23) we obtain

$$\mathbf{D} = [1 - 4bX - 2dY]\mathbf{E} + [2cY + dX]\mathbf{B} + \dots, \tag{4.27}$$

$$\mathbf{H} = [1 - 4bX - 2dY]\mathbf{B} - [2cY + dX]\mathbf{E} + \dots. \tag{4.28}$$

As expected, the non-linear vacuum polarization is a purely quantum effect. In the absence of CP violation — i.e. if $d = 0$ — a purely electric (magnetic) external field would induce a purely electric polarization (magnetization) along the same direction, i.e.

$$\mathbf{B} = 0, \mathbf{E} \neq 0 \overset{\text{CP}}{\Longrightarrow} \mathbf{D} = 4bE^2\mathbf{E}, \tag{4.29}$$

$$\mathbf{E} = 0, \mathbf{B} \neq 0 \overset{\text{CP}}{\Longrightarrow} \mathbf{H} = -4bB^2\mathbf{B}. \tag{4.30}$$

This condition is no longer verified if CP is broken. In fact, if $d \neq 0$, a purely magnetic (electric) external field can generate an electric polarization (magnetization) along the same direction, i.e.

$$\mathbf{B} \neq 0, \mathbf{E} = 0 \overset{\text{CP-viol.}}{\Longrightarrow} \mathbf{D} = dB^2\mathbf{B}, \tag{4.31}$$

$$\mathbf{E} \neq 0, \mathbf{B} = 0 \overset{\text{CP-viol.}}{\Longrightarrow} \mathbf{H} = dE^2\mathbf{E}. \tag{4.32}$$

The relationship (4.31) can be used to compute the effective coefficient of the leading CP-odd term in the effective Lagrangian (4.23). In fact, the calculation we performed in section 4.1.2 implies that the vacuum electric dipole moment at finite θ is

$$\mathbf{D} = \frac{5}{9}\frac{\alpha^2\theta}{m_{\eta'}^2(4\pi f_\pi)^2}\ B^2\ \mathbf{B}, \tag{4.33}$$

The strong contribution to the coefficient d is then immediately obtained by matching Eq. (4.33) with Eq. (4.31) and reads

$$d = \frac{5}{9}\frac{\alpha^2\theta}{m_{\eta'}^2(4\pi f_\pi)^2}. \tag{4.34}$$

We also note that using eq. (4.32) and (4.34), it is immediate to obtain the CP-odd magnetization induced by an external electric field

$$\mathbf{M} = -\frac{5}{9}\frac{\alpha^2\theta}{m_{\eta'}^2(4\pi f_\pi)^2}\ E^2\ \mathbf{E}. \tag{4.35}$$

In the next sections, we evaluate the contribution of the CP-odd component of the low-energy photon-photon interaction (4.23) to the induced ellipticity of an electromagnetic wave, propagating in a cavity.

4.2.3 CP-even Vacuum Birefringence

Let us consider an electromagnetic wave, characterized by the fields $(\mathbf{e}, \mathbf{b})$, propagating along the $\hat{z}$ direction and linearly polarized along an axis rotated by an angle α_0 with respect to the $\hat{y}$-axis (see Fig. 4.6):

$$\mathbf{e}(\mathbf{x}, t) = e_0\ \left(\cos\alpha_0\ \hat{y} + \sin\alpha_0\ \hat{x}\right)\ e^{i(k_z z - \omega t)}. \tag{4.36}$$

The wave enters a cavity filled with a constant and uniform magnetic field $\mathbf{B}$, directed along the $\hat{y}$ axis. After traveling for a distance L, the electromagnetic wave develops an elliptic polarization, which has both CP-even and CP-odd components. Let us first review the calculation of the CP-conserving contribution [41].

The dynamics of the electromagnetic field is conveniently described in terms of the vacuum electric and magnetic permeability tensors ε_{ij} and μ_{ij}, which are defined as

$$d_i = \varepsilon_{ij}\, e_j, \qquad h_i = \mu_{ij}\, b_j, \tag{4.37}$$

where and $\mathbf{d}$ and $\mathbf{h}$ are the usual displacement vector and auxiliary magnetic field,

$$\mathbf{d} = \frac{\partial\mathcal{L}}{\partial\mathbf{e}}, \qquad \mathbf{h} = -\frac{\partial\mathcal{L}}{\partial\mathbf{b}}. \tag{4.38}$$

In terms of the CP-even coefficients of the effective Lagrangian (4.23), the electric and magnetic permeability tensors have the following expression

$$\varepsilon_{ij} = \left(1 - 4bB^2\right)\delta_{ij} + 2cB_iB_j, \tag{4.39}$$
$$\mu_{ij} = \left(1 - 4bB^2\right)\delta_{ij} - 8bB_iB_j. \tag{4.40}$$

Since $\mathbf{d}$ and $\mathbf{h}$ must satisfy a wave equation, ε and μ must depend only on the external magnetic field $\mathbf{B}$ and not fields $\mathbf{e}$ and $\mathbf{b}$. Maxwell's Eq.s imply

$$\mathbf{k}\cdot\mathbf{b} = 0, \tag{4.41}$$
$$\mathbf{k}\cdot\mathbf{d} = 0, \tag{4.42}$$
$$\mathbf{k}\times\mathbf{e} = \omega\mathbf{b}, \tag{4.43}$$
$$\mathbf{k}\times\mathbf{h} = -\omega\mathbf{d}, \tag{4.44}$$

where $\mathbf{k}$ is the propagation vector of the wave. By substituting $\mathbf{b}$ of Eq.(4.43) in Eq.(4.44) we obtain

$$\epsilon_{ijq}\ k_j[\mu_{ql}\ (\mathbf{k}\times\mathbf{e})_l] + \omega^2\varepsilon_{il}e_l = 0, \tag{4.45}$$

where ϵ_{ijq} denotes the usual rank-3 completely anti-symmetric tensor. Using the relationships (4.39) and (4.40), Eq. (4.45) can be written in the following matrix form

$$\begin{pmatrix}\lambda_1 & 0\\ 0 & \lambda_2\end{pmatrix}\ \begin{pmatrix}e_1\\ e_2\end{pmatrix} = 0, \tag{4.46}$$

with

$$\lambda_1 = -\frac{\mathbf{k}^2}{\omega^2}[1 - 12\,b\ \mathbf{B}^2] + 1 - 4b\mathbf{B}^2, \tag{4.47}$$
$$\lambda_2 = -\frac{\mathbf{k}^2}{\omega^2}[1 - 4\,b\ \mathbf{B}^2] + 1 + 2(c-2b)\mathbf{B}^2. \tag{4.48}$$

The two solutions of this equation give the refraction indeces along $\hat{x}$ and $\hat{y}$, respectively:

$$n_1 = 1 + 4\,b\ \mathbf{B}^2 + \ldots, \tag{4.49}$$
$$n_2 = 1 + c\ \mathbf{B}^2 + \ldots. \tag{4.50}$$

If the incoming wave is linearly polarized along the eigenvectors of λ_1 and λ_2 —i.e. along the $\hat{x}$ and $\hat{y}$ axis— it will remain linearly polarized, even inside the region permeated by the magnetic field. On the other hand, if the incoming wave is polarized along an axis forming a finite angle α_0 with respect to the direction selected by the eigenvector with the greatest eigenvalues —i.e. the $\hat{y}$ axis—, it will acquire an ellipticity [41]

$$\Psi_{\text{CP-even}}(\mathbf{B}, L) = \frac{\pi}{\lambda}(n_2(\mathbf{B}) - n_1(\mathbf{B}))L \times \sin 2\alpha_0 \tag{4.51}$$
$$= \frac{\pi}{\lambda}\ (c-4b)\ \mathbf{B}^2\ L\sin 2\alpha_0. \tag{4.52}$$

4.2.4 CP-odd Contribution to Vacuum Birefringence

We now compute the ellipticity induced on the electromagnetic wave, in the presence of CP-violating vacuum polarization. In this case, the electric displacement field $\mathbf{d}$ and auxiliary magnetic field $\mathbf{h}$ receive additional contributions $\Delta\mathbf{d}$ and $\Delta\mathbf{h}$, which depend on the CP-odd effective coefficient d,

$$\mathbf{d} = \mathbf{d}_{\text{CP-even}} + \Delta\mathbf{d}, \tag{4.53}$$

$$\mathbf{h} = \mathbf{h}_{\text{CP-even}} + \Delta\mathbf{h}, \tag{4.54}$$

with

$$\Delta\mathbf{d} = 2d\,\mathbf{B}[\mathbf{b}\cdot\mathbf{B}] + d\,\mathbf{b}\,\mathbf{B}^2, \tag{4.55}$$

$$\Delta\mathbf{h} = -2d\,\mathbf{B}[\mathbf{e}\cdot\mathbf{B}] - d\,\mathbf{e}\,\mathbf{B}^2. \tag{4.56}$$

Maxwell's Eq.s now give

$$\epsilon_{ijq}\ k_j[\mu_{ql}\ (\mathbf{k}\times\mathbf{e})_l] + \omega^2\varepsilon_{il}e_l = 2d\,[(\epsilon_{ijq}k_jB_q)e_lB_l + B_i([(\mathbf{k}\times\mathbf{B})_je_j]. \tag{4.57}$$

The CP-odd interactions introduce non-diagonal elements in the matrix (4.45), which now becomes:

$$\begin{pmatrix}\lambda_1 & C\\ C & \lambda_2\end{pmatrix}\ \begin{pmatrix}e_1\\ e_2\end{pmatrix} = 0, \tag{4.58}$$

where λ_1 and λ_2 are the same as in Eq.s (5.73),(4.48) and

$$C = 2\,\frac{k}{\omega}d\,\mathbf{B}^2. \tag{4.59}$$

As in the CP-even case, an incoming wave which is linearly polarized along the eigenvectors of the matrix (4.58) does not acquire ellipticity. Up to higher corrections in the effective coefficient d, the eigenvalues of (4.58) — i.e. the refraction indexes— are the same as those of (4.50). On the other hand, the new eigenvectors are rotated by an angle β given by

$$\beta = \frac{d}{c-4b} + O(\mathbf{B}^2). \tag{4.60}$$

Consequently, the final expression for the ellipticity acquired in the cavity, in the presence of CP-violation reads

$$\Psi = \frac{\pi}{\lambda}\ (c-4b)\mathbf{B}^2\ L\sin 2(\alpha_0-\beta). \tag{4.61}$$

We expect CP-violation to provide at most a small correction to the total ellipticity, i.e. $\beta \ll \alpha_0$. In this case,

$$\Psi \simeq \Psi_{\text{CP-even}} + \Psi_{\text{CP-odd}}, \tag{4.62}$$

with

$$\Psi_{\text{CP-odd}} = -2\pi d \frac{L}{\lambda} \mathbf{B}^2 \cos 2\alpha_0. \tag{4.63}$$

This Eq. has been independently obtained in [38] and [39].

Within the Standard Model, the CP-odd correction is indeed extremely small. For example, if we consider a set-up characterized by an angle $\alpha_0 = \pi/8$, for which the trigonometric factor cancels out, then the ratio between the $\Psi_{\text{CP-even}}$ and $\Psi_{\text{CP-odd}}$ is

$$\left(\frac{\Psi_{\text{CP-odd}}}{|\Psi_{\text{CP-even}}|} \right)_{\alpha=\pi/8} \simeq \frac{2d}{c-4b} \simeq \theta \times 10^{-12} < 10^{-22}. \tag{4.64}$$

However, it is important to stress that the CP-odd and CP-even contributions to the ellipticity are *qualitatively* different and therefore can be experimentally disentangled. In particular, if α_0 is chosen to be $0, \pi/2, \ldots$, then the CP-even contribution vanishes and the entire ellipticity is due to CP-violating quantum photon-photon interactions. In this case, any significant deviation from our estimate,

$$\Psi_{\text{CP-odd}} \simeq -\frac{10\pi\alpha^2\theta}{9m_{\eta'}^2(4\pi f_\pi)^2} \frac{L}{\lambda} \mathbf{B}^2, \tag{4.65}$$

would represent a clear signature of CP-violating physics beyond the Standard Model. In the next section, we shall discuss the possibility of measuring the CP-odd ellipticity using a Fabry-Perot cavity.

4.2.5 Propagation of Light in a Fabry-Perot Cavity

We now consider an electromagnetic wave propagating in a Fabry-Perot cavity: after travelling a distance L given by the cavity length, the wave is reflected and turns back along the same path to the entrance of the cavity, where it is reflected again...

After a single reflection, both the polarization vector $\mathbf{e}$ and the wave vector $\mathbf{k}$ change sign: this affects both the angles α_0 and β. In fact, the angle α_0 will undergo a rotation of 180°

$$\alpha_0 \quad \longrightarrow \alpha_0^{'} = \alpha_0 + \pi, \tag{4.66}$$

$$\beta \quad \longrightarrow \beta^{'} = -\beta, \tag{4.67}$$

while the angle β changes sign. The latter effect occurs because β is proportional to the coefficient C in Eq.(4.58): since C is linear in k, by inverting the direction of the electromagnetic wave the sign of β changes. On the

contrary, the indexes of refraction n_1 and n_2 remain unchanged, because λ_1 and λ_2 are quadratic in k, see Eq.s(5.73) and (4.48).

Thus, the contribution to the total ellipticity during the return part of the round trip is given by

$$\Psi^{'} = \frac{\pi}{\lambda}\,(c-4b)\mathbf{B}^2\; L\sin 2(\alpha_0^{'}-\beta^{'}) \tag{4.68}$$

$$= \frac{\pi}{\lambda}\,(c-4b)\mathbf{B}^2\; L\sin 2(\alpha_0+\beta), \tag{4.69}$$

Hence, the total amount of CP-odd ellipticity of the wave after a round trip is

$$\Psi_{\text{CP-odd,R}} = \Psi_{\text{CP-odd}} + \Psi^{'}_{\text{CP-odd}} = 0. \tag{4.70}$$

After being reflected 2N times in the resonant cavity, the total ellipticity gained by the electromagnetic wave will be

$$\Psi_{TOT} = (2N+1)\Psi_{\text{CP-even}} + \Psi_{\text{CP-odd}}. \tag{4.71}$$

Thus, we conclude that the experimental setup formed by a magnetic field in a resonant cavity is not suitable for measurements of CP-odd ellipticity: there is no enhancement of the CP-odd signal after several round trips.

Cavity permeated by Magnetic and Electric Fields

We now show that if the cavity is also permeated by an electric field set up in the plane perpendicular to $\mathbf{k}$, the CP-odd ellipticity does not cancel out, in general, after a round trip. To this end, one as to perform again the calculations in the previous seection, considering an external electromagnetic field $(\mathbf{E},\mathbf{B})$ instead of only $(\mathbf{0},\mathbf{B})$. After a tedious but straightforward calculation one obtains the following results for the *forward* and *backward* ellipticities Ψ^f and Ψ^b:

$$\Psi^f_{\text{CP-even}} = \frac{\pi}{\lambda}(c-4b)\left[\mathbf{B}^2\times\sin 2\alpha_B - \mathbf{E}^2\times\sin 2\alpha_E - 2|\mathbf{E}|\,|\mathbf{B}|\cos(\alpha_B+\alpha_E)\right],$$

$$\Psi^f_{\text{CP-odd}} = -2d\frac{\pi}{\lambda}\left[\mathbf{B}^2\times\cos 2\alpha_B - \mathbf{E}^2\times\cos 2\alpha_E + 2|\mathbf{E}|\,|\mathbf{B}|\sin(\alpha_B+\alpha_E)\right],$$

$$\Psi^b_{\text{CP-even}} = \frac{\pi}{\lambda}(c-4b)\left[\mathbf{B}^2\times\sin 2\alpha_B - \mathbf{E}^2\times\sin 2\alpha_E + 2|\mathbf{E}|\,|\mathbf{B}|\cos(\alpha_B+\alpha_E)\right],$$

$$\Psi^b_{\text{CP-odd}} = 2d\frac{\pi}{\lambda}\left[\mathbf{B}^2\times\cos 2\alpha_B - \mathbf{E}^2\times\cos 2\alpha_E - 2|\mathbf{E}|\,|\mathbf{B}|\sin(\alpha_B+\alpha_E)\right].$$

After a round trip, the total ellipticity amounts to

$$\Psi_{\text{CP-even,R}} = \Psi^f_{\text{CP-even}} + \Psi^b_{\text{CP-even}}$$

$$= 2\frac{\pi}{\lambda}(c-4b)\left[\mathbf{B}^2\times\sin 2\alpha_B - \mathbf{E}^2\times\sin 2\alpha_E)\right], \tag{4.72}$$

$$\Psi_{\text{CP-odd,R}} = \Psi^f_{\text{CP-odd}} + \Psi^b_{\text{CP-odd}}$$

$$= -8d\frac{\pi}{\lambda}|\mathbf{E}|\,|\mathbf{B}|\sin(\alpha_B+\alpha_E). \tag{4.73}$$

Hence after 2N reflections, the total ellipticity is

$$\Psi_{\rm TOT} = N\left[\Psi_{\text{CP-even,R}} + \Psi_{\text{CP-odd,R}}\right] + \left[\Psi^{f}_{\text{CP-even}} + \Psi^{f}_{\text{CP-odd}}\right]. \quad (4.74)$$

Notice that the CP-odd ellipticity is maximum if $(\alpha_B + \alpha_E) = \pi/2, 3\pi/2, ..$ and vanishes for $(\alpha_B + \alpha_E) = 0, \pi, ...$ Notice also that, if the electric and magnetic fields are orthogonal to each other — i.e. if $\alpha_E - \alpha_B = \pm\pi/2$—, then one recovers the structure of the CP-even and CP-odd ellipticities in Eq.s(4.51) and (4.63)

$$\Psi_{\text{CP-even}} = 2\frac{\pi}{\lambda}(c-4b)\left[\mathbf{B}^2 + \mathbf{E}^2\right]\sin 2\alpha_B, \quad (4.75)$$

$$\Psi_{\text{CP-odd}} = \mp 8d\frac{\pi}{\lambda}|\mathbf{E}|\,|\mathbf{B}|\cos 2\alpha_B, \quad (4.76)$$

On the contrary, if the electric and magnetic fields are parallel to each other — i.e. $\alpha_B = \alpha_E$— both contributions will be proportional to $\sin 2\alpha_B$

$$\Psi_{\text{CP-even}} = 2\frac{\pi}{\lambda}(c-4b)\left[\mathbf{B}^2 - \mathbf{E}^2\right]\sin 2\alpha_B, \quad (4.77)$$

$$\Psi_{\text{CP-odd}} = -8d\frac{\pi}{\lambda}|\mathbf{E}|\,|\mathbf{B}|\sin 2\alpha_B. \quad (4.78)$$

In the next section we study the effects of modulating the external fields on the spectrum of the intensity of the outgoing wave.

4.2.6 Consequences on PVLAS-like Experiments

The main goal of the experiments PVLAS [43] and BMV [44] is to study the birefringence and the dichroism induced by the quantum fluctuations in the QED vacuum, in the presence of an external magnetic field **B**. In the following, we restrict our attention to the implications of CP-violating quantum fluctuations on the vacuum birefringence. We compare two scenarios, one in which only the magnetic field permeates the cavity and one in which also an electric field **E** is present.

Let us begin with the first case, which is the one implemented at PVLAS and BMV. The experimental setup consists of a Fabry-Perot cavity, placed between two crossed polarizers (Fig. 4.7). The cavity is uniformly filled with a magnetic field **B**, rotating with angular frequency ω_B, along the plane perpendicular to the wave vector of the incoming light. Since the magnetic field is rotating, the total induced ellipticity is time-dependent, $\Psi = \Psi(\omega_B t + \alpha_B)$, where α_B is the angle between the polarization vector and the magnetic field at the time $t = 0$.

It can be shown that the intensity of the outgoing wave has the following form [43][45]

$$I_{out} = I_{in}\left|\frac{2\mathcal{F}}{\pi}\, i\,\Psi_{\text{CP-even}}\left(\omega_B\, t + \alpha_B\right) + i\,\Psi_{\text{CP-odd}}\left(\omega_B\, t + \alpha_B\right)\right|^2, \quad (4.79)$$

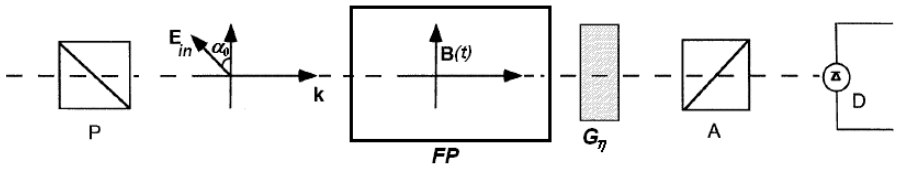

Figure 4.7: Schematic representation of the experimental setup of PVLAS (see text). P and A are the cross-polarizers, FP is the Fabry-Perot cavity, G_η is generator of the additional ellipticity $\eta(t)$ and D is the detector. Picture taken from [43].

where I_0 is the intensity of the incoming wave, $\mathcal{F}$ is the so-called finesse of the Fabry-Perot cavity.

The ellipticity Ψ generated by the quantum vacuum polarization is in general expected to be a small effect. Hence, in order to increase the intensity of the wave coming out the last polarizer, an additional time-dependent classical ellipticity $\eta(t)$ is introduced by means of a modulator. This way, the intensity of the outgoing wave becomes linear in the ellipticity $\Psi(t)$:

$$I_{out} \simeq I_{in}\eta(t)\left\{\eta(t) + 4\frac{\mathcal{F}}{\pi}\Psi_{\text{CP-even}}\left(\omega_B\, t + \alpha_0\right) + 2\Psi_{\text{CP-odd}}\left(\omega_B\, t + \alpha_B\right)\right\} + O\left(\psi^2\right) \quad (4.80)$$

In particular, let us consider the case in which the classical ellipticity $\eta(t)$ is modulated with a frequency ω_η,

$$\eta(t) = \eta_0\, \cos(\omega_\eta\, t + \alpha_\eta). \quad (4.81)$$

In this case, the intensity of the outgoing wave is

$$\begin{aligned} I_{out,\psi}(t) \;=\; & L\frac{\pi}{\lambda}\,\mathbf{B}^2\, I_{in}\,\eta_0\Big[2\frac{\mathcal{F}}{\pi}(c-4b)\big\{\sin\left[(\omega_\eta + 2\omega_B)t + \alpha_\eta + 2\alpha_0\right] \\ & - \sin\left[(\omega_\eta - 2\omega_B)t + \alpha_\eta - 2\alpha_0\right]\big\} - 2d\big\{\cos\left[(\omega_\eta + 2\omega_B)t + \alpha_\eta + 2\alpha_0\right] \\ & + \cos\left[(\omega_\eta - 2\omega_B)t + \alpha_\eta - 2\alpha_0\right]\big\}\Big]. \end{aligned} \quad (4.82)$$

The CP-even and CP-odd contributions to the induced ellipticity can be disentangled by Fourier analysis. In fact, we see that the Fourier spectrum of $I_{out,\psi}$ contains:

- Two CP-even Fourier components with amplitude given by

$$A_{even} = 2(c-4b)\,\frac{L}{\lambda}\,\mathbf{B}^2\, I_0\,\eta_0\,\mathcal{F}, \quad (4.83)$$

  and frequency and phase given by

$$\Omega_{even,\pm} = \omega_\eta \pm 2\omega_B; \qquad \Phi_{even,\pm} = \alpha_\eta \pm 2\alpha_0. \quad (4.84)$$

- Two CP-odd Fourier components of amplitude given by

$$A_{odd} = 2\,d\,L\frac{\pi}{\lambda}\,\mathbf{B}^2\,I_0\,\eta_0, \tag{4.85}$$

and frequency and phase given by

$$\Omega_{odd,\pm} = \omega_\eta \pm 2\omega_B; \qquad \Phi_{odd,\pm} = \alpha_\eta \pm \left(2\alpha_0 - \frac{\pi}{2}\right). \tag{4.86}$$

Note that, except for $\alpha_0 = \frac{\pi}{8}$, the phases of the CP-even and CP-odd components are different. This fact implies that, at least in principle, it should be possible to probe directly the CP-odd part of the photon-photon interaction by analyzing the spectrum of the outgoing wave. Unfortunately, as we noticed in the previous sections, the amplitude (4.85) of the CP-odd ellipticity is suppressed by a factor $\mathcal{F} \propto N$, where N is the number of round trips in the cavity, respect to the CP-even amplitude (4.83): any signal of CP-violation would be hardly measurable.

Cavity Permeated by Electric and Magnetic Fields

We now discuss what would happen if a time dependent electric field is placed in the Fabry-Perot cavity, along with the magnetic field. If the electric field is modulated with frequency ω_E and phase α_E, by replacing Eq.s(4.72) and (4.73) in Eq.(4.79) the intensity of the outgoing wave in Eq.(4.87) gives, up to $O(\mathcal{F}^0)$

$$\begin{aligned} I_{out,\psi}(t) \;=\; & 2\frac{L}{\lambda}\,I_{in}\,\eta_0\,\mathcal{F}\Big[(c-4b)\mathbf{B}^2\big\{\sin\left[(\omega_\eta+2\omega_B)t+\alpha_\eta+2\alpha_B\right]+ \\ & -\sin\left[(\omega_\eta-2\omega_B)t+\alpha_\eta-2\alpha_B\right]\big\}+ \\ - \;& (c-4b)\mathbf{E}^2\big\{\sin\left[(\omega_\eta+2\omega_E)t+\alpha_\eta+2\alpha_E\right] \\ & -\sin\left[(\omega_\eta-2\omega_E)t+\alpha_\eta-2\alpha_E\right]\big\}+ \\ - \;& 4d|\mathbf{E}|\,|\mathbf{B}|\big\{\sin\left[(\omega_\eta+\omega_B+\omega_E)t+\alpha_\eta+\alpha_B+\alpha_E\right] \\ & -\sin\left[(\omega_\eta-\omega_B-\omega_E)t+\alpha_\eta-\alpha_B-\alpha_E\right]\big\}\Big]. \end{aligned} \tag{4.87}$$

Thus, the spectrum of the outgoing intensity has six characteristic Fourier components

- Two CP-even Fourier components with amplitude given by

$$A_{even,B} = 2(c-4b)\,\frac{L}{\lambda}\,\mathbf{B}^2\,I_0\,\eta_0\;\mathcal{F}, \tag{4.88}$$

and frequency and phase given by

$$\Omega_{even,\pm} = \omega_\eta \pm 2\omega_B; \qquad \Phi_{even,B,\pm} = \alpha_\eta \pm 2\alpha_B. \tag{4.89}$$

- Two CP-even Fourier components with amplitude given by

$$A_{even,E} = 2(c - 4b)\,\frac{L}{\lambda}\,\mathbf{E}^2\,I_0\,\eta_0\;\mathcal{F}, \tag{4.90}$$

and frequency and phase given by

$$\Omega_{even,\pm} = \omega_\eta \pm 2\omega_E; \qquad \Phi_{even,E,\pm} = \pi + \alpha_\eta \pm 2\alpha_E. \tag{4.91}$$

- Two CP-odd Fourier components of amplitude given by

$$A_{odd} = 8\,d\,\frac{L}{\lambda}\,|\mathbf{E}|\,|\mathbf{B}|\,I_0\,\eta_0\mathcal{F}, \tag{4.92}$$

and frequency and phase given by

$$\Omega_{odd,\pm} = \omega_\eta \pm (\omega_B + \omega_E); \qquad \Phi_{odd,\pm} = \pi + \alpha_\eta \pm (\alpha_B + \alpha_E))\,. \tag{4.93}$$

Conclusive Remarks

We then realize that for an experimental setup in which $\alpha_E - \alpha_B = \pi/2$ and $\omega_E = \omega_B$, the four CP-even peaks merge into two peaks. The CP-odd Fourier components of the outgoing intensity spectrum have the same frequency of the CP-even ones, but their phases are shifted by $\pi/2$. Hence, we have recovered our previous result with

$$(c - 4b)\mathbf{B}^2 \qquad \longrightarrow (c - 4b)\left[\mathbf{B}^2 + \mathbf{E}^2\right]\mathcal{F}, \tag{4.94}$$

$$d\mathbf{B}^2 \qquad \longrightarrow \frac{4}{\pi} d\,|\mathbf{E}|\,|\mathbf{B}|\,\mathcal{F}. \tag{4.95}$$

The presence of an electric field in the cavity can significantly increase the sensitivity of the experimental set-up to the CP-odd ellipticity only if the round-trip contribution $\propto d|\mathbf{E}|\,|\mathbf{B}|\mathcal{F}$ is much larger than the one-way contribution, $\propto d\mathbf{B}^2$. This condition is verified if

$$\frac{A_{odd,\mathbf{E}}}{A_{odd,\mathbf{E}=\mathbf{0}}} = \frac{4|\mathbf{E}|\,\mathcal{F}}{\pi|\mathbf{B}|} \gg 1. \tag{4.96}$$

For example, for a typical finesse of 10^5, the condition (4.96) holds for electric fields $\gg 10V/cm$.

The contribution to the coefficient d coming form the θ-term of QCD is at least 20 order of magnitudes smaller than the coefficient of the CP-even term $c-4b$. Given such a huge difference, it is difficult to imagine that an experiment with a resonant cavity will be able to reach the sensitivity required to resolve the Standard Model contribution. Hence, observing evidence for the peaks (4.93) in the spectrum of the outgoing wave would represent a clean signature of CP-violation coming from microscopic dynamics beyond the Standard Model.

Chapter 5

Effective Statistical Theory for Topological Vacuum Gauge Configurations

In the previous chapter we have used ChPT to calculate quantitatively non-perturbative effects at low energies such as CP-odd vacuum polarization; as expected from phenomenological considerations, such an effect is driven by an underlying microscopic dynamics ruled by gluonic configurations with non-trivial topological charge.

We now address the problem of describing explicitely the dynamics of these topological degrees of freedom. In chapter 2, we have seen that this may be achieved by performing a rigorous reparametrization of the QCD path-integral in terms of collective coordinates γ of the topological configurations

$$Z_{QCD} = \int \mathrm{d}\gamma_1 \dots \mathrm{d}\gamma_k e^{-F(\gamma_1,\dots,\gamma_k)}; \tag{5.1}$$

the collective coordinates $\gamma = (\gamma_1, \dots, \gamma_k)$ represents a set of effective low-energy gluonic degrees of freedom, while all other infinite degrees of freedom are explicitly integrated out from the path integral: this give raise to an effective interaction $F(\gamma)$.

In the present chapter, we develop a rigorous formalism which enables to determine the effective interaction $F(\gamma)$ for a generic family of non-perturbative gauge fields, using lattice simulations.

5.1 Effective Interactions from Lattice Simulations

We now present a rigorous description of the reparametrization of the QCD path integral, and give a definition of effective interaction $F(\gamma_1, \ldots, \gamma_k)$ for a generic family of non-perturbative configurations defined by a set of collective coordinate $\gamma = (\gamma_1 \ldots \gamma_k)$. We will then sketch an algorithm for computing such an effective interaction, using lattice gauge simulations.

Our starting point is the Euclidean Yang-Mills path integral

$$Z_{p.g.} = \int \mathcal{D}A_\mu \; e^{-\frac{1}{4g^2}\int d^4x \, G_a^{\mu\nu} G_a^{\mu\nu}}. \tag{5.2}$$

Our goal is reducing the dynamical gauge degrees of freedom of this generating functional, from an infinite set of gluonic excitations to a finite number of effective degrees of freedom, and obtain the following integral representation

$$Z_{p.g.} = \int \mathrm{d}\gamma_1 \ldots \mathrm{d}\gamma_k e^{-F(\gamma_1,\ldots,\gamma_k)}. \tag{5.3}$$

In order to compute the effective interaction $F(\gamma)$, we begin by observing that for any choice of collective coordinates, a generic *gauge fixed* gauge field configuration can be decomposed as

$$A_\mu(x) \equiv \tilde{A}_\mu(x;\gamma) + B_\mu(x). \tag{5.4}$$

From now on we will refer at $B_\mu(x)$ as the "fluctuation field".
Notice that, in general, neither the backgorund field $\tilde{A}$ nor the fluctuation field are solutions of the Euclidean equation of motion: we are not adopting a semiclassical approach.

In Eq.(5.3) we have introduced k additional integral γ_k, we then have to set an equal number of constraints on the fluctuation field. A natural way is by imposing a set of k orthogonality conditions:

$$(B(x) \cdot g_{\gamma_i}(x,\bar{\gamma})) \equiv \mathrm{Tr}_c \left\{ \int \mathrm{d}^4x \; B_\mu(x) \; g_{\gamma_i,\mu}(x,\bar{\gamma}) \right\} = 0, \tag{5.5}$$

$$g_{\gamma_i,\mu}(x,\bar{\gamma}) = \frac{\partial}{\partial\gamma_i}\tilde{A}_\mu(x;\gamma)\Big|_{\gamma=\bar{\gamma}}. \qquad i = 1,\ldots,k. \tag{5.6}$$

Notice that the fucntions $\{g_{\gamma_i}(x,\bar{\gamma})\}$ identify the k directions tangent to the manifold $\mathcal{M}$ of curvilinear coordinates $\bar{\gamma}$, see Fig(5.1). We then consider only choices of the manifold and of $\bar{\gamma}$ such that the vectors (5.6) defines a system of coordinates on the manifold.

In the path integral formalism, the orthogonality conditions in Eq.(5.5) can be implemented by introducing a Fadeev-Popov representation of the

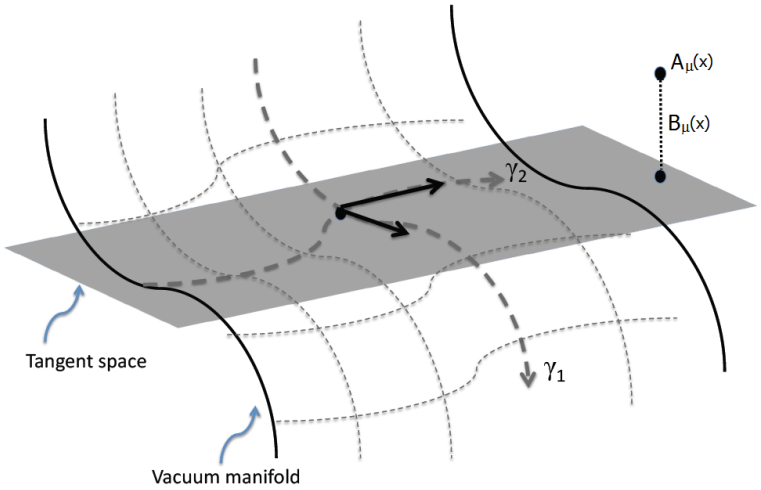

Figure 5.1: Pictorical representation of the projection of the configuration $A_\mu(x)$ onto the vacuum field manifold $\mathcal{M}$. A generic configuration $A_\mu(x)$ is represented by a point in this picture. The constraints (5.5) imply that the the fluctuation field $B_\mu(x)$ is perpendicular to the plane tangent to the manifold in the point of the curvilinear abscissas $\gamma = \bar{\gamma}$.

unity. After some formal manipulation (see e.g. [46]) one arrives to the expression (5.3) where $F(\gamma)$ is a gauge dependent function defined as

$$\begin{aligned} F(\gamma) &= -\log\left\{\int \mathcal{D}B\ \delta(\partial_\mu B_\mu)\left(\prod_i \delta(B\cdot g_{\gamma_i}(\bar{\gamma}))\right)\times \right. \\ &\left. \times\Phi[\tilde{A}(x,\gamma)+B(x)]e^{-S[\tilde{A}(x,\gamma)+B(x)]}\right\}, \end{aligned} \tag{5.7}$$

while, in the Landau Gauge, the Jacobian factor Φ is defined as

$$\Phi^{-1}[A_\mu(x)] = \int\prod_{l=1}^{k} d\gamma_l \int \mathcal{D}U^\Omega\ \delta(\partial_\mu A^\Omega_\mu)\left(\prod_i \delta[(A^\Omega_\mu(x)-\tilde{A}_\mu(x,\gamma))\cdot g_{\gamma_i}(\bar{\gamma})]\right) \tag{5.8}$$

In the last Eq., $U^\Omega(x)$ denotes a generic gauge transformation and A^Ω_μ is result of gauge transforming A_μ according to U^Ω. It is important to emphasize that the gauge dependence of the effective interaction $F(\gamma)$ does not spoil the gauge invariance of the path integral. On the other hand, the choice of the gauge enters through a delta-function in the definition of the effective interaction Eq.(5.7) and in the structure of the Jacobian factor Φ, defined in Eq. (5.8).

5.1.1 A Projection Technique

We now present an algorithm — to which we will refer as the "projection technique"— to compute $F(\gamma)$ non-perturbatively and ab-initio:

1) we use Lattice QCD simulations to generate a statistically representative ensemble of N_{conf} gauge-fixed fields $\{A^g_{\mu,1}(x), \ldots, A^g_{\mu,N_{conf}}(x)\}$

2) Eq.(5.4) and the orthogonality conditions in Eq.(5.5) enable us to build a set of k non-linear equations for the $\gamma_1, \ldots, \gamma_k$ variables

$$\begin{cases} \Phi^g_1[A^g_\mu(x)] = (A^g \cdot g^g_{\gamma_1}(\bar\gamma)) \equiv (\tilde A^g(\gamma) \cdot g^g_{\gamma_1}(\bar\gamma)) \equiv \Psi^g_1(\gamma); \\ \qquad\qquad\qquad\qquad\qquad\qquad ... \\ \Phi^g_k[A^g_\mu(x)] = (A^g \cdot g^g_{\gamma_k}(\bar\gamma)) \equiv (\tilde A^g(\gamma) \cdot g^g_{\gamma_k}(\bar\gamma)) \equiv \Psi^g_k(\gamma). \end{cases} \tag{5.9}$$

The quantities Φ^g_k on the left-hand-side are numbers which are determined numerically by projecting the given lattice configuration $A^g_\mu(x)$ onto the system of coordinates defined by the tangent vectors $g^g_{\gamma_k,\mu}(x,\bar\gamma)$. On the other handm the quantities $\Psi^g_k(\gamma)$ are determined once and for all from the choice of the backgroun field manifold and the projection point $\bar\gamma$. By solving numerically such a system of equations, a value for the curvilinear coordinates can be assigned to each configuration.

3) By repeating this procedure for a large number N_{conf} of independent configurations, one can count the occurancy of a given set of coordinates γ and hence calculate the probability $P(\gamma)$ of projecting an equilibrium configuration onto the background field manifold.
The effective interaction $F(\gamma)$ is then trivially given by

$$F(\gamma_1, \ldots, \gamma_k) = -\log P(\gamma_1, \ldots, \gamma_k).$$

5.1.2 Gauge Invariance of the Projection Technique

We note that the system of Eq.s(5.9) is not manifestly gauge invariant. In fact, there is in general no guarantee that the orthogonality condition defined in a specific gauge,

$$\left(B^g \cdot g^g_{\gamma_i}(\bar\gamma)\right) = 0 \qquad i = 1, \ldots, k, \tag{5.10}$$

it is satisfied also in any other gauges. We now show that, in spite of this fact, Eq. (5.9) holds irrespectively of the gauge chosen. To see this, let us assume that such an equation is satisfied in one particular gauge and analyze how the different terms entering the equation change under a generic gauge transformation $U^{g'}(x)$. Obviously, all fields transform according to

$$A^g_\mu(x) \xrightarrow{g'} A^{g'}_\mu(x) = U^{g'}(x) A_\mu(x) U^{g',\dagger}(x) - i \left[\partial_\mu U^{g'}(x)\right] U^{g',\dagger}(x). \tag{5.11}$$

On the other hand, the basis vector defined on the tangent space transform according to

$$g^{g}_{\gamma_i,\mu}(x,\bar{\gamma}) \xrightarrow{g'} g^{g'}_{\gamma_i,\mu}(x,\bar{\gamma}) = \frac{\partial}{\partial\gamma_i}\tilde{A}^{g'}_{\mu}(x;\gamma)\Big|_{\gamma=\bar{\gamma}} = U^{g'}(x) g_{\gamma_i,\mu}(x,\bar{\gamma}) U^{g',\dagger}(x).$$

These Eq.s, together with Eq.(5.5) imply that

$$(B^{g'} \cdot g^{g'}_{\gamma_i}(\bar{\gamma})) = -i\left(U^{g',\dagger}(x)\left[\partial_\mu U^{g'}(x)\right]\cdot g^{g}_{\gamma_i,\mu}(x,\bar{\gamma})\right) \neq 0. \tag{5.12}$$

However, using the relations in Eq.(5.11) it is immediate to show that the functional $\Phi^g_i[A^g_\mu(x)]$ and the function $\Psi^g_i[\gamma]$ transform as

$$\begin{aligned}
\Phi^g_i[A^g_\mu(x)] &\xrightarrow{g'} \Phi^{g'}_i[A^{g'}_\mu(x)] = \Phi^g_i[A^g_\mu(x)] - i\left(U^{g',\dagger}(x)\left[\partial_\mu U^{g'}(x)\right]\cdot g^{g}_{\gamma_i,\mu}(x,\bar{\gamma})\right), \\
\Psi^g_i[\gamma] &\xrightarrow{g'} \Psi^{g'}_i[\gamma] = \Psi^g_i[\gamma] - i\left(U^{g',\dagger}(x)\left[\partial_\mu U^{g'}(x)\right]\cdot g^{g}_{\gamma_i,\mu}(x,\bar{\gamma})\right),
\end{aligned}$$

which implies

$$\Phi^{g'}_i[A^{g'}_\mu(x)] = \Psi^{g'}_i[\gamma] \qquad \forall g'. \tag{5.13}$$

Hence, we have shown that, if the system of Eq.s (5.9) is satisfied in one gauge, it holds also in any other gauge. As result, the projection procedure is well defined in gauge theories.

5.1.3 Consistency of Vacuum Reparametrization

The effective theory defined by the partition function (5.3) allows to perform approximate calculations of the vacuum expectation value of arbitrary operators $\mathcal{O}$,

$$\langle\mathcal{O}\rangle = \frac{1}{Z_{QCD}}\int \mathcal{D}A_\mu\mathcal{D}\bar{q}\mathcal{D}q\ \mathcal{O}[A_\mu,q,\bar{q}]\ e^{-\frac{1}{\hbar}S_{QCD}}. \tag{5.14}$$

In fact, if instantons (in this case) are the non-perturbative gauge configurations which rule the microscopic dynamics underlying the operator $\mathcal{O}$, then

$$\mathcal{O}[A_\mu] \simeq \hat{\mathcal{O}}[\hat{\gamma}],$$

and

$$\langle\hat{\mathcal{O}}\rangle \simeq \frac{1}{Z_{QCD}}\int\prod_{l=1}^{k} d\ \gamma_l\ \hat{\mathcal{O}}[\hat{\gamma}]\ e^{-\frac{1}{\hbar}F(\gamma_1,\ldots,\gamma_k)}. \tag{5.15}$$

On the other hand, we note that while the partition function (5.3) is independent on the choice of $\bar{\gamma}$ — which specifies the system of coordinates on

the manifold— the effective interaction $F(\gamma)$ and vacuum expectation values of operators may in principle depend on such a parameter. However, such a dependence is generated only by the projection of configurations which contain very large fluctuations, i.e. lie far from the vacuum manifold. To see this, let us consider the projection of a configuration $A_\mu(x)$ which lies very close to a point on the vacuum manifold $\tilde{A}_\mu(x;\gamma')$, i.e.

$$||A_\mu(x) - \tilde{A}_\mu(x;\gamma')|| \simeq 0, \tag{5.16}$$

for some γ'. Then, the projection Eq.s (5.9) read:

$$(A_\mu(x)\cdot g_{\gamma_1}(x;\bar{\gamma})) \simeq (\tilde{A}_\mu(x;\gamma')\cdot g_{\gamma_1}(x;\bar{\gamma})) = (\tilde{A}_\mu(x;\gamma)\cdot g_{\gamma_1}(x;\bar{\gamma})) \tag{5.17}$$

$$\ldots$$

$$(A_\mu(x)\cdot g_{\gamma_k}(x;\bar{\gamma})) \simeq (\tilde{A}_\mu(x;\gamma')\cdot g_{\gamma_k}(x;\bar{\gamma})) = (\tilde{A}_\mu(x;\gamma)\cdot g_{\gamma_k}(x;\bar{\gamma})). \tag{5.18}$$

A solution of such set of Eq.s is trivially $\gamma' = \gamma$, for any choice of the projection point $\bar{\gamma}$. If the vacuum field manifold captures the physically important configurations, the vacuum expectation values of operators $\mathcal{O}[A_\mu]$ will be dominated by the configurations in the functional vicinity of the manifold. In the limit in which the relevant configurations are only those very close to the manifold, the system of Eq.s (5.9) have a unique solution and the expressions (5.14) become independent on the choice of the coordinate system on the manifold, i.e. of the parameter $\bar{\gamma}$. Clearly, this condition can be verified by comparing the results obtained projecting onto different points of the manifold.

In order to illustrate how the approach works for a generic system, in the next section we will first consider the simple case of a one-dimensional quantum mechanical particle, interacting with a double-well potential. We will then turn back to the QCD case in section 5.3.

5.2 An Illustrative Application: 1-Dimensional Quantum Mechanics

Results in this section have been published in [49].
Before applying our formalism to gauge theories, it is instructive to consider first a toy-model: the 1-dimensional quantum mechanical problem of a particle moving in a potential $U(x)$.

We briefly sketch the vacuum reparametrization for a quantum mechanical system. The system has boundary conditions

$$x[-T/2] = x_i \qquad x[T/2] = x_f, \tag{5.19}$$

and the imaginary time path integral is given by

$$Z[x_f, x_i|T] = \langle x_f|e^{-HT}|x_i\rangle = \int_{x[-T/2]=x_i}^{x[T/2]=x_f} \mathcal{D}x\ e^{-\frac{S[x]}{\hbar}}, \tag{5.20}$$

where

$$S[x] = \int_{-T/2}^{T/2} \mathrm{d}t\ \left[m\frac{\dot{x}^2(t)}{2} + U(x)\right]. \tag{5.21}$$

is the usual Euclidean action.

As for the QCD case, we can consider a generic family of vacuum field configurations $\tilde{x}(t;\gamma)$, which form a differentiable manifold $\mathcal{M}$, parametrized by the curvilinear coordinates $\gamma_1, \ldots, \gamma_k$. Again, for every given choice of the parameters γ it is possible to decompose a generic configuration $x(t)$ contributing to the path integral (5.20) as a sum of a field configuration $\tilde{x}(t;\gamma)$, belonging to the manifold $\mathcal{M}$, and of a residual fluctuation field $y(t)$:

$$x(t) \equiv \tilde{x}(t;\gamma) + y(t). \tag{5.22}$$

The k orthogonality conditions are then given by

$$(y(t) \cdot g_{\gamma_i}(t,\bar{\gamma})) \equiv \int_{-T/2}^{T/2} dt\ y(t)\ g_{\gamma_i}(t,\bar{\gamma}) = 0, \qquad i = 1, \ldots, k \tag{5.23}$$

where the functions $g^i_{\bar{\gamma}}(t)$ are defined as

$$g_{\gamma_i}(t,\bar{\gamma}) = \frac{\partial}{\partial\gamma_i}\tilde{x}(t;\gamma)\Big|_{\gamma=\bar{\gamma}}, \tag{5.24}$$

and identify the k directions tangent to the manifold $\mathcal{M}$ of vacuum fields, in the point of curvilinear coordinates $\bar{\gamma} = (\bar{\gamma}_1, \ldots, \bar{\gamma}_k)$. Configurations which lie in a functional neighborhood of the manifold can be projected onto the same system of coordinates. The components of such configurations $x(t)$ are

$$\Psi_1[x(t)] = (x(t) \cdot g_{\gamma_1}(t,\bar{\gamma})) = \int_{-T/2}^{T/2} dt\ x_i(t)\ g_{\gamma_1}(t,\bar{\gamma}), \tag{5.25}$$

$$\ldots$$

$$\Psi_k[x(t)] = (x(t) \cdot g_{\gamma_k}(t,\bar{\gamma})) = \int_{-T/2}^{T/2} dt\ x_i(t)\ g_{\gamma_k}(t,\bar{\gamma}). \tag{5.26}$$

Hence, the condition (5.23) imposes that fluctuation fields $y(t)$ should have vanishing coordinates on the system of coordinates defined by the vector $\{g_{\gamma_i}(t,\bar{\gamma})\}_{i=1,\ldots,k}$.

As in section 5.1, but withouth the complication of gauge fixing, the path integral (5.20) can be formally re-written as

$$Z(T; x_i, x_f) = \int \prod_{l=1}^{k} d\ \gamma_l\ e^{-\frac{1}{\hbar}F(\gamma_1,\ldots,\gamma_k)}, \tag{5.27}$$

where $F(\gamma)$ is defined as

$$\begin{aligned} F(\gamma) &= -\hbar \log \int_{y(-T/2)=0}^{y(T/2)=0} \mathcal{D}y \quad \left(\prod_i \delta^{(k)}(y(t) \cdot g_{\gamma_i}(t, \bar{\gamma})) \right) \times \\ &\quad \times \Phi[\tilde{x}(t;\gamma) + y(t)] e^{-\frac{1}{\hbar}S[\tilde{x}(t;\gamma)+y(t)]}, \end{aligned}$$

and $\Phi[x]$ is a functional coming from a Fadeev-Popov transformation.

5.2.1 Toy Model: Double Well Potential

We now restric our discussion to the potential

$$U(x) = m\alpha \left(x^2 - \beta^2\right)^2, \tag{5.28}$$

where m is the mass of the particle, and α and β are parameters charachterizing the height and width of the potential. We consider the path integral with boundary conditions

$$x_i = x_f = -\beta \qquad (\text{ or equivalently: } x_i = x_f = +\beta\ ). \tag{5.29}$$

In this specific system, a choice of the effective degrees of freedom is suggested semi-classical arguments. We choose the vacuum field manifold to be the one generated by the superposition of N instantons and N antiinstantons

$$\hat{x}_I(t; t_I) = \beta \tanh\left[\sqrt{2\alpha}\beta(t - t_I)\right], \tag{5.30}$$

$$\hat{x}_{\bar{I}}(t; \hat{t}_{\bar{I}}) = -\beta \tanh\left[\sqrt{2\alpha}\beta(t - \hat{t}_{\bar{I}})\right], \tag{5.31}$$

which are the tunneling solutions connecting the two classical vacua

$$\hat{x}_{cl}(t) = \pm\beta.$$

Obviously, the choice of the optimal number of pseudo-particles depends on the time interval T. If the barrier is sufficiently high, one can fix N from the semi-classical tunneling rate [47]

$$2N \simeq \kappa T, \tag{5.32}$$

where κ is the one-instanton measure

$$\kappa \simeq 4\sqrt{\frac{2(2\alpha)^{3/2}\beta^2}{\pi\hbar}}. \tag{5.33}$$

The curvilinear coordinates $\gamma_1 = t_1, \gamma_2 = \hat{t}_1, \ldots, \gamma_{2N-1} = t_N, \gamma_{2N} = \hat{t}_N$ represent the collective coordinates of each instanton or antiinstanton, i.e. their positions in the imaginary time axis. In particular, we adopt the so-called "sum-*ansatz*", which consists in simply adding-up the instanton and antiinstanton fields:

$$\tilde{x}_{S_{2N}}(t; t_1, \ldots \hat{t}_N) \equiv -\beta + \sum_{k=1}^{N} \left[\hat{x}_I(t - t_k) + \hat{x}_{\hat{I}}(t - \hat{t}_k)\right], \tag{5.34}$$

where we have labeled with $t_1, \ldots t_N$ $(\hat{t}_1, \ldots, \hat{t}_N)$ the centers of the instantons (antiinstantons). The path integral, re-written as in Eq.(5.27) reads

$$Z[T; -\beta, -\beta] = \int dt_1, \int d\hat{t}_1 \ldots \int dt_N \int d\hat{t}_N \; e^{-\frac{1}{\hbar} F(t_1, \hat{t}_1, \ldots, t_N, \hat{t}_N)}. \tag{5.35}$$

Notice that this expression is the equivalent of Eq.(2.86) in the 1-dimensional double well potential.

We also note that there are only two choices of such collective coordinates for which the field configuration (5.34) becomes an exact solution of the Euclidean EoM:

1. When all nearest neighbour instanton-antiinstantons pairs are infinitely separated from each other, i.e.

$$|t_i - \hat{t}_i| \to \infty, |t_{i+1} - \hat{t}_i| \to \infty;$$

2. When all nearest neighbour instanton-antiinstantons pairs are infinitely close to each other, i.e.

$$t_i = \hat{t}_i.$$

In the former case, one obtains a dilute instanton gas configuration. In the latter case, all pairs annihilate and the field reduces a trivial classical vacuum, i.e. $x(t) = -\beta$. For any other choice of the collective coordinates $t_1, \ldots, \hat{t}_N$, the field configuration (5.34) is not an extremum of the action.

Two-body Effective Interaction

The relative statistical weight of each configuration in the path integral (5.20) is provided by the exponential factor appearing in Eq. (5.35), which plays the role of the free energy in the statistical mechanical analogy. Hence,

the function $F(t_1, \ldots, \hat{t}_N)$ expresses the statistical and dynamical correlations between the pseudo-particles, induced by all other field configurations in the path integral. For example, in the high barrier limit in which the semi-classical dilute instanton gas approximation is justified, one has

$$e^{-\frac{1}{\hbar}\ F(t_1,\ldots,\hat{t}_N)} \simeq \theta(\hat{t}_1 - t_1)\ \theta(t_2 - \hat{t}_1) \ldots \theta(\hat{t}_N - t_N)\ \kappa^{2N}. \qquad (5.36)$$

As the height of the barrier is adiabatically reduced, the dilute instanton gas approximation becomes worse and worse and eventually breaks down. In this regime, the vacuum fields behave as an interacting liquid and the effective interaction $F(t_1, \ldots, \hat{t}_N)$ deviates from the expression (5.36) and can be written as

$$F(\hat{t}_1, \ldots, \hat{t}_N) \simeq \sum_{i=1}^{N} F_2^{IA}(\hat{t}_i - t_i) + F_2^{AI}(t_{i+1} - \hat{t}_i), \qquad (5.37)$$

where F_2^{IA} (F_2^{AI}) expresses the two-body instanton-antiinstanton (antiinstanton-instanton) correlations [1]. For very low barriers, the average instanton distance becomes smaller than the instanton size, and the pseudoparticles "melt". Clearly, in such a regime, instantons and antiinstanton fields no longer represent a good choice of low-energy vacuum degrees of freedom. In the following sections, we shall consider systems for which the dilute liquid regime is appropriate.

In order to compute $F_2^{IA}(\hat{t}_i - t_i)$ and $F_2^{AI}(t_{i+1} - \hat{t}_i)$ it is convenient to integrate out from (5.35) all instanton degrees of freedom, except those of a single pair of pseudo particles. To this end, we rewrite the path integral as :

$$\begin{aligned} Z[T; -\beta, -\beta] &= \frac{1}{2}\Big[\int dt_1 \int d\hat{t}_1 \left(\int dt_2\ d\hat{t}_2 \ldots d\hat{t}_N\ e^{-\frac{1}{\hbar}F} \right) + \\ &\quad \int d\hat{t}_1 \int dt_2\ \left(\int dt_1\, d\hat{t}_2\, dt_3 \ldots d\hat{t}_N\ e^{-\frac{1}{\hbar}F} \right) \Big] \\ &= \frac{1}{2}\ \int dt_1 \int dt_2\ \left[g_2^{IA}(t_2 - t_1) + g_2^{AI}(t_2 - t_1) \right]. \qquad (5.38) \end{aligned}$$

The first term corresponds to the case in which the pseudo-particle of coordinate t_1 is an instanton, while the second of coordinate t_2 is an anti-instanton and $g_2^{IA}(t_2 - t_1)$ is the corresponding pair-correlation function. Conversely, the second term corresponds to the case in which the pseudo-particle at t_1 is an anti-instanton and that at t_2 is an instanton. In the dilute liquid regime, the functions $g^{IA(AI)}(t_2 - t_1)$ relate directly to $F_2^{IA(AI)}(t_2 - t_1)$ by

$$e^{-\frac{1}{\hbar}\ F_2^{IA(AI)}(t_2 - t_1)} \propto\ g_2^{IA(AI)}(t_2 - t_1), \qquad (5.39)$$

where the proportionality factor is controlled by the density.

[1] Eq. (5.37) can be generalized to include higher-order (e.g. three-body, four-body, etc...) correlations.

5.2.2 Projection Technique for the Double-Well Problem

In order to extract the instanton-antiinstanton pair correlation function g_2^{IA} we consider the path integral with boundary condition $x_f = x_i = -\beta$ and parametrize a generic configuration $x(t)$ using the sum ansatz for an instanton-antiiinstanton pair, Eq.(5.34)

$$\begin{aligned} x(t) &= \tilde{x}_{S_2}^{IA}(t;t_1,t_2) + y(t) \qquad (5.40)\\ &= -\beta\left\{1 - \tanh\left[\sqrt{2\alpha}\,\beta\,(t-t_1)\right] + \tanh\left[\sqrt{2\alpha}\,\beta\,(t-t_2)\right]\right\} + y(t), \end{aligned}$$

where $y(t)$ is a configuration of boundary conditions $y(\pm T/2) = 0$, and t_1 and t_2 are the coordinates of the two pseudoparticles, in the Euclidean time axis. Conversely, in order to evaluate g_2^{AI}, one should consider the path integral with boundary conditions $x_f = x_i = \beta$ and adopt a vacuum manifold based on the anti-instanton instanton pair:

$$\begin{aligned} x(t) &= \tilde{x}_{S_2}^{AI}(t;t_1,t_2) + y(t) \qquad (5.41)\\ &= \beta\left\{1 - \tanh\left[\sqrt{2\alpha}\,\beta\,(t-t_1)\right] + \tanh\left[\sqrt{2\alpha}\,\beta\,(t-t_2)\right]\right\} + y(t). \end{aligned}$$

Since the two calculations are identical, in the following we shall focus on determining g_2^{IA} and the IA suffix will be implicitly assumed.

It is convenient to introduce the relative variables

$$\begin{aligned} \chi &= \frac{1}{2}(t_1 + t_2),\\ \xi &= t_2 - t_1. \end{aligned}$$

Notice that variable χ is the "center of mass" of the pair, while ξ represents the "relative distance" between the instanton and antiinstanton. Notice also that Eq.(5.38) implies

$$F_2(t_1,t_2) = F_2(t_2 - t_1) \equiv F_2(\xi), \qquad (5.42)$$

that is to say we expect the effective interaction to be independent from the center of mass of the pair. This is a consequence of the time translational invariance of the vacuum.

We recall that the multi-instanton field configuration and the fluctuation field have to fulfill the orthogonality conditions (5.23), which is enforced in a specific point $\gamma = \bar{\gamma}$ of the manifold. The basis vector of the tangent space of the manifold defined by the sum ansatz (5.34) are, for an arbitrary point $\gamma = (\bar{t}_1, \bar{t}_2)$

$$\begin{aligned} g_{t_1}(t;\bar{t}_1,\bar{t}_2) &= \partial_{t_1}\tilde{x}_{S_2}(t;t_1,t_2)\Big|_{t_1=\bar{t}_1,t_2=\bar{t}_2} = -\sqrt{2\alpha}\beta^2\mathrm{sech}^2\left[\sqrt{2\alpha}\beta(t-\bar{t}_1)\right],\\ g_{t_2}(t;\bar{t}_1,\bar{t}_2) &= \partial_{t_2}\tilde{x}_{S_2}(t;t_1,t_2)\Big|_{t_1=\bar{t}_1,t_2=\bar{t}_2} = \sqrt{2\alpha}\beta^2\mathrm{sech}^2\left[\sqrt{2\alpha}\beta(t-\bar{t}_2)\right]. \end{aligned}$$

Equivalently, in terms of the χ and ξ coordinates, the basis vectors of the tangent space in the generic point $\gamma = (\xi, \chi)$ read

$$g_\chi(t;\bar\chi,\bar\xi) = \partial_\chi\, \tilde x_{S_2}\left(t;\chi-\frac{1}{2}\xi,\chi+\frac{1}{2}\xi\right)\Big|_{\chi=\bar\chi,\xi=\bar\xi} \tag{5.43}$$

$$= \sqrt{2\alpha}\beta^2\left\{\mathrm{sech}^2\left[\sqrt{2\alpha}\beta\left(t-\bar\chi-\frac{\bar\xi}{2}\right)\right]-\mathrm{sech}^2\left[\sqrt{2\alpha}\beta\left(t-\bar\chi+\frac{\bar\xi}{2}\right)\right]\right\},$$

$$g_\xi(t;\bar\chi,\bar\xi) = \partial_\xi\, \tilde x_{S_2}\left(t;\chi-\frac{1}{2}\xi,\chi+\frac{1}{2}\xi\right)\Big|_{\chi=\bar\chi,\xi=\bar\xi} \tag{5.44}$$

$$= \sqrt{\frac{\alpha}{2}}\beta^2\left\{\mathrm{sech}^2\left[\sqrt{2\alpha}\beta\left(t-\bar\chi-\frac{\bar\xi}{2}\right)\right]+\mathrm{sech}^2\left[\sqrt{2\alpha}\beta\left(t-\bar\chi+\frac{\bar\xi}{2}\right)\right]\right\}.$$

Hence, without loss of generality, in the following we shall consider

$$x(t;\chi,\xi) := -\beta\left\{1-\tanh\left[\sqrt{2\alpha}\,\beta\,\left(t-\chi+\frac{\xi}{2}\right)\right]+\tanh\left[\sqrt{2\alpha}\,\beta\,\left(t-\chi-\frac{\xi}{2}\right)\right]\right\}+y(t),$$

with the conditions

$$\left(y(t)\cdot g_\chi(t;\bar\chi,\bar\xi)\right)=0, \tag{5.45}$$

$$\left(y(t)\cdot g_\xi(t;\bar\chi,\bar\xi)\right)=0. \tag{5.46}$$

Although our ultimate goal is to evaluate $F_2^{IA}(\xi)$ and $F_2^{IA}(\xi)$ in a fully non-perturbative way, it is instructive to discuss first a perturbative analysis, which yields information about the contribution to the quantum effective interactions in the short instanton-antiinstanton distance limit: this will help us clarify the validity of the projection technique.
The perturbative calculation is presented in the next section, while the fully non-perturbative calculation is reported in section 5.2.4.

5.2.3 Perturbative Calculation

Perturbation theory deals with small quantum fluctuations around a *classical* vacuum. In particular, a calculation of $F_2^{IA}(\xi)$ and $F_2^{IA}(\xi)$ at small ξ requires to assign to each point in the vicinity of the trivial vacuum

$$\tilde x_{S_2}\equiv -\beta, \tag{5.47}$$

a point on the intanton-antiinstanton functional manifold. Since quantum fluctuations can be arbitrarily small, the orthogonality conditions (5.45) and (5.46) have to be imposed at a point which is arbitrarily close to the same classical vacuum. In principle, the most natural choice would be impose the orthogonality conditions *at* the classical vacuum. However, problems arise

due to the fact that it is not possible to define the tangent space in such a point, since

$$g_\chi(t;\bar{\chi},0) \equiv 0, \tag{5.48}$$

for all $\bar{\chi}$. To overcome this difficulty, we have used stochastic quantization formalism to construct a rigorous approach in which the tangent space which is defined at a point which is *arbitrarily* close to classical point, but does not coincide with it.

Let us begin by briefly reviewing Pairsi and Wu quantization technique [53]. The starting point is to allow the field configuration $x(t)$ to depend on an additional parameter, the so-called stochastic "time" τ. The dynamics of the field in such an additional dimension is postulated to obey a Langevin equation:

$$x'(t,\tau) \equiv \frac{d}{d\tau}\, x(t,\tau) = -k\frac{\delta\, S[x]}{\delta\, x(t,\tau)} + \sqrt{\hbar}\,\eta(t,\tau), \tag{5.49}$$

where k is an arbitrary diffusion coefficient and $\eta(t,\tau)$ Gaussian distributed stochastic field

$$P[\eta] \;\; \propto \;\; \exp\left\{-\frac{1}{4k}\int_{-\infty}^{\infty}\mathrm{d}t\int_{0}^{\infty}\mathrm{d}\tau\;\eta^2(t,\tau)\right\}, \tag{5.50}$$

which obeys the fluctuation-dissipation relationship

$$\langle\eta(t,\tau)\eta(t',\tau')\rangle \;\; = \;\; \int \mathcal{D}\eta\,\eta(t,\tau)\eta(t',\tau')P[\eta] = 2\;k\;\delta(t'-t)\;\delta(\tau'-\tau).$$

For any value of the stochastic time τ, the probability to for the field to assume a given configuration $x(t,\tau)$ is described by a (functional) probability distribution $\mathcal{P}[x](\tau)$, which is a solution of the Fokker-Planck Eq. associated to the Langevin Eq. (5.49):

$$\frac{d}{d\tau}\mathcal{P}[x] = k\;\frac{\delta^2}{\delta x^2}P[x] + k\;\frac{\delta}{\delta x}\left(\mathcal{P}[x]\;\frac{\delta S[x]}{\delta x}\right). \tag{5.51}$$

A general property of the Fokker Planck Eq. is that its solutions converge to the static, "Boltzmann" weight, in the long time limit:

$$\mathcal{P}[x] \overset{(\tau\to\infty)}{\to} \frac{1}{\int\mathcal{D}x(t)\exp\left\{-\frac{1}{\hbar}S[x(t)]\right\}}\exp\left\{-\frac{1}{\hbar}S[x(t)]\right\}, \tag{5.52}$$

regardless of the initial condition, $x(t,\tau=0)$ and of the value of the diffusion coefficient k. Hence, the Langevin Eq. (5.49) generates configurations which, at equilibrium, are distributed according to the statistical weight appearing in the Euclidean quantum path integral. Such configurations can

be used to compute quantum mechanical Green's functions.

In stochastic perturbation theory, a generic configuration $x(t,\tau)$ obeying Langevin Eq. (5.49) with boundary conditions (5.45) and (5.46) is written as a power series in $\varepsilon = \sqrt{\hbar}$:

$$x(t,\tau) = \sum_{i=i}^{\infty} \varepsilon^i x_i(t,\tau), \tag{5.53}$$

$x_0(t,\tau)$ is the classical content of the configuration, while all other terms represent quantum corrections. In the double-well problem, the classical solution with boundary conditions (5.29) is $x_0(t,\tau) = -\beta$.

By inserting the expansion (5.53) into the Langevin Eq. (5.49) and matching the keft-handside and right-handside, order by order in ε, one generates a tower of coupled stochastic differential Eq.s, for the components $x_i(t,\tau)$, which appear in Eq. (5.53):

$$O(\varepsilon^0): \quad x_0'(t,\tau) = k\,m\left(\partial_t^2 - 4\alpha\,[x_0^2(t,\tau) - \beta^2]\,\right)\,x_0(t,\tau); \tag{5.54}$$

$$O(\varepsilon^1): \quad x_1'(t,\tau) = k\,m\left(\partial_t^2 - 4\alpha\,[3\,x_0^2(t,\tau) - \beta^2]\,\right)\,x_1(t,\tau) + \eta(t,\tau); \tag{5.55}$$

$$O(\varepsilon^2): \quad x_2'(t,\tau) = k\,m\left[\left(\partial_t^2 - 4\alpha\,[3\,x_0^2(t,\tau) - \beta^2]\,\right)\,x_2(t,\tau) - 12\alpha\,x_0(t,\tau)x_1^2(t,\tau)\right]; \tag{5.56}$$

$$O(\varepsilon^3): \quad x_3'(t,\tau) = k\,m\left[\left(\partial_t^2 - 4\alpha\,[3\,x_0^2(t,\tau) - \beta^2]\,\right)\,x_3(t,\tau) - 4\alpha\,x_1^3(t,\tau) - 24\alpha x_0(t,\tau)x_1(t,\tau)x_2(t,\tau)\right]; \tag{5.57}$$

...

In practice, the perturbative expansion is truncated and one solves a finite set of stochastic differential Eq.s, starting from a given initial condition. For example, truncating the expansion to order ε^2 and choosing the initial condition

$$x_0(t,\tau=0) = -\beta, \tag{5.58}$$

$$x_i(t,\tau=0) = 0, \qquad (i=1,2,\ldots), \tag{5.59}$$

which corresponds to the classical vacuum state, we find

$$x_0(t,\tau) = -\beta; \tag{5.60}$$

$$x_1(t,\tau) = \int_{-\infty}^{\infty}\frac{\mathrm{d}\omega}{2\pi}e^{-i\omega t}\int_0^{\infty}\mathrm{d}\tau'\theta\left[\tau-\tau'\right]e^{-km(8\alpha\beta^2+\omega^2)(\tau-\tau')}\tilde{\eta}(\omega,\tau'); \tag{5.61}$$

$$x_2(t,\tau) = 12\alpha\beta km\int_{-\infty}^{\infty}\frac{\mathrm{d}\omega}{2\pi}e^{-i\omega t}\int_0^{\infty}\mathrm{d}\tau'\theta\left[\tau-\tau'\right]e^{-km(8\alpha\beta^2+\omega^2)(\tau-\tau')}\times \times\int_{-\infty}^{\infty}\mathrm{d}t'e^{i\omega t'}x_1^2(t',\tau'). \tag{5.62}$$

The corresponding perturbative solution is

$$x(t,\tau) = x_0(t,\tau) + \varepsilon x_1(t,\tau) + \varepsilon^2 x_2(t,\tau). \tag{5.63}$$

It is important to stress that only the asymptotic equilibrium solution $x(t,\tau = \infty)$ enters in the evaluation of physical observables. Such equilibrium solutions are independent on the choice of the initial condition of the perturbative stochastic equations (5.54)-(5.57).

Let us now show how the stochastic perturbation theory technique can be used to gain information about the $F_2^{IA}(\xi)$ and $F_2^{AI}(\xi)$ distributions. To this end, we begin by decomposing the field as in Eq. (5.22),

$$x(t) \equiv \tilde{x}_{S_2}(t;\chi,\xi) + y(t). \tag{5.64}$$

Next we need to promote the manifold field $\tilde{x}(t;\chi,\xi)$ and fluctuation field $y(t)$ to dynamical variables, under the stochastic time evolution. There is some freedom associated to the definition of such a stochastic dynamics. For example, a possible choice may be one in which the τ dependence enters entirely through the fluctuation field $y(t,\tau)$, while the smooth vacuum field $\tilde{x}_{S_2}$ is assumed to be static, under stochastic evolution, i.e. $\tilde{x}_{S_2}(t,\tau) = \tilde{x}_{S_2}(t)$. Instead, a crucial point of the present approach is to make a different choice and allow both the fluctuation field and the smooth vacuum field to vary with the stochastic time τ. This is done in practice by promoting the curvilinear coordinates ξ and χ to dynamical stochastic degrees of freedom [54], i.e. $\xi \to \xi(\tau)$ and $\chi \to \chi(\tau)$. Consequently, at a generic stochastic instant τ, the quantum field $x(t,\tau)$ reads:

$$x(t,\tau) \;\; = \;\; \tilde{x}_{S_2}\left(t;\chi(\tau),\xi(\tau)\right) + y(t,\tau). \tag{5.65}$$

Let us now construct a perturbative solution of the Langevin Eq. (5.49), based on the decomposition (5.65). We recall that the multi-instanton field is not a classical solution of the EoM, except in the points where $\xi = 0$. As a consequence, quantum corrections will appear not only in the fluctuation field, but also in the background field. To account for this fact, we expand $y(t,\tau)$, $\chi(\tau)$ and $\xi(\tau)$ as power series in $\varepsilon = \sqrt{\hbar}$:

$$y(t,\tau) \;\; = \;\; \sum_{i=1}^{\infty} \varepsilon^i y_i(t,\tau); \tag{5.66}$$

$$\chi(\tau) \;\; = \;\; \sum_{i=0}^{\infty} \varepsilon^i \; \chi_i(\tau); \tag{5.67}$$

$$\xi(\tau) \;\; = \;\; \sum_{i=0}^{\infty} \varepsilon^i \; \xi_i(\tau). \tag{5.68}$$

Let us now define the tangent space in a generic point $\bar{\xi}, \bar{\chi}$ of the manifold. It is possible to show that the orthogonality conditions (5.45) and (5.46) hold order-by-order in perturbation theory and at any stochastic time i.e.:

$$\Big(y_i(t,\tau) \cdot g_\chi(t;\bar{\chi},\bar{\xi}) \Big) = 0; \tag{5.69}$$

$$\Big(y_i(t,\tau) \cdot g_\xi(t;\bar{\chi},\bar{\xi}) \Big) = 0, \qquad \forall i. \forall \tau. \tag{5.70}$$

From Eq.s (5.53), (5.66), (5.67) and (5.68) it is immediate to obtain an expression for each of the $x_i(t,\tau)$ components in Eq. (5.53):

$$x_i(t,\tau) \equiv \frac{1}{i!}\frac{\partial^i}{\partial \varepsilon^i} \left(\hat{x}_{S_2} \left(t; \sum_{n=0}^{\infty} \varepsilon^n \chi_n, \sum_{m=0}^{\infty} \varepsilon^m \xi_m \right) + \sum_{l=1}^{\infty} \varepsilon^l y_l(t,\tau) \right) \Bigg|_{\varepsilon=0} \tag{5.71}$$

For example, the first orders are

$$x_0(t,\tau) = \tilde{x}_{S_2} \left(t; \chi_0 - \frac{\xi_0(\tau)}{2}, \chi_0 + \frac{\xi_0(\tau)}{2} \right); \tag{5.72}$$

$$x_1(t,\tau) = \chi_1(\tau)\ g_\chi\big(t;\chi_0,\xi_0(\tau)\big) + \xi_1(\tau)\ g_\xi\big(t;\chi_0,\xi_0(\tau)\big) + y_1(t,\tau) \tag{5.73}$$

$$\begin{aligned} x_2(t,\tau) = {} & \chi_2(\tau)\ g_\chi\big(t;\chi_0,\xi_0(\tau)\big) + \xi_2(\tau)\ g_\xi\big(t;\chi_0,\xi_0(\tau)\big) + \\ & -\frac{1}{2}\left(\chi_1^2(\tau) + \frac{\xi_1^2(\tau)}{4}\right)\ \dot{g}_\chi\big(t,\chi_0,\xi_0(\tau)\big) - \\ & \chi_1(\tau)\ \xi_1(\tau)\ \dot{g}_\xi\big(t,\chi_0,\xi_0(\tau)\big) + y_2(t,\tau) \end{aligned} \tag{5.74}$$

$$\ldots \quad .$$

where we have used the fact that χ_0 is independent on τ. The terms on the left-handiside of Eq.s (5.72)-(5.74) coincide with the perturbative solution results (5.60)-(5.62). On the other hand, the terms on the right-handside represent the decomposition of the same functions in terms of the low-energy vacuum field configurations and of the corresponding fluctuation fields.

In order to make contact with the effective interaction, we need to introduce the tangent space which enters the projection Eq.s (5.69) and (5.70). At this point, we face the above mentioned problem that the tangent space at the classical vacuum $-\beta$ is not defined. To overcome this problem, we let the tangent space vary with the stochastic time in such a way that the point $\bar{\xi}, \bar{\chi}$ asymptotically approaches the classical vacuum, but does not coincide with it at any finite τ. In practice, we promote $\bar{\xi}$ to a stochastic variable and we impose

$$\bar{\xi}(\tau) \overset{\tau\to\infty}{\to} 0. \tag{5.75}$$

In particular, we choose $\bar{\xi}(\tau) \equiv \xi_0(\tau)$, since $\xi_0(\tau \to \infty) \to 0$.

Using such a decomposition, we are now in a condition to analytically compute arbitrary moments of the equilibrium distribution for χ and ξ, i.e. $\langle \xi^k \rangle$ and $\langle \chi^k \rangle$.

By projecting and inverting Eq.s (5.73) and (5.74), we obtain the following expression for the collectives coordinates up to $\mathcal{O}(\hbar)$

$$\begin{aligned}
\chi_1(\tau) &= \frac{(x_1(t,\tau) \cdot g_\chi(t;\chi_0,\xi_0(\tau)))}{(g_\chi(t;\chi_0,\xi_0(\tau) \cdot g_\chi(t;\chi_0,\xi_0(\tau))}, && (5.76)\\
\xi_1(\tau) &= \frac{(x_1(t,\tau) \cdot g_\xi(t;\chi_0,\xi_0(\tau)))}{(g_\xi(t;\chi_0,\xi_0(\tau) \cdot g_\xi(t;\chi_0,\xi_0(\tau))}, && (5.77)\\
\chi_2(\tau) &= \frac{(x_2(t,\tau) \cdot g_\chi(t;\chi_0,\xi_0(\tau))) + \chi_1(\tau)\xi_1(\tau)\left(\dot{g}_\xi(t;\chi_0,\xi_0(\tau)) \cdot g_\chi(t;\chi_0,\xi_0(\tau))\right)}{(g_\chi(t;\chi_0,\xi_0(\tau)) \cdot g_\chi(t;\chi_0,\xi_0(\tau)))}, \\
\xi_2(\tau) &= \frac{(x_2(t,\tau) \cdot g_\xi(t;\chi_0,\xi_0(\tau))) + \frac{1}{2}\left(\chi_1^2(\tau) + \frac{1}{2}\xi_1^2(\tau)\right)\left(\dot{g}_\chi(t;\chi_0,\xi_0(\tau)) \cdot g_\xi(t;\chi_0,\xi_0(\tau))\right)}{(g_\xi(t;\chi_0,\xi_0(\tau) \cdot g_\xi(t;\chi_0,\xi_0(\tau))}, \\
\dots &\quad .
\end{aligned}$$

Using the fluctuation-dissipation relationships (5.51), and the fact that $\xi_0(\tau)$ is independent from $\eta(t,\tau)$ we find

$$\begin{aligned}
\langle \chi_1(\tau) \rangle &= 0, \\
\langle \chi_2(\tau) \rangle &= 0, \\
\langle \xi_1(\tau) \rangle &= 0, \\
\langle \xi_2(\tau) \rangle &\overset{\tau\to\infty}{\longrightarrow} \frac{9}{32}\frac{1}{m\alpha\beta^4}. && (5.78)
\end{aligned}$$

Hence we have obtained a closed analytical expression for the first moments:

$$\begin{aligned}
\langle \chi \rangle &= \langle \chi_0 + \varepsilon\chi_1 + \varepsilon^2\chi_2 \rangle = \chi_0 + O(\hbar^2), && (5.79)\\
\langle \xi \rangle &= \langle \xi_0 + \varepsilon\xi_1 + \varepsilon^2\xi_2 \rangle = \frac{9}{32}\frac{\hbar}{m\alpha\beta^4} + O(\hbar^2). && (5.80)
\end{aligned}$$

Now, in order to compute the second moments, we observe that the general expression up to order $O(\varepsilon^2)$ is

$$\begin{aligned}
\chi^2(\tau) &= \chi_0^2(\tau) + 2\varepsilon\chi_0\chi_1(\tau) + \varepsilon^2[2\chi_0\chi_2(\tau) + \chi_1^2(\tau)] + \dots && (5.81)\\
\xi^2(\tau) &= \xi_0^2(\tau) + 2\varepsilon\xi_0(\tau)\xi_1(\tau) + \varepsilon^2[2\xi_0(\tau)\xi_2(\tau) + \xi_1^2(\tau)] + \dots && (5.82)
\end{aligned}$$

which immediately gives

$$\begin{aligned}
\langle \chi^2 \rangle &= \infty; && (5.83)\\
\langle \xi^2 \rangle &= \hbar\langle \xi_1^2 \rangle = \frac{9}{32}\frac{\hbar}{m\alpha\beta^4}\left(\frac{\pi^2 - 9}{3\sqrt{2\alpha}\beta}\right). && (5.84)
\end{aligned}$$

Some comments on these results are in order.
The distribution of the instanton-antiinstanton distance ξ is not symmetric around the origin, since $\langle\xi\rangle \neq 0$. Such a symmetry breaking comes from fluctuations which explore the non-harmonic region of the potential function $U(x)$. Since the potential on the left of the equilibrium configuration raises more steeply than that on the right, quantum paths in the direction of the barrier are statistically favored. The divergence $\langle\chi^2\rangle = \infty$ emerges because the distribution of collective coordinates is independent on χ, as consequence of the time-translational invariance of the system. In the language of stochastic quantization, this implies that the center of mass of the instanton-antiinstanton pair performs Brownian motion in stochastic time and $\langle\chi^2\rangle \propto \tau$, according to Einstein relationship. We also stress the fact that there is no contribution to the effective interaction, at the classical level: $F_2(\xi)$ is an entirely quantum effect.

We emphasize once again that in this calculation we have never requested that the multi-instanton configurations should be approximate solutions of the classical EoM. The only request is that the configuration corresponding to the classical vacuum must belong to the manifold parametrized by the set of relevant low-energy degrees of freedom γ_i. To our knowledge, this represents the first perturbative analysis of the dynamics of short-distance instanton-antiinstanton fluctuations.

5.2.4 Non-Perturbative Calculation

Let us now take the main step of the present work and perform a fully non-perturbative calculation of $F_2(\xi)$ which describes the correlations between consecutive tunneling events.

Let $\{x^1(t,\tau=\infty),\ldots,x^l(t,\tau=\infty)\}$ be an ensemble of l equilibrium field configurations, which were obtained non-perturbatively, for example by integrating numerically directly the stochastic equations 5.49, or by means of a lattice Monte Carlo simulation. The pair correlation function $g_2^{IA}(\xi)$ can be extracted by projecting the set of equilibrium configurations onto the low-energy vacuum field manifold spanned by an instanton-antiinstanton pair. To this end, we define the functionals of the field configuration $x(t,\tau)$

$$\Phi_\chi[x_\tau] := \left(x(t,\tau), g_\chi(t;\bar\chi,\bar\xi)\right), \tag{5.85}$$
$$\Phi_\xi[x_\tau] := \left(x(t,\tau), g_\xi(t;\bar\chi,\bar\xi)\right), \tag{5.86}$$

which represents the projection of an arbitrary field configuration onto the tangent space, at the point $(\bar\chi,\bar\xi)$. We also introduce the functions of the

collective coordinate χ and ξ

$$\Psi_\chi(\chi,\xi) := \left(\tilde{x}_{S2}\left(t;\chi,\xi\right), g_\chi(t;\bar{\chi},\bar{\xi})\right), \tag{5.87}$$
$$\Psi_\xi(\chi,\xi) := \left(\tilde{x}_{S2}\left(t;\chi,\xi\right), g_\xi(t;\bar{\chi},\bar{\xi})\right), \tag{5.88}$$

which represents the projection of a generic point of the instanton-antiinstanton field manifold onto the same tangent space. In the specific case of the double-well potential one has simple analytical expressions

$$\begin{aligned}\Psi_\chi(\chi,\xi) &= \zeta\left[\left(\chi-\frac{\xi}{2}\right)-\left(\bar{\chi}+\frac{\bar{\xi}}{2}\right)\right]-\zeta\left[\left(\chi+\frac{\xi}{2}\right)-\left(\bar{\chi}+\frac{\bar{\xi}}{2}\right)\right]+\\ &+\zeta\left[\left(\chi+\frac{\xi}{2}\right)-\left(\bar{\chi}-\frac{\bar{\xi}}{2}\right)\right]-\zeta\left[\left(\chi-\frac{\xi}{2}\right)-\left(\bar{\chi}-\frac{\bar{\xi}}{2}\right)\right], \qquad (5.89)\\ \Psi_\xi(\chi,\xi) &= -2\beta^2+\frac{1}{2}\zeta\left[\left(\chi-\frac{\xi}{2}\right)-\left(\bar{\chi}+\frac{\bar{\xi}}{2}\right)\right]-\frac{1}{2}\zeta\left[\left(\chi+\frac{\xi}{2}\right)-\left(\bar{\chi}+\frac{\bar{\xi}}{2}\right)\right]+\\ &-\frac{1}{2}\zeta\left[\left(\chi-\frac{\xi}{2}\right)-\left(\bar{\chi}+\frac{\bar{\xi}}{2}\right)\right]+\frac{1}{2}\zeta\left[\left(\chi+\frac{\xi}{2}\right)-\left(\bar{\chi}+\frac{\bar{\xi}}{2}\right)\right], \qquad (5.90)\end{aligned}$$

where

$$\zeta[X]=2\beta^2\left\{\sqrt{2\alpha}\beta X\sinh^{-2}\left[\sqrt{2\alpha}\beta X\right]-\coth\left[\sqrt{2\alpha}\beta X\right]\right\}. \tag{5.91}$$

By setting Eq.s (5.85) and (5.86) to be equal to Ψ_χ and Ψ_ξ respectively, we obtain a complete system of equations for the variables χ and ξ.

$$\begin{cases}\Phi_\chi[x_\tau] \equiv \Psi_\chi\big[\chi(\tau),\xi(\tau)\big];\\ \Phi_\xi[x_\tau] \equiv \Psi_\xi\big[\chi(\tau),\xi(\tau)\big].\end{cases} \tag{5.92}$$

Such a system has a unique solution for any choice of the projection point $(\bar{\chi},\bar{\xi})$, with $\bar{\xi}\neq 0$. Hence, it is possible to assign a value of χ and ξ to every non-perturbatively generated configuration $x(t,\tau)$.

Repeating such a projection for the entire ensemble of equilibrium configurations, one obtains an histogram which by construction is proportional to the pair correlation function $g_2^{IA}(\xi)$. The effective potential $F_2(\xi)$ is immediately extracted from:

$$F_2^{IA}(\xi) = -\hbar\ \log[\ g_2^{IA}(\xi)]+\text{const.}. \tag{5.93}$$

Clearly, the calculation of $F_2^{AI}(\xi)$ would be completely analog. In practice, such a calculation is not necessary, since the function $F_2^{AI}(\xi)$ can be inferred directly by symmetry arguments:

$$F_2^{AI}(\xi)=F_2^{IA}(-\xi). \tag{5.94}$$

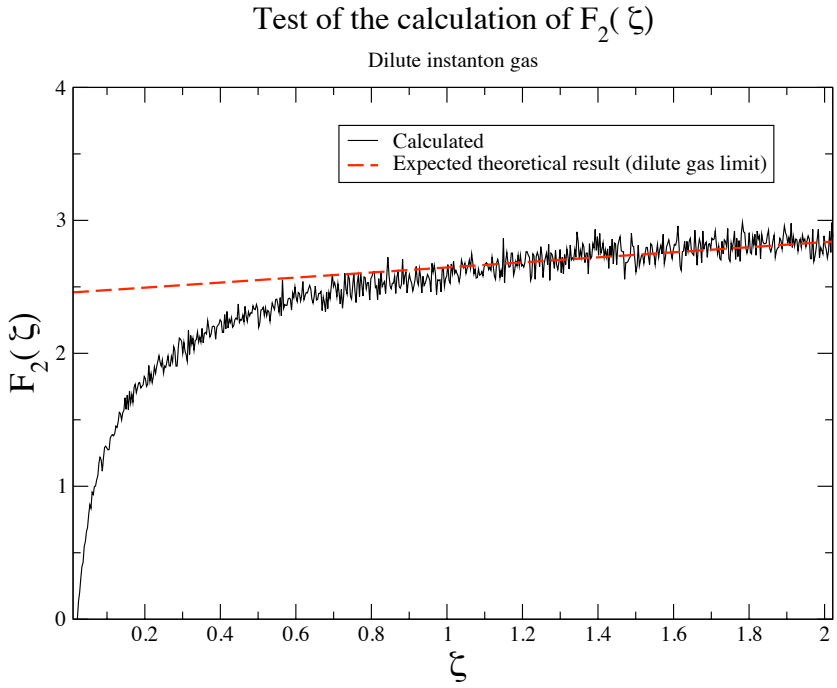

Figure 5.2: Non-perturbative calculation of the effective interaction $F_2(\xi)$ for a dilute instanton gas with $\alpha = 7$, $m = 1$, $\beta = 1$ in a volume $T = 200$. The points are the results obtained from projecting 1000 configurations, while the dashed line is the expected theoretical results for ξ much larger than the instanton size (which is 0.26, in these units).

Once the effective interaction has been determined, one can evaluate the instanton density of the liquid by minimizing the free-energy of the ensemble. In the next section, we present the results of some numerical investigations, in order to illustrate the method and assess the accuracy of the determination of the instanton-antiiinstanton interaction.

5.2.5 Test: Non-Perturbative Calculations in DIGA

In order to show that our method yields the correct result, let us first consider a model for which the effective interaction can be evaluated analytically. The two-body part of the effective interaction for a dilute instanton gas can be easily computed from Eq. (5.36), by integrating out all the collective coordinates, except for those of a single instanton-antiinstanton pair. The result is

$$e^{-\frac{1}{\hbar}F_2^{IA}(\xi)} = \text{const.} \times e^{-(\kappa T-1)\log(T-\xi)}. \tag{5.95}$$

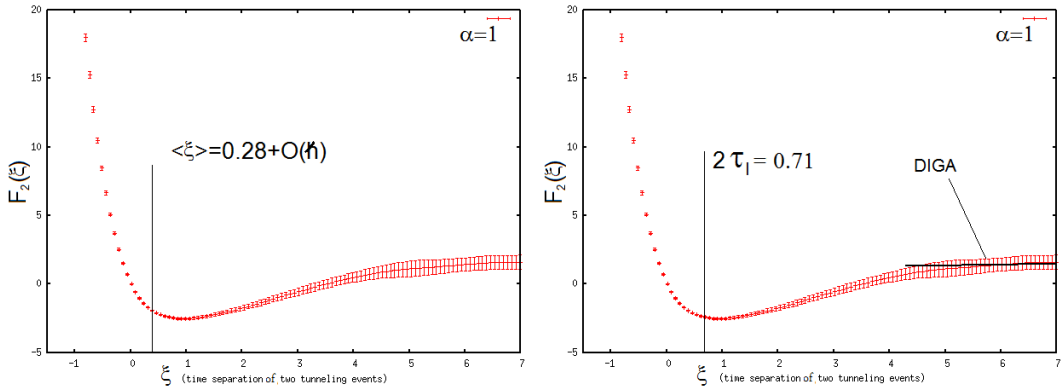

Figure 5.3: Non-perturbative calculation of the effective interaction $F(\xi)$ for $\alpha = 1$. Left panel: non-perturbative result compared to perturbative calculation. Right panel: non-perturbative result compared to DIGA, and instanton size.

This result holds for high barriers and distances ξ much larger than the instanton size. Notice that, in the thermodynamic limit — $N, T \to \infty$ and $N/T = \kappa$ fixed— the effective interaction $F_2^{IA}(\xi)$ should scale linearly, with a slope controlled by the instanton rate κ.

We now address the question if our projection technique is able to reconstruct the effective interaction in Eq.(5.95). To this end, we have generated an ensemble of 1000 dilute gas configurations, by randomly sampling the positions of instantons and anti-instantons, in a box of size $T = 200$ for a well with $\alpha = 7, m = 1, \beta = 1$. In Fig. 5.2, we compare the expected theoretical curve (dashed line) with the result of our numerical calculation (points). We see that, as soon as the distance ξ becomes larger than few instanton sizes —which is 0.26 in this units— the numerical results agree with the expected curve. A linear fit of the data for $\xi > 1$ yields a slope of 0.32 ± 0.01, in excellent agreement with the exact theoretical result, which is 0.31. Hence, we conclude that our projection method is indeed able to quantitively reconstruct the structure of the exact distribution used to generate the ensemble of configurations.

5.2.6 Toy Model: Results and Conclusive Remarks

Let us now discuss for completeness the structure of the effective interaction for our original quantum double-well system. At this level, we no longer consider the semi-classical dilute gas model: we account for quantum fluctuations to all orders. As the barrier becomes higher and higher, performing a sampling of multiple barrier-crossing paths contributing to the functional integral with dynamical algorithms such as Molecular Dynamics of Monte Carlo becomes highly inefficient, and computationally expensive.

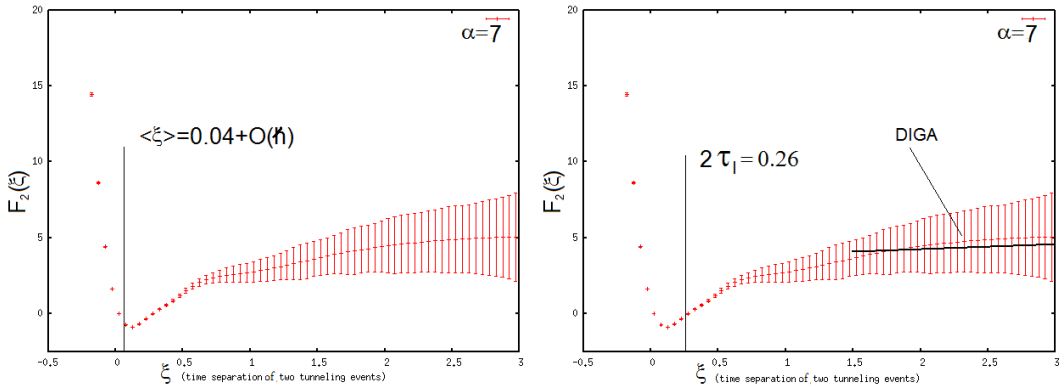

Figure 5.4: Non-perturbative calculation of the effective interaction $F(\xi)$ for $\alpha = 7$. Left: non-perturbative result compared to perturbative calculation. Right panel: non-perturbative result compared to DIGA, and instanton size.

To cope with this problem, we have evaluated the instanton-antiinstanton interactions using the importance sampling approach described in appendix B.

Fig. 5.3 and 5.4 shows the results of such a non-perturbative calculation for a well with $\alpha = 1$ (low barrier) and $\alpha = 7$ (high barrier). Some comments on these results are in order. First of all we note that the minimum of the effective interaction $F_2^{IA}(\xi)$ is located at positive values of ξ, in qualitative agreement with our perturbative calculation. The range of ξ in which the effective interaction $F_2^{IA}(\xi)$ is not flat corresponds to close, largely overlapping instanton-antiinstanton pair configurations. When the distance becomes of the order of twice the instanton size, the effective interaction starts to raise and eventually reaches the dilute gas limit. On the other hand, for low barriers, the instanton density is large and the attraction and repulsion generated by $F_2^{IA}(\xi)$ become important. In such a regime, the vacuum behaves like a one-dimensional liquid, rather than as an ideal gas. We note that this is precisely the physical picture underlying the instanton liquid model of the vacuum [48].

5.3 Projection Technique in Gauge Theories

Let us now apply the projection technique to Gauge Theories. In particular, we will use it to perform a rigorous calculation of effective interactions in the Instanton Vacuum: due to the extremely large number of results that have been obtained for this particular vacuum parametrization, it will be easier to test the validity of the projection techinque in Gauge Theories.

As we have seen in section 2.9, we can parametrize the vacuum with a family of configurations constructed from the classical fields of N^+ instantons and N^- antiinstantons: this can be done according to some prescriptions, in the following we will consider the simplest choice, in which one simply adds up the contribution of individual fields — *sum ansatz* — in *singular gauge*

$$\tilde{A}_\mu(x;\gamma) = \sum_{i=1}^{N^+} \tilde{A}_\mu^{I,sing}(x;\gamma_i) + \sum_{i=1}^{N^-} \tilde{A}_\mu^{\bar{I},sing}(x;\hat{\gamma}_i),$$

in the following we will consider $N = N^+ = N^-$ which corresponds to a vacuum with vanishing θ: as we have seen in section 2.5, this is a good approximation since $\theta \leq 10^{-10}$.

The Yang Mills path-integral over the gauge configurations is then replaced by a sum over the configurations of a grand-canonical statistical ensemple of singular gauge instantons and antiinstantons

$$Z_{p.g.} = \sum_N \frac{1}{(N!)^2} \int \prod_{i=1}^{N} \mathrm{d}\gamma_i \mathrm{d}\hat{\gamma}_i e^{-F(\gamma_i,\hat{\gamma}_i)},$$

where $F(\gamma,\hat{\gamma})$ is the effective interaction which represents the result of performing functional integral over the luctuations around the instanton vacuum manifold.

In general the effective interaction $F(\gamma,\hat{\gamma})$ contains the information about many-bosy correlations between the pseudo-particles. If the instanton vacuum ensemble is sufficiently dilute, it is possible to neglect three-body, ... and higher correlations and we re-write, in analogy to the quantum mechanical problem of the previous section

$$\begin{aligned} \exp\{-F(\gamma,\hat{\gamma})\} &\simeq \sum_i [G_1(\gamma_i) + G_1(\hat{\gamma}_i)] + \\ &+ \sum_{i<j} [G_2(\gamma_i,\gamma_j) + G_2(\hat{\gamma}_i,\hat{\gamma}_j)] + \sum_{i,j} G_2'(\gamma_i,\hat{\gamma}_j) + \ldots \end{aligned} \quad (5.96)$$

The 1-body term $G_1(\gamma)$ is the so-called instanton-density, or instanton size distribution. Gauge invariance and traslational invariance of the vacuum

imply that it must only depend on the instanton size ρ_i and that it must be equal for instanton and antiinstantons. The terms G_2 and G_2' desctibe the two bosy interactions between pseudo-particles of same and different kind, and so on.
As a first application we focus on the calculation of the instanton size distribution.

5.4 Non-Perturbative Calculation of the Instanton Size Distribution

In order to calculate $G_1(\rho)$ we recall that every gauge field of the path-integral will be decomposed as

$$A_\mu(x) \equiv \tilde{A}_\mu^{sing}(x;\gamma) + B_\mu(x), \tag{5.97}$$

we know that $G_1(\rho)$ must be the same for instanton and anti-instantons: we then choose $\tilde{A}_\mu$ to be an instanton in singular gauge:

$$A_\mu(x;x^I,\rho^I,\Delta^I) = U(\Delta^I)\tau^a U^\dagger(\Delta^I)\bar{\eta}^a{}_{\mu\nu}\frac{\rho_I^2}{(x-x^I)^2}\frac{(x-x^I)_\nu}{(x-x^I)^2+\rho_I^2}, \tag{5.98}$$

and the orthogonality conditions for the fluctuation fields are defined by imposing a set of k orthogonality conditions

$$(B(x)\cdot g_{\gamma_i}(x,\bar{\gamma})) \equiv \mathrm{Tr}_c\left\{\int \mathrm{d}^4x\ B_\mu(x)\ g_{\gamma_i,\mu}(x,\bar{\gamma})\right\} = 0, \tag{5.99}$$

$$g_{\gamma_i,\mu}(x,\bar{\gamma}) = \frac{\partial}{\partial\gamma_i}\tilde{A}_\mu(x;\gamma)\Big|_{\gamma=\bar{\gamma}}, \qquad i=1,\dots,k \tag{5.100}$$

from section 2.7 we recall that by definition, $g_{\gamma_i,\mu}$ are the zero mode of the fluctuation operator, which can be interpreted as vectors of the tangent space of the manifold parametrized by the coordinates of a single instanton. We now give an explicit example of such vectors (we recall that we are in Landau Gauge):

$$g_{\rho,\mu}(x;\bar{\gamma}) = U(\bar{\Delta}^I)\tau^a U^\dagger(\bar{\Delta}^I)\bar{\eta}^a{}_{\mu\nu}\frac{2\bar{\rho}_I(x-\bar{x}^I)_\nu}{[(x-\bar{x}^I)^2+\bar{\rho}_I^2]^2};$$

$$\begin{aligned} g_{x^I_\sigma,\mu}(x;\bar{\gamma}) = \ - \ & U(\bar{\Delta}^I)\tau^a U^\dagger(\bar{\Delta}^I)\bar{\eta}^a{}_{\mu\nu}\left[\frac{\bar{\rho}_I^2}{(x-x^I)^2}\frac{\delta_{\nu\sigma}}{(x-x^I)^2+\rho_I^2} - \right. \\ & \left. +\bar{\rho}_I^2\frac{(x-\bar{x}^I)_\nu(x-\bar{x}^I)_\sigma[\bar{\rho}_I^2+2(x-\bar{x}^I)^2]}{(x-\bar{x}^I)^2[(x-\bar{x}^I)^2+\bar{\rho}_I^2]^2}\right]; \end{aligned}$$

if we consider $N_C = 2$ we can also give an analytical expression for the zero-modes defined along the gauge orientation of the instanton, because we

have the analytical expression for $U(\mathbf{\Delta})$ given in Appendix A.1.

We also recall that in order to compue $G_1(\rho)$ the projection technique presecribe to generate a statistically representative ensemble of N_{conf} landau gauge-fixed field configurations $\{A^g_{\mu,1}(x), \ldots, A^g_{\mu,N_{conf}}(x)\}$, project them onto the tangent space of the single-instanton manifold and solve numerically the system of equations

$$\begin{cases} \Phi^g_1[A^g_\mu(x)] = (A^g \cdot g^g_{\gamma_1}(\bar{\gamma})) \equiv (\tilde{A}^g(\gamma) \cdot g^g_{\gamma_1}(\bar{\gamma})) \equiv \Psi^g_1(\gamma); \\ \qquad\qquad\qquad\qquad ... \\ \Phi^g_k[A^g_\mu(x)] = (A^g \cdot g^g_{\gamma_k}(\bar{\gamma})) \equiv (\tilde{A}^g(\gamma) \cdot g^g_{\gamma_k}(\bar{\gamma})) \equiv \Psi^g_k(\gamma). \end{cases} \tag{5.101}$$

in the variables γ for each configuration.

The system of equations 5.101 involves $4N_C$ equations for $4N_C$ variables γ in $SU(N_C)$. Since we know that instantons in $SU(N_C)$ are embeddings of $SU(2)$ instantons, in this work we will consider $N_C = 2$ for simplicty: we will then have to solve a system of 8 equations for 8 variables.
In addiction, due to the comlex non-linearity of the functions $\Psi^g(\gamma)$, we will not compute them analytically as in the Toy Model of section 5.2; instead, we will solve a discretized version of 5.101, where the projection vectors are substituted by "finite difference" derivatives, e.g.

$$\tilde{g}_{\gamma_i,\mu}(x,\bar{\gamma}) = \frac{\tilde{A}_\mu(x;\bar{\gamma}_i + \Delta\gamma) - \tilde{A}_\mu(x;\bar{\gamma}_i)}{\Delta\gamma},$$

and scalar products are calculated numerically

$$\tilde{\Phi}^g_i[A^g_\mu(x)] = a^4 \sum_n \mathrm{Tr}_C \left[A^g_\mu(n) \tilde{g}^g_{\gamma_i}(n;\bar{\gamma}) \right]; \tag{5.102}$$

$$\tilde{\Psi}^g_i[\gamma] = a^4 \sum_n \mathrm{Tr}_C \left[\tilde{A}^g_\mu(n;\gamma) \tilde{g}^g_{\gamma_i}(n;\bar{\gamma}) \right], \tag{5.103}$$

where a is the lattice spacing of the discretized configurations, and n runs over the lattice points: for consistency we will use $\Delta\gamma$ much smaller than a.

5.4.1 Test: Non-Perturbative Calculations in DIGA

Before performing the non-perturbative calculations in $SU(2)$ QCD, we test the projection technique on multi-instanton configurations generated with a given instanton size-distribution, without fluctuations; these configurations are discretized on a lattice and the projection and inversion are performed numerically.

This example is equivalent to the test performed on the Toy Model, where configurations have been generated starting by a distribution calculated analytical in the Dilute Instanton Gas regime. Here we generate

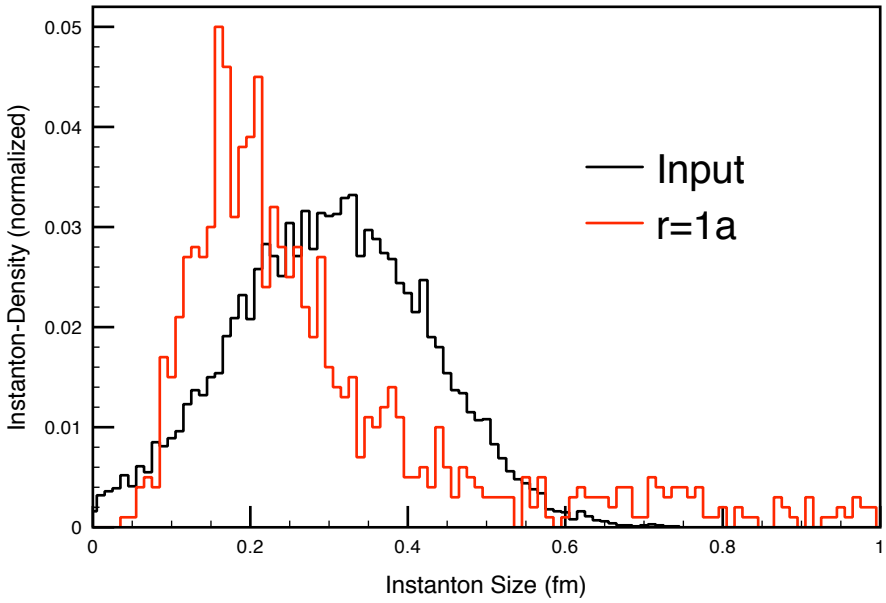

Figure 5.5: Test: Instanton size distribution of an instanton-antiinstanton ensemble with density $n \simeq 0.75(fm^{-4})$ and instanton size distribution *Input*. Results obtained with projection technique are in red (1000 configurations): the size of the projector is $\rho = 1a$ lattice spacings.

configurations with an instanton ensemble whose parameter are determined by phenomenology: we decide in particular to mimic the $N_c = 3$ Instanton Models, and choose a density of $n \simeq 0.75 fm^{-4}$ and a size-distribution with gaussian form, peaked on $\rho = 0.3 fm$. We perform our calculations on a lattice of size $V = (L = 2.7 fm)^4$, with $N = 16$ lattice points in each 4-direction: the lattice spacing is equal to $a \simeq 0.17 fm$. The choice of such a value is motivated by the LQCD configurations that will be used in the next sections.

The ensemble we have chosen is very dilute, so we expect that the projection technique is able to discriminate very well between separate pseudoparticles[2]. In order to test the goodness of the technique we then project our ensemble into different points of the instanton manifold, and check if the effective interactions depend on the choice of such a parameter, and which are the conditions for the given size distribution to be correctly reproduced. Due to translational invariance and gauge invariance, we do not expect the projection technique to be sensitive on different choices of the Euclidean position $\bar{x}^I_\nu$, and of the color orientation $\bar{\mathbf{\Delta}}$: we will perform our calculations on three different points $\bar{\rho}$ of the instanton manifold, and on random points

[2]See discussion in section 5.1.1.

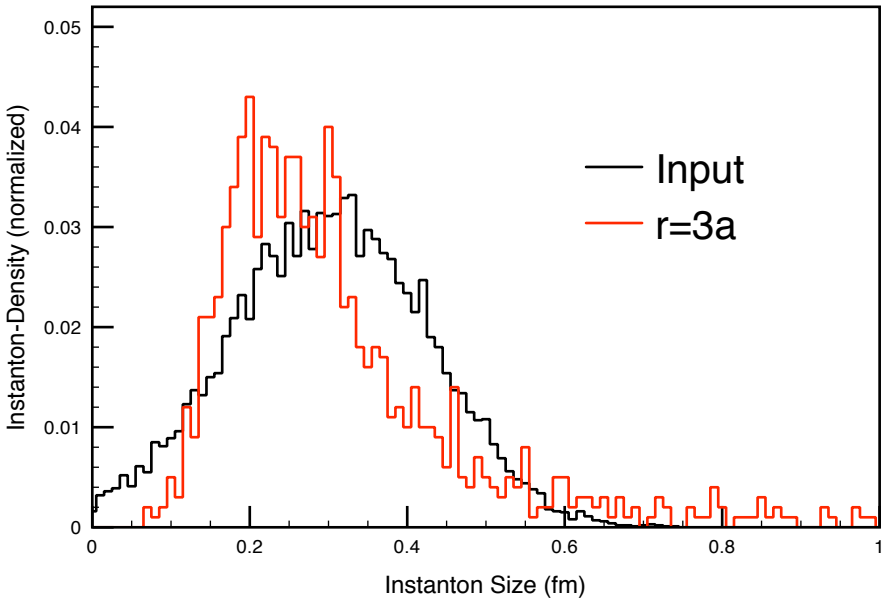

Figure 5.6: Test: Instanton size distribution of an instanton-antiinstanton ensemble with density $n \simeq 0.75(fm^{-4})$ and instanton size distribution *Input*. Results obtained with projection technique are in red (1000 configurations): the size of the projector is $\bar{\rho} = 3a$ lattice spacings.

x_ν^I and $\mathbf{\Delta}$.

In Fig.(5.5), Fig.(5.6) and Fig.(5.7) we show the results of the instanton size distributions calculated by projecting 1000 configurations in the points $\bar{\rho} = 1a$, $\bar{\rho} = 3a$ and $\bar{\rho} = 5a$ respectively, where we recall that "a" is the lattice spacing. As we can see, if $\bar{\rho}$ — which we will call this "size of the projector" from now on — is too close to the value of the lattice spacing, that is to say if $\bar{\rho} \simeq 1a \div 3a$ the projection technique will be sensitive only to small instantons, i.e. instantons which have roughly the same size of the projector. This implies that the correct size distribution cannot be recovered. If the projector is large at least 5 lattice spacings, on the other hand, we can see that the instanton size distribution is correctly reproduced, see Fig(5.7).

Notice that the instanton size distribution at very short range $\rho < a$ is similar for different sizes of projector, and differ from the expected result; this is not surprizing, in fact we do not expect the discretized theory to give us exact results at very small $\ll a$ and very large $\gg L$ distances.

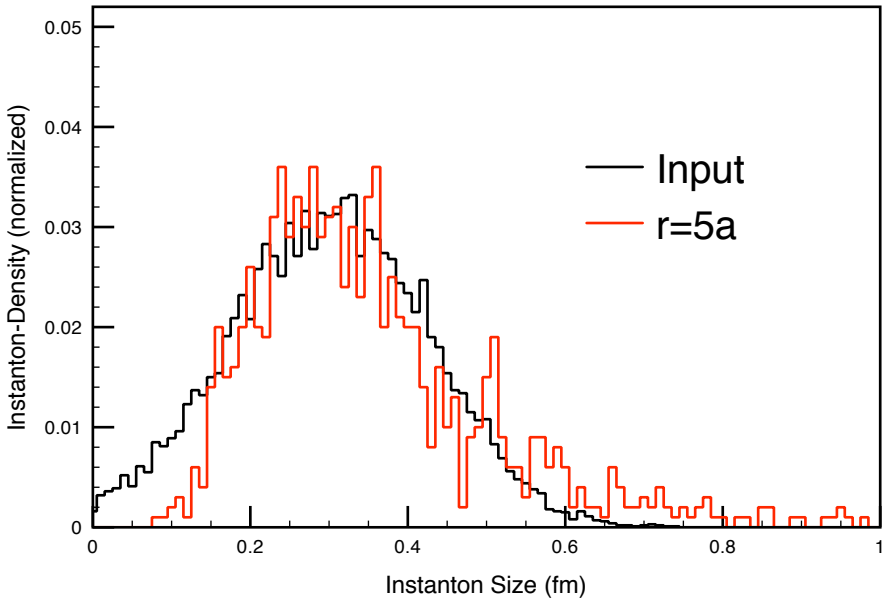

Figure 5.7: Test: Instanton size distribution of an instanton-antiinstanton ensemble with density $n \simeq 0.75(fm^{-4})$ and instanton size distribution *Input*. Results obtained with projection technique are in red (1000 configurations): the size of the projector is $\bar{\rho} = 5a$ lattice spacings.

5.4.2 On the Importance of Gauge Fixing

In the previous section we have seen the outcome of projections of configurations with a dilute instanton ensemble; from a geometrical point of view this is equivalent to say that projected configurations where very close to the manifold parametrized by configurations of a single instanton.
We now perform another test in order to see what one would expect if the configurations are extremely far from the projection manifold: we project gauge unfixed configurations.

In section 5.1 we have seen that the projection technique is gauge invariant: the only prescription is that we project configurations in a given gauge — Landau gauge, temporal gauge, etc. . .— onto a projection manifold parametrized by the collective coordinates of a family of configurations with the *same gauge fixing*. If this does not occur in fact, we cannot assign the correct collective coordinates to the projected configurations, because the projection technique is inconsistent: the system of equations 5.101 is shifted by a gauge-dependent random number

$$K_i = -i \left(U^{g',\dagger} \left[\partial_\mu U^{g'} \right] \cdot g_{\gamma_i,\mu} \right),$$

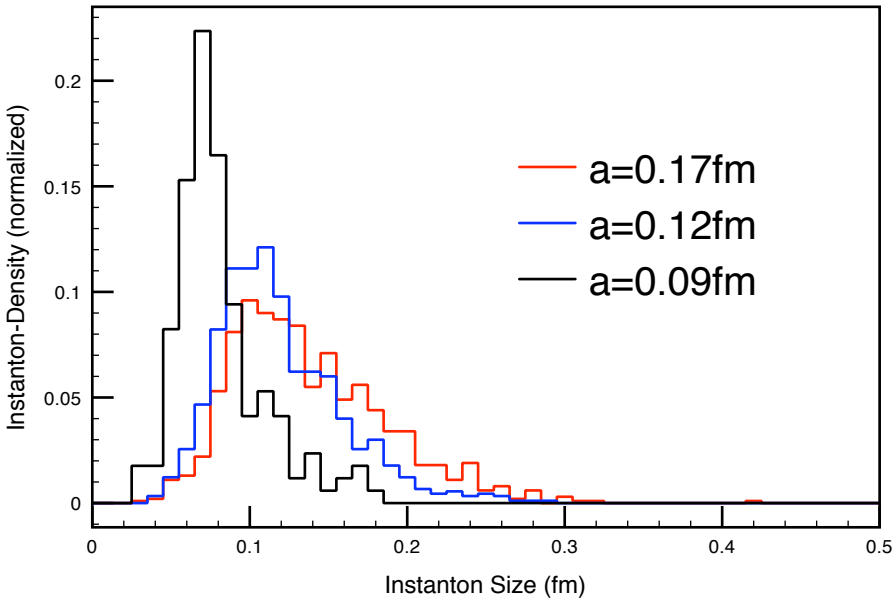

Figure 5.8: Test: Instanton size distribution obtained with projection technique, from 1000 gauge unfixed configurations. Results exhibit a lattice spacing dependence.

equation by equation.

We then project a set of *gauge-unfixed* configurations discretized on lattices of similar size $V \simeq (2.8fm)^4$ but different lattice spacings: $a_1 = 0.17fm$, $a_2 = 0.12fm$ and $a_3 = 0.09fm$. We present the results for the projection in Fig(5.8). As we can see, the results are clearly lattice-spacing-dependent; in addiction, the peak of the calculated instanton-density (whose gauge-fixed form is presented in the next-section) are found at values of ρ much smaller than the lattice spacing. This means that the projector cannot resolve the instanton content of the configurations: since the only physical scale is the lattice spacing, all configuration are projected in the submanifold with $0 < \rho < a$, that is to say that the projection technique interprets $O(a)$ fluctuations as signal.

5.5 Instanton Size Distribution: Results

In the previous section we have tested the behaviour and "regime of validity" of the projection technique applied to gauge theories: we have seen that the size of the projector must be much bigger than the lattice spacing and that if the obtained results depends from the choice of lattice spacing, it is a clear signal that the chosen set of collective coordinates are not a good

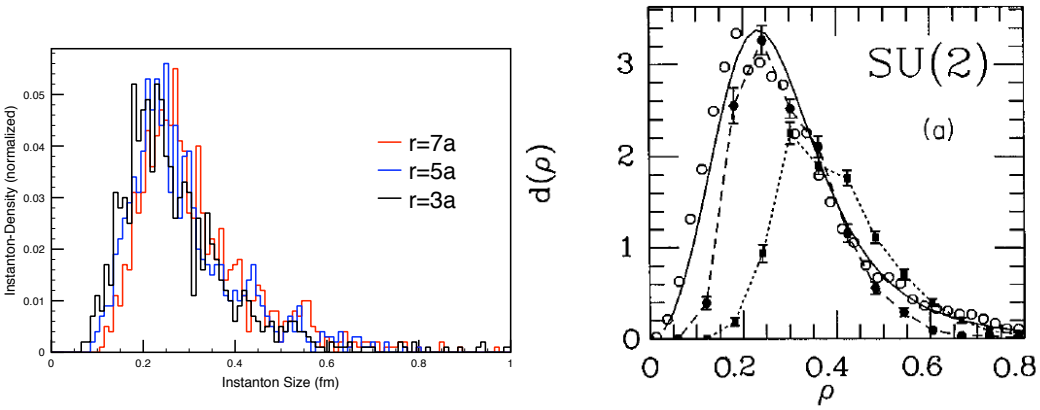

Figure 5.9: (Panel on the left:) Instanton size distribution obtained with projection technique, from *gauge-fixed* configurations of set 1), see 5.5. The results are presented for three different values of the size $\bar{\rho}$. Results exhibit a lattice spacing dependence. (Panel on the right:) Results for pure gauge $SU(2)$ obtained: (black dots) by C.Michael and S.Spencer with cooling [52]; (circled white dots) by Shuryak [20]. Picture taken from [20].

set of variables for reparametrizing the path integral.

In this section we will present the first calculations of the full instanton density from first principles. We will apply the projection technique to three different sets of $SU(2)$ pure gauge Lattice QCD configurations generated using the Standard Wilson action[3]:

1) 100 configurations: $\beta = 2.3$; $N = 16$. $L \simeq 2.7fm$; $a \simeq 0.17fm$;

2) 100 configurations: $\beta = 2.4$; $N = 24$. $L \simeq 2.9fm$; $a \simeq 0.12fm$;

3) 25 configurations: $\beta = 2.5$; $N = 32$. $L \simeq 2.8fm$; $a \simeq 0.09fm$.

Each configuration is projected in 10 different points of the lattice, in order to increase the statistics: 1000 projections for sets 1) and 2); 250 projections for set 3).
The configurations have been gauge fixed to Landau gauge using an overrelaxation algorithm, for a detailed analysis see [51]. This algorithm minimizes the divergence of a combination of gauge links

$$\mathcal{A}_\mu(x) = \frac{1}{2ai}\left(U_\mu(x) - U_\mu(x)^\dagger\right),$$

which in the continuum limit is equivalent to a physical gauge field

$$\mathcal{A}_\mu(x) \stackrel{a\to 0}{\longrightarrow} A_\mu(x).$$

[3]These LQCD Configurations have been obtained by Andre Sternbeck et al. [50].

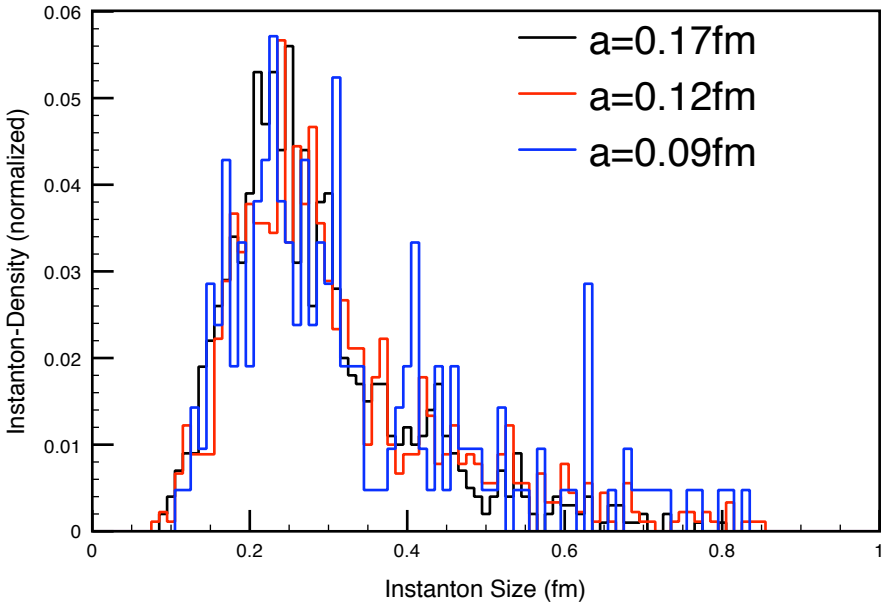

Figure 5.10: Instanton size distribution obtained with projection technique, from *gauge-fixed* configurations of set 1), 2) and 3), see 5.5.

Since we know from the previous section, that the gauge fixing condition is essential in the projection technique, we are going to use $\mathcal{A}_\mu(x)$ as a discretized definition of gauge field for our set of configurations.

We now show the results for the instanton size distribution for the first set of configurations: in Fig(5.9) we present the instanton size distribution calculated with tree different sizes $\bar{\rho}$ of the projector. As we can see, the obtained distribution is peaked around $\rho = 0.25fm$ and is independent from the choice of the parameter $\bar{\rho}$: results are in agreement with other calculations.

We also present the results for the instanton density for the three sets of configurations, i.e. at different lattice spacings, Fig(5.10): within the statistical error, the results are independent from the value of a. The gauge unfixed configurations we have used in the previous sections are those coming from these three sets, taken before berforming the gauge-fixing overrelaxation algorithm, see Fig(5.11) for a comparison.

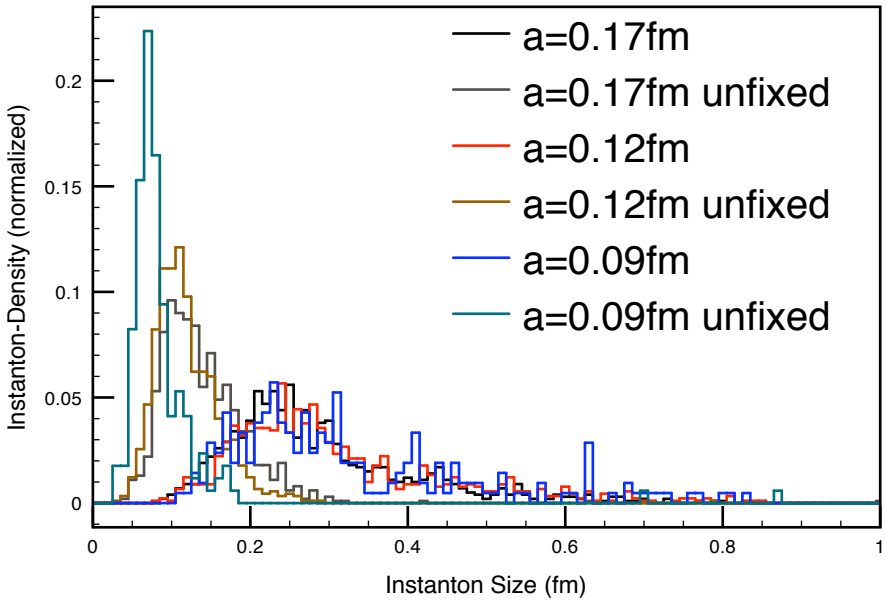

Figure 5.11: Instanton size distribution obtained with projection technique, from *gauge-fixed* and *gauge-unfixed* configurations of set 1) and 2), see 5.5.

Conclusive Remarks

The results in this section have been obtained without a direct modification of the LQCD configurations: unlike cooling, smearing and eigenvalue filtering[4], the results presented here come from unmodified LQCD configurations.

We recall that these results have been obtained without making any assumption on the nature of the non-perturbative configuration: the projection technique is not based on semiclassical arguments and hence can be applied to any family of non-perturbative configurations.

In the near future, we are going to calculate the two-body correlation function $G_2(\gamma, \gamma)$ for instantons and anti-instantons, in the sum-ansatz. If the inston density is low, this result together with the results for the $G_1(\gamma)$ would in principle enable to approximately calculate generic matrix elements of gluonic and fermionic operators, without using phenomenological interactions — Instanton Models — but using interactions calculated from first principles. These calculations can clarify the role of instantons in non-perturbative processes.

[4]See chapter 3.

We are also planning to apply this technique to other family of gauge configurations, such as monopoles and dyons or other topological configurations. Application of this technique at finite temperature T may give new insights on the role of topological configurations to confinement. For example, one could calculate monopole-instanton interactions, or instanton-instanton interactions in a background gauge field which mimic long-range interactions, as in the $PNJL$ model, and so forth.

Chapter 6

Conclusions

In this work we have discussed the role of topological degrees of freedom in the dynamics of non-perturbative processes. We have analyzed their role in the anomalous breaking of $U_A(1)$ symmetry and in the spontaneous breaking of chiral symmetry below the energy scale Λ_{SChSB}, and we have seen that their existence is responsible for the emergence of CP-violation in hadronic processes. We have seen in particular that the combination of axial anomaly and electromagnetic anomaly, may induce a CP-odd polarization in hadronic systems permeated by external magnetic fields. Ab initio calculations of such an effect, are limited by the possibility of solving QCD non-perturbatively.

The contribution of topological degrees of freedom in non-perturbative processes can be rigorously accounted for at very low-energies, in the ChPT approach at large N_c. We have discussed in particular the realization of Strong CP-violating interactions and anomalous interactions, and shown that at low energies these are both mediated by the $\eta^{'}$ pseudoscalar meson.

In chapter 4 we have used ChPT formalism to calculate the CP-odd vacuum polarization in the presence of an external magnetic field, at zero and finite temperature. We have seen that indeed the interplay between axial and electromagnetic anomaly give raise to a polarization of quantum fluctuations whose amplitude is proportional to the CP-breaking parameter θ. Results have been obtained at leading chiral $O(p^6)$ order and show that vacuum behaves as a non-linear medium: at zero temperature the CP-odd vacuum polarization is cubic in the external magnetic field B; at finite temperature the effect is enhanced by thermal fluctuations and the polarization vector is linear in the magnetic field and quadratic in the temperature.

As expected, such an effect is extremely weak and may be observed only in systems permeated by an intense magnetic field coherent over large scales.

Implications on Magnetars have been discussed.
We have also shown that Strong CP-violating interactions can also induce a CP-odd photon-photon interactions in low-energy QED, and we calculated the QCD contribution to the leading order CP-odd coefficient ruling the CP-odd photon dynamics. We also calculated the CP-odd contribution to the vacuum birefringence induced by a non-vanishing θ and we have also analyzed the dynamics of polarized light propagating in a Fabry Perot cavity permeated by an external electromagnetic field.

ChPT cannot be applied at high energies or at temperatures comparable to $T \simeq T_c$, because fundamental degrees of freedom become manifest and have to be explicitely included in the dynamics; the only approach which enables to solve QCD non-perturbatively from first principles is Lattice QCD. In the second part of this project we have then proposed to investigate the dynamics of non-perturbative configurations, using a technique which enables to rigorously reparametrize the QCD partition in terms of a finite numebr of effective low-energy degrees of freedom. All other infinite degrees of freedom are explicitly integrated out from the path integral using lattice QCD simulations.
This technique has been applied to the calculation of instanton size distribution in pure gauge $SU(2)$ QCD at $T = 0$: results are in agreement with other calculations, based e.g. on UV filtering. However it is worth stressing that, unlike such approach, the present method does not filter out gauge configurations. On the contrary the integral over such fluctuations is performed by means of LQCD. As a consequence our method does not introduce additional scales to the theory. For example, it does not involve choosing a scale at which stopping the cooling procedure. In addition, the projection technique is not based on semiclassical arguments and hence can be applied to any family of non-perturbative configurations.

Future work will consist in the calculation of the two-body correlation function $G_2(\gamma, \gamma)$ for instantons and anti-instantons, in the sum-ansatz. These calculations can clarify the role of instantons in non-perturbative processes.

Another interesting possibility is to apply this technique to investigate monopoles, dyons, vortices or other non-perturbative configurations, both at zero and finite temperature T: results may give crucial information on the role of topological configurations to non-perturbative processes such as confinement.

Appendix A

Topology of Lie Groups

Here we give a brief introduction of the theory of $SU(N)$ Lie Groups. We will show how their local properties are encoded in the $\mathfrak{su}(N)$ Lie algebras, and we will discuss how $SU(N)$ global — topological — properties are defined by the Homotopy groups $\pi_k[SU(N)]$. For a more comprehensive discussion see [55] and [56].

A Lie Group $\mathcal{G}$ is a group of continuous transformations $G(\bar{\xi})$, with $\bar{\xi}$ a finite set of real continuous parameters. Lie groups are differentiable manifolds: every group element "infinitely close" to the identity $I := G(\bar{0})$ can be written in terms of vectors of the tangent space $X^a[I]$ at the identity

$$G(\mathrm{d}\bar{\xi}) = I + i(\mathrm{d}\xi_1 X^1[I] + \ldots \mathrm{d}\xi_n X^n[I]).$$

Commutation relations among vector X^a, which are called generators of the group $\mathcal{G}$, define the Lie Algebra $\mathfrak{g}$

$$[X_a, X_b] = 2i{C_{ab}}^c X_c.$$

The coefficients ${C_{ab}}^c$ are called *structure constants*, and encode information on the *local properties* of the group $\mathcal{G}$. In fact, every group element "sufficiently close" to the identity can be represented as an expansion in $\bar{\xi}$ whose coefficients are uniquely determined by the structure constants ${C_{ab}}^c$; multiplication properties of such elements are also fixed by ${C_{ab}}^c$.

A.1 $SU(3)$ and $SU(2)$

$SU(N)$ Lie groups can be represented by unitary transormations[1]

$$G(\xi_a) = e^{i\xi_a \frac{X^a}{2}}; \qquad \text{s.t. } GG^\dagger = I,$$

[1] This is always true for Compact Lie Groups.

where the generators X^a are N^2-1 matrices in the adjoint representation: traceless, $N \times N$ hermitian matrices. In the $\mathfrak{su}(3)$ case, a perfect choise is given by the Gellmann matrices

$$\lambda_1 = \begin{pmatrix} 0 & 1 & 0 \\ 1 & 0 & 0 \\ 0 & 0 & 0 \end{pmatrix} \qquad \lambda_2 = \begin{pmatrix} 0 & -i & 0 \\ i & 0 & 0 \\ 0 & 0 & 0 \end{pmatrix} \qquad \lambda_3 = \begin{pmatrix} 1 & 0 & 0 \\ 0 & -1 & 0 \\ 0 & 0 & 0 \end{pmatrix}$$
$$\lambda_4 = \begin{pmatrix} 0 & 0 & 1 \\ 0 & 0 & 0 \\ 1 & 0 & 0 \end{pmatrix} \qquad \lambda_5 = \begin{pmatrix} 0 & 0 & -i \\ 0 & 0 & 0 \\ i & 0 & 0 \end{pmatrix} \tag{A.1}$$
$$\lambda_6 = \begin{pmatrix} 0 & 0 & 0 \\ 0 & 0 & 1 \\ 0 & 1 & 0 \end{pmatrix} \qquad \lambda_7 = \begin{pmatrix} 0 & 0 & 0 \\ 0 & 0 & -i \\ 0 & i & 0 \end{pmatrix} \qquad \lambda_8 = \sqrt{\tfrac{1}{3}} \begin{pmatrix} 1 & 0 & 0 \\ 0 & 1 & 0 \\ 0 & 0 & -2 \end{pmatrix};$$

$$\mathrm{Tr}[\lambda_a, \lambda_b] = 2\delta_{ab}.$$

The first three elements of $\mathfrak{su}(3)$ — λ_1, λ_2, λ_3 — form a sub-algebra. This is $\mathfrak{su}(2)$, whose generators in the adjoint representation are

$$\tau_1 = \begin{pmatrix} 0 & 1 \\ 1 & 0 \end{pmatrix} \qquad \tau_2 = \begin{pmatrix} 0 & -i \\ i & 0 \end{pmatrix} \qquad \tau_3 = \begin{pmatrix} 1 & 0 \\ 0 & -1 \end{pmatrix}; \tag{A.2}$$

$$[\tau_a, \tau_b] = 2i\varepsilon_{abc}\tau_c, \tag{A.3}$$

where τ_i are the pauli matrices and ε_{abc} is the totally antisymmetric tensor with $\varepsilon_{123} = 1$. $SU(2)$ group elements have simple analitical representations in terms of pauli matrices

$$G_{SU(2)}(\xi_1, \xi_2, \xi_3) = \mathrm{Cos}[\Xi] I_{2\times 2} + i\xi_a \frac{\tau_a}{2} \frac{\mathrm{Sin}[\Xi]}{\Xi}; \tag{A.4}$$
$$\Xi = \frac{1}{2}\sqrt{\xi_a \xi_a}. \tag{A.5}$$

A.2 Homotopy Groups of $SU(N)$

$SU(N)$ Lie Groups are *Compact* — or *Connected* —, that is to say that it is always possible to reach the group identity I from every other group element of $G(\hat{\xi})$ with a continuous path $\gamma_{0,\hat{\xi}}[t]$ in the group manifold, s.t.

$$G(\gamma_{0,\hat{\xi}}[0]) = I; \tag{A.6}$$
$$G(\gamma_{0,\hat{\xi}}[t]) = G_\gamma(\bar{\xi}); \quad 0 < t < 1; \tag{A.7}$$
$$G(\gamma_{0,\hat{\xi}}[1]) = G(\hat{\xi}), \tag{A.8}$$

where $G_\gamma(\bar{\xi}) \to I$ when $t \to 0$, and $G_\gamma(\bar{\xi}) \to G(\hat{\xi})$ when $t \to 1$.

Compact Lie Groups may be *simply connected*, depending on the properties of closed paths $\gamma_{0,0}$: if it is possible to continuously deform any closed path $\gamma_{0,0}$ in $\mathcal{G}$ into the infinitely short path

$$\gamma_I[t] = \bar{0}; \quad \text{s.t. } G_\gamma(\gamma_I[t]) = I,$$

then the group is simply connected. The set of all paths $\gamma_{0,0}$ that can be continuously deformed into another path $\hat{\gamma}_{0,0}$, is called the *homotopy class* of $\hat{\gamma}_{0,0}$: the set of homotopy classes form a group. The homotopy group of closed paths in $\mathcal{G}$ is called first homotopy group $\pi_1[\mathcal{G}]$ or fundamental group of $\mathcal{G}$: if all paths $\gamma_{0,0}$ in $\mathcal{G}$ are in the homotopy class of γ_I then $\pi_1[\mathcal{G}] = 0$. The fundamental group $\pi_1[\mathcal{G}]$ can be generalized to the 2−nd, 3−rd, ..., k−th homotopy group $\pi_k(\mathcal{G})$ by considering how spheres, tri-spheres, ..., k−sphere can be mapped into the $\mathcal{G}$ manifold. Hence, Homotopy groups give information on global — topological — properties of a Lie Group.

Homotopy groups can be calculated with the help of topologically invariant functionals of the elements of the group $\mathcal{G}$; the first homotopy class, for example, is given by the Cartan-Maurer integral

$$\mathcal{J}^1_{\mathcal{G}}(G) = \int_{S^1} \mathrm{d}x_1 \big(\partial G_{S^1}(\bar{\xi}[x_1])]\big) G^\dagger_{S^1}(\bar{\xi}[x_1])]. \tag{A.9}$$

Elements which belong to the same homotopy class will have the same Cartan-Maurer number, thus by solving $\mathcal{J}^1_{\mathcal{G}}(G)$ for all $G \in \mathcal{G}$ the first homotopy class of $\mathcal{G}$ can be determined; a simple analytical example can be given for $\pi_1[U(1)]$, which is obtained by parametrizing closed paths $\gamma_{0,0}$ into the abelian group manifold. The fundamental homotopy group of $U(1)$ can be can be easiliy calculated, and is equivalent to

$$\pi_1[U(1)] = Z,$$

which is the set of all integer numbers. The homotopy classes are the sets of paths equivalent to

$$G_{\gamma^n_{0,0}}(x) = e^{inx}; \qquad n \in Z.$$

The 1-dimensional Cartan-Maurer Integral is given by

$$\begin{aligned} \mathcal{J}^1_{U(1)}(G_{\gamma^n_{0,0}}) &= i\,n \int_0^{2\pi} \mathrm{d}x e^{-inx} e^{inx} && \text{(A.10)} \\ &= 2i\,n\pi. && \text{(A.11)} \end{aligned}$$

Hence, every homotopy class has its charachteristic value for the Cartan-Maurer Integral.

We now focus on $SU(N)$: the general result for the Homotopy groups is

$$\pi_1[SU(N)] = 0; \qquad \forall N; \tag{A.12}$$

$$\pi_{2k}[SU(N)] = 0; \qquad k \geq 1; \quad N \geq \frac{2k+1}{2}; \tag{A.13}$$

$$\pi_{2k+1}[SU(N)] = 0; \qquad k \geq 1; \quad N \geq k+1. \tag{A.14}$$

The most important relation is $\pi_3[SU(N)] = Z$: this proves crucial in the study of the topology of classical QCD vacuum. In fact it enables to distinguish vacuum gauge fields in different homotopy class: $n = 0$ for the trivial vacuum, $n = \pm 1, \pm 2, \ldots$ for vacuums with non-trivial topology.
The Cartan-Maurer Integral can be generalized to a generic π_k, so the third homotopy class can be calculated by means the following expression

$$\mathcal{J}^3_{\mathcal{G}}(G) = \int_{S^3} \mathrm{d}x_1 \mathrm{d}x_2 \mathrm{d}x_3 \; \varepsilon_{abc} Y^a \left[G_{S^3}(\mathbf{x})\right]] \, Y^b \left[G_{S^3}(\mathbf{x})\right] Y^c \left[G_{S^3}(\mathbf{x})\right], \tag{A.15}$$

where

$$Y^a \left[G\right] = \big(\partial^a G\big) G^\dagger.$$

The homotopy group of other Lie Groups such as the Coset Space $H = SU(2)/U(1)$, enables to identify other families of topological configurations: $\pi_2[H] = Z$ is related to the existence of monopoles in QCD. In this work we are be interested mainly $\pi_3[SU(N)]$, and we will not enter in further details.

Appendix B

Algorithm Used in the Evaluation of $F_2^{IA}(\xi)$

We are interested in computing numerically the integral

$$
\begin{aligned}
g_2^{IA}(\xi) \;=\; & \mathcal{N} \int \mathcal{D}y \, \exp\left\{ - \int \mathrm{d}t \, \mathcal{L}[\tilde{x}_{S_2}(t; \chi - \frac{1}{2}\xi, \chi + \frac{1}{2}\xi) + y(t)] \right\} \times \\
& \times \delta\Big(y \cdot g_\chi(\bar{\chi}, \bar{\xi}) \Big) \delta\Big(y \cdot g_\xi(\bar{\chi}, \bar{\xi}) \Big) \times \\
\times \Big[& \Big(g_\chi(\chi, \xi) \cdot g_\chi(\bar{\chi}, \bar{\xi}) \Big) \Big(g_\xi(\chi, \xi) \cdot g_\xi(\bar{\chi}, \bar{\xi}) \Big) - \Big(g_\chi(\chi, \xi) \cdot g_\xi(\bar{\chi}, \bar{\xi}) \Big) \Big(g_\xi(\chi, \xi) \cdot g_\chi(\bar{\chi}, \bar{\xi}) \Big) \Big],
\end{aligned}
$$

where the term inside the square brackets is the explicit representation of the Jacobian factor $\Phi[y]$.

The meta-stability of the double well system makes it rather computationally challenging to generate a statistically significative ensemble of field configurations, using algorithms based on Metropolis or by Langevin dynamics. The main problem is that, for such a meta-stable system, ergodicity is reached only in an exponentially large computational time.

The problem has no easy solution within a dynamical Monte Carlo approach. However, because of the low dimensionality of our system, simpler importance sampling technique are available and efficient[1]. Since the system is time-translationally invariant, without loss of generality we can set $\chi = 0$, $\bar{\chi} = 0$ — i.e. we can remove completely the dependance from the center of mass—, and set $\bar{\xi} = 0$. Then, the resulting expression for the pair

[1] Note that this problem is unrelated to our projection approach, which is a prescription about the measurement of an effective action, once a significant sample of configurations has been provided in some way.

correlation function can be re-written as

$$g_2^{IA}(\xi) = \mathcal{N} \int \mathcal{D}y \; \delta(y(t) \cdot g_\xi(t;0)) \; \Phi[y] \; \hat{P}[y(t)] \; \frac{e^{-S\left[\tilde{x}_{S_2}\left(t,-\frac{1}{2}\xi,\frac{1}{2}\xi\right)+y(t)\right]}}{\hat{P}[y(t)]}, \tag{B.1}$$

where $\hat{P}[y(t)]$ is a probability distribution to be defined below. We stress that now the integral can be restricted to the small region in which the projection function is not exponentially small. The discretized version of Eq. (B.1) is

$$g_2^{IA}(\xi) = \mathcal{N} \; \int \prod_{k=1}^{N} \mathrm{d}y(t_k) \delta \left(\sum_{k=1}^{N} y(t_k) g_\xi(t_k, 0) \right) \; \Phi[y] \; \hat{P}[y] \; \frac{e^{-S_{\mathrm{lat}}\left[\tilde{x}_{S_2}\left(t_k,-\frac{1}{2}\xi,\frac{1}{2}\xi\right)+y\right]}}{\hat{P}[y]} \tag{B.2}$$

where N is the number of points in the lattice and S_{lat} is the discretised version of S.

For $\hat{P}[y]$ we choose:

$$\hat{P}[y] \propto \exp\left(-\frac{1}{8m\Delta t} \sum_{k=0}^{N} (y(t_{k+1}) - y(t_k))^2 \right), \tag{B.3}$$

with the constraint $y(t_0) = y(t_{N+1}) = 0$. We eliminate the delta function by setting the last coordinate $y(t_N)$ equal to

$$y(t_N) = -\sum_{i=1}^{N-1} y(t_i) g_\xi(t_i) / g_\xi(t_N). \tag{B.4}$$

Notice that, in this way, the orthogonality condition is satisfied configuration by configurations. The statistical weight of resulting each configurations was evaluated from

$$w_i(\xi) = \frac{\exp(-S_{\mathrm{lat}}[\tilde{x}_s(t_k, \xi) + y_i])}{\hat{P}[y_i]}. \tag{B.5}$$

Up to an overall multiplicative factor, $g^{IA}(x)$ can be extracted from

$$g_2^{IA}(\xi) = \text{const.} \times \sum_i w_i(\xi). \tag{B.6}$$

By taking the logarithm, one obtains $F_2^{IA}(\xi)$, up to an overall additive constant.

Notation

We define

Minkowskian Metric

$$\eta_{\mu\nu} = \begin{pmatrix} -1 & 0 & 0 & 0 \\ 0 & 1 & 0 & 0 \\ 0 & 0 & 1 & 0 \\ 0 & 0 & 0 & 1 \end{pmatrix}.$$

Gamma matrices

$$\{\gamma^\mu, \gamma^\nu\} = 2\eta^{\mu\nu} \; ; \quad \gamma_5 = i\gamma_0\gamma_1\gamma_2\gamma_3.$$

Perturbative Vs. Non-Perturbative Notation in QCD

$$A_\mu^{np} \leftrightarrow gA_\mu^p;$$

$$G_{\mu\nu}^{np} \to gG_{\mu\nu}^p.$$

Euclidean Notation

$$x_4 = ix^0 = -ix_0;$$

$$\partial_4 = i\partial^0 = -i\partial_0'$$

$$A_4^a = iA^{a,0};$$

$$\gamma_4 = i\gamma^0;$$

$$\mathrm{d}^4x_E = i\mathrm{d}^4x = \mathrm{d}x_1\mathrm{d}x_2\mathrm{d}x_3\mathrm{d}x_4.$$

Bibliography

[1] A.C. Davis, M. Dine and N Seiberg, Phys.Lett.**B125** (1983) 487; A.V. Belitsky, S Vandoren and P. van Nieuwenhuizen *Yang-Mills and D-Instantons* Class.Quant.Grav.17 (2000) 3521 1

[2] N.K. Nielsen and B.Schroer *Saturation of Gauge Invariant Schwniger Model Correlation Functions by Instantons* Phys.Lett**B66** (1977) 373; A.V. Smilga *Instantons in Schwinger Model* Phys.Rev.**D49** (1994) 5480 1

[3] The STAR Collaboration: Abelev, B.I *et al. Azimuthal Charged-Particle Correlations and Possible Local Strong Parity Violation*, Phys.Rev.Lett 103 (2009) 251601 1

[4] D.Kharzeev and A. Zhitnitski, *Charge Separation by P-odd Bubbles in QCD Matter* Nucl.Phys**A797** (2007) 67; K. Fukushima, D. Kharzeev and H. Warringa *The Chiral Magnetic Effect* Phys.Rev.**D78** (2008) 074033; H. J. Warringa *Implications of CP-Violating Transitions in Hot Quark Matter on Heavy-Ion Collisions* J. Phys. G: Nucl. Part. Phys. 35 (2008) 104012 1, 2.4.1

[5] D.J. Gross, F. Wilczek *Ultraviolet Behaviour of Non-Abelian Gauge Theories*, Phys.Rev.Lett 30 (1973) 1343; H.D. Politzer , Phys.Rev.Lett 30 (1973) 1346 2.2

[6] Crewther, R.J.; Di Vecchia, P. and Veneziano, G. *Chiral estimate of the electric dipole moment of the Neutron in Quantum Chromodynamics* Phys.Lett.B88:123 (1979) 2.5.2

[7] Particle Data Group: http://pdg.lbl.gov 2.52

[8] Peccei, R.D. and Quinn, H.R. *CP Conservation in the Presence of Pseudoparticles* Phys. Rev. Lett. 38, 25, 1440 (1977) 2.5.2

[9] Kim, J.E. *Weak-Interaction Singlet and Strong CP Invariance* Phys. Rev. Lett. P **43**, 103 (1979) 2.5.2

[10] Shifman, M.A.; Vainshtein, A.I. and Zakharov, V.I Nucl. Phys. *Can Confinement Ensure Natural CP Invariance of Strong Interactions?* **B166**, 493 (1980) 2.5.2

[11] Dine, M.; Fischler, W. and Srednicki, M. Phys. Lett. *A Simple Solution to the Strong CP Problem with a Harmless Axion* **B104**, 199 (1981) 2.5.2

[12] *On Possible Suppression of the Axion Hadron Interactions* Zhitnitsky, A.R. Sov. J. Nucl. Phys. **31**, 260 (1980) 2.5.2

[13] A.A. Belavin *et. al.*, Phys.Lett.**B59** (1975) 85 2.7

[14] G. 't Hooft, Phys.Rev.Lett 37 (1976) 8 2.7

[15] M.F. Atiyah and I.M Singer, Proc.Nat.Acad.Sci **81** (1984) 2597 2.8.1

[16] T. Banks and A. Casher, Nucl.Phys**B169** (1980) 103 2.8.2

[17] M. Cristoforetti, P. Faccioli, J.W.Negele and M. C. Traini, Phys. Rev. **D 75** (2007), 034008. M. Cristoforetti, P. Faccioli, and M. C. Traini, Phys. Rev. **D 75**, (2007) 054024. 2.9

[18] P. Faccioli, A. Schwenk, and E. Shuryak, Phys. Lett. **B 549**, 93 (2002). P. Faccioli, Phys. Rev. **C 69** (2004), 065211. P. Faccioli, A. Schwenk, and E. Shuryak, Phys. Rev. **D 67** (2003), 113009. M. Cristoforetti, P. Faccioli, E. Shuryak, and M. Traini, Phys. Rev. **D 70** (2004), 054016 . 2.9

[19] F. Lenz , J. W. Negele , M. Thies, Annals Phys. **323** (2008),1536. 2.9

[20] T. Schaefer and E. Shuryak, Rev. Mod. Phys. **70**, 323 (1998). 2.9, 9, 2.9, 5.9

[21] T.Schafer, E.V Shuryak and J.J.M. Verbaarschot *The Chiral Phase Transition and Instanton-AntiInstanton Molecules* Phys.Rev**D51** (1995) 1267; E.V Shuryak and T.Schafer *Instantons and Chiral Symmetry Restoration in QCD-Like Theories* Nucl.Phys.**B53** (1997) 472; E.V Shuryak and J.J.M. Verbaarschot *Chiral Symmetry Breaking and Correlations in the Instanton Liquid* Nucl.Phys**B341**(1990)1 2.9

[22] Weinberg, S. *Phenomenological Lagrangians*, Physica A96, 327 (1979) 3.1.1, 3.1.1

[23] 't Hooft, G. Nucl. Phys. **B72** 461 (1974) 3.1.2

[24] Witten, E. *Current algebra theorems for the* $U(1)$ *"Goldstone Boson"* (1979) 3.1.2

[25] Pich, A. *η-decays and chiral Lagrangians* Presented at Workshop on Rare Decays of Light Mesons, Gif-sur-Yvette, France, Mar 29-30 (1990) 3.1.2

[26] Ecker, G.; Gasser, J.; Pich, A. and de Rafael, E. *The role of resonances in chiral perturbation theory* Nucl.Phys.B321:311 (1988) 3.1.2

[27] Witten, E. *Large N chiral dynamics* Annals Phys.128:363 (1980) 3.1.4

[28] Witten, E. *Global aspects of current algebra* Nucl. Phys. B223, 422 (1983) 3.1.7

[29] Pich, A. *Chiral Perturbation Theory* Rept.Prog.Phys.58:563-610 (1995) 3.1.4

[30] Wess, J. and Zumino, B. *Consequences of anomalous Ward Identity* Phys. Lett. B37, 95 (1971) 3.1.7

[31] Gupta, R. *Introduction to Lattice QCD: Course* Piblished in: Les Houches 1997, Probing the Standard Model of Particle Interactions, Pt.2 83-219Beane, S.R. *et al Nuclear Physics from Lattice QCD* (2010) arXiv:1004.2935; F. Di Renzo and L. Scorzato *Numerical Stochastic Perturbation Theory for Full QCD* JHEP (2004) 0410:073 3.2

[32] K.G. Wilson, *Confinement of Quarks* Phys. Rev. D10 (1974) 2445. 3.2.4

[33] J. Kogut and L. Susskind, *Hamiltonian Formulation of Wilson's Lattice Gauge Theories* Phys. Rev. D11 (1975) 395; T. Banks, J. Kogut, and L. Susskind, *Strong Coupling Calculation of Lattice Gauge Theories: (1+1)-Dimensional Exercises* Phys. Rev. D13 (1996) 1043; L. Susskind, *Lattice Fermions* Phys. Rev. D16 (1977) 3031. 3.2.4

[34] S. Solbrig *et.al. Smearing and Filtering Methods in Lattice QCD: a Quantitative Comparison* PoS LAT2007:334; F. Bruckmann *et.al. Quantitative comparison of filtering methods in lattice QCD* Eur.Phys.J.**A33** (2007) 333 3.2.6

[35] R. Millo and P. Faccioli, *Strong CP-Violation and Primordial Magnetic Field* Phys. Rev. **D77**(2008) 065013. 4.1, 4.1.2

[36] R.Millo, *Strong CP-Violation in External Magnetic Fields* MsC Thesis, Trento University (2007) 4.1.2, 4.1.4

[37] R.Millo and P.Faccioli *Cp-Violation in Low-Energy Photon-Photon Interactions* Phys.Rev.**D79**(2010) 065020 4.2

[38] Xue-Peng Hu, Yi Liao, Eur. Phys. *Effective Field Theory Approach to Light Propagation in an External Magnetic Field* J. **C53** (2008) 685. 4.2, 4.2.4

[39] B. Pinto da Souza *et al. P, T Violating Magneto-Electro-Optics* Eur. Phys. J. **D40** (2006) 445. 4.2, 4.2.4

[40] Yi Liao *Impact od Spin-Zero Particle-Photon Interactions on Light Polarization in External Magnetic Fields* Phys. Lett. **B650** (2007) 257. 4.2

[41] Kruglov, S.I. *Vacuum Birefringence from Effective Lagrangian of the Electromagnetic Field* Phys. Rev. **D75** (2007) 117301; S.L. Adler, Ann. Phys. **67** (1971) 599. 4.2, 4.2.3, 4.2.3

[42] W. Heisenberg, H. Euler , Z. Phys. **98** (1936) 718; J. Schwinger , Physical Review **82** (1951) 664. 4.2.1

[43] Zavattini, E. et al. *PVLAS: Probing Vacuum with Polarized Light* Nucl.Phys.Proc.Suppl.164:264-269 (2007) 4.2.6, 4.2.6, 4.7

[44] R. Battesti *et. al.* Eur. Phys. J. **D46** (2008) 323 4.2.6

[45] F. Brandi, E. Polacco, G. Ruoso , Meas. Sci. Technol. **12** (2001) 1502, G. Zavattini *et al.* Appl. Phys. **B83** (2006) 571. 4.2.6

[46] D.I. Dyakonov and V.Yu Petrov, *Instanton-Based Vacuum from the Feynman Variational Principles* Nucl. Phys. **B245**(1984) 259. 5.1

[47] Coleman, S., 1977, "The uses of instantons", Prooceedings of the 1977 School of Subnuclear Physics, Erice (Italy), reproduced in Aspects of Symmetry (Cambridge University Press, Cambridge, England, 1985), p. 265. 5.2.1

[48] E.V. Shuryak, *Toward the Quantitative Theory of the "Instanton Liquid" 4. Tunneling in the Double Well Potential* Nucl. Phys. **B302** (1988) 621 5.2.6

[49] R.Millo, P.Faccioli, L.Scorzato *Quantum Interactions Between Non-Perturbative Vacuum Fields* Phys.Rev.**D82**(2010) 074019 5.2

[50] A. Sternbeck *et.al. Comparing SU(2) to SU(3) Gluodynamics on Large Lattices* PoS LAT2007:340 (2007) 3

[51] J.Mandula and M.Ogilvie *Efficient Gauge Fixing Via Overrelaxation* Phys.Lett**B248** (1990) 157 5.5

[52] C.Michael and P.S. Spencer *Cooling and the SU(2) Vacuum* Phys. Rev. **D52** (1995) 4691. 5.9

[53] G. Parisi, Yongshi Wu , *Perturbation Theory Without Gauge Fixing* Sci.Sin.**24** (1981) 483 5.2.3

[54] Y. Grandati, A. Berard, P. Grange , *Stochastic Quantization of Instantons* Ann. of Phys. **246** 2 (1996) 291 5.2.3

[55] Weinberg, S. *The Quantum Theory of Fields: Foundations. I* Cambridge University Press (2005) A

[56] Weinberg, S. *The Quantum Theory of Fields: Modern Applications. II* Cambridge University Press, (2005) A

[57] Scherer, S. *Intrduction to chiral perturbation theory* Adv.Nucl.Phys.27:277 (2003)

[58] le Bellac, M *Thermal Field Theory* Cambridge University Press (1996)

[59] Heyl, J.S. and Hernquist, L. *Birefringence and Dichroism of the QED Vacuum* J.Phys.A30:6485-6492 (1997)

[60] P.H. Damgaard and H. Hueffel *Stochastic Quantization* Phys.Rept 152 (1987) 227

[61] M.Hutter, *Instantons in QCD* Ph.D. Thesis, Ludwig Maximilians University Munich (1995), arXiv:hep-ph/0107098.

[62] M. Chu, J. Grandy, S. Huang, and J. W. Negele, Phys. Rev. **D 49** (1994), 6039.

[63] C. T. H. Davies *et al.*, Phys. Rev. **D**37 (1988) 1581.

[64] L. Giusti, M. L. Paciello, C. Parrinello, S. Petrarca and B. Taglienti, Int. J. Mod. Phys. **A**16, 3487 (2001) [arXiv:hep-lat/0104012].

[65] Le Bellac, M. *Quantum and Statistical Field Theory* Oxford Science Publications (1995)

[66] Donoghue, J.F.; Golowich, E. and Holstein, B.R. *Dynamics of the Standard Model* Cambridge University Press (1992)

[67] Landau, L. and Lifchitz, E. *Physique théorique: Theorie des Champs* Editions MIR Moscou (19..)

[68] Kaiser, R. and Leutwyler, H. *Large N_c in chiral perturbation theory* hep-ph/0007101 v1 (2000)

[69] Pich, A. and de Rafael, E. *Strong CP Violation in an effective chiral Lagrangian approach* Nucl.Phys.B367:313-333 (1991)

[70] Peccei, R.D. *The Strong CP problem and axions* hep-ph/0607268 (2006)

[71] Lepage, G.P. *How to renormalize the Schroedinger equation* nucl-th/9706029 (1997)

[72] Pich, A. *Effective Field Theory* Talk given at Les Houches Summer School in Theoretical Physics, Session 68: Probing the Standard Model of Particle Interactions, Les Houches, France, 28 Jul - 5 Sep (1998)

[73] Mallik, S. *Current algebra derivation of temperature dependence of hadron couplings with currents* Eur.Phys.J.C45:777-782 (2006)

[74] Treiman, S.B.; Jackiw, R.; Zumino, B. and Witten, E. *Current algebra and anomalies* Princeton series in Physics (1985)

[75] Peskin, M.E and Schroeder, E.V. *An Introduction to Quantum Field Theory* Perseus Books (1995)

[76] Schaefer, T. and Shuryak, E.V. *Instantons in QCD* Rev.Mod.Phys.70:323-426 (1998)

[77] R. Bertle, J. Greensite, S. Olejnik, "Quark Confinement and the Hadron Spectrum IV: Proceedings." , edited by Wolfgang Lucha and Khin Maung Maung, World Scientific, Singapore, 2002. ArXiv: hep-lat/0009017.

[78] S.Weinberg *The U(1) Problem* Phys.Rev**D11** 3583

[79] J.J.M. Verbaarshot *Streamlines and Conformal Invariance in Yang-Mills Theories* Nucl.Phys**B362** (1991) 33

[80] H.Forkel *A Primer on Instantons in QCD* hep-ph/0009136